Renewable Bioplastics and Biocomposites From Biogas Methane and Waste-Derived Feedstock: Development of Enabling Technology, Life Cycle Assessment, and Analysis of Costs

CalRecycle
California Department of Resources Recycling and Recovery

August 2014

Contractor's Report
Produced Under Contract By:

Craig S. Criddle
Sarah L. Billington
Department of Civil and Environmental Engineering
Stanford University

Curtis W. Frank
Department of Chemical Engineering
Stanford University

STATE OF CALIFORNIA

Edmund G. Brown Jr.
Governor

Matt Rodriquez
Secretary, California Environmental Protection Agency

DEPARTMENT OF RESOURCES RECYCLING AND RECOVERY

Caroll Mortensen
Director

Department of Resources Recycling and Recovery
Public Affairs Office
1001 I Street (MS 22-B)
P.O. Box 4025
Sacramento, CA 95812-4025
www.calrecycle.ca.gov/Publications/
1-800-RECYCLE (California only) or (916) 341-6300

Publication # DRRR-2014-1502

To conserve resources and reduce waste, CalRecycle reports are produced in electronic format only. If printing copies of this document, please consider use of recycled paper containing 100 percent postconsumer fiber and, where possible, please print images on both sides of the paper.

Prepared as part of contract number DRRR10020 / $1,874,328.

The California Department of Resources Recycling and Recovery (CalRecycle) does not discriminate on the basis of disability in access to its programs. CalRecycle publications are available in accessible formats upon request by calling the Public Affairs Office at (916) 341-6300. Persons with hearing impairments can reach CalRecycle through the California Relay Service, 1-800-735-2929.

Disclaimer: This report was produced under contract by Stanford University. The statements and conclusions contained in this report are those of the contractor and not necessarily those of the Department of Resources Recycling and Recovery (CalRecycle), its employees, or the State of California and should not be cited or quoted as official Department policy or direction.

The state makes no warranty, expressed or implied, and assumes no liability for the information contained in the succeeding text. Any mention of commercial products or processes shall not be construed as an endorsement of such products or processes.

Table of Contents

Acknowledgments

The following faculty, staff, and students contributed to this report:

Department of Civil and Environmental Engineering, Stanford University

Faculty: Craig S. Criddle (Professor, Principal Investigator), Sarah L. Billington (Associate Professor, Co-Principal Investigator), Michael Lepech (Assistant Professor)

Staff: Weimin Wu (Senior Research Engineer); Gary Hopkins (Senior Research Engineer), Julie Stevens (Administrative Associate)

Graduate Students: Allison Pieja, Margaret-Catherine Morse, Eric Sundstrom, Katherine Rostkowski, Andrew Pfluger, Cecily Ryan, Wil Srubar, Aaron Michel, Nathan Strong, Francis Meerberg, Wakuna Gallega, Jaewook Myung, Sabbie Miller

Department of Chemical Engineering, Stanford University

Faculty: Curtis W. Frank (Professor, Co-Principal Investigator)

Students: Qi Liao, Zachary Wright, Amy Tsui

Collaborations:

Department of Chemical Engineering, Michigan State University

Faculty: Ramani Narayan (Professor)

Students: Chad Lefeldt, Mohan Patil

Department of Chemical Engineering and Applied Chemistry, University of Toronto

Faculty: Elizabeth Edwards (Professor)

Staff: Alexander Yakunin, (Director, Center for Structural Proteomics)

Graduate Student: Mahbod Hajigsaema

Executive Summary

Currently, the State of California recycles about 5 percent of its plastic waste stream.[1] The reclaimed plastic is typically downcycled in a single cycle to lower-value products. The remaining 95 percent follows a linear path from fossil carbon feedstock to plastic products to disposal in landfills or release to natural systems. Plastics discarded to the environment often accumulate, filling landfills and littering land, lakes, and oceans. Society needs materials that are truly renewable, economical, and safe, with excellent in-use performance. Recognizing this need, the state's Department of Toxic Substances Control and Department of Resources Recycling and Recovery (CalRecycle) have supported research to develop enabling technologies and cradle-to-cradle life cycles for bioplastics and biocomposites.

This report focuses on use of biogas methane as a feedstock and on the development and analysis of cradle-to-cradle cycles for polyhydroxybutyrate (PHB), a biodegradable biopolymer in the polyhydroxyalkanoate (PHA) family, and for polylactic acid (PLA), the most common in commercial use today. At present, PHAs and PLA are recycled through carbon dioxide and photosynthesis. The cycle begins with fixation of carbon dioxide by cultivated crops. The harvested crops are processed to create feedstock for PHAs (sugars, fatty acids, oils) and for PLA (lactic acid). At end-of-life, bioproducts made from these bioplastics are designed to degrade back to carbon dioxide, creating a cycle. A problem with this cycle is its dependency upon the cultivation of crops, with the associated demands for energy, water, nutrients, and land, and its vulnerability to changes in the price of food crops and energy. These requirements can result in appreciable cost and environmental impact. A cheap and reliable waste feedstock is desirable.

A promising candidate feedstock is biogas, a mixture of methane (50 to 70 percent) and carbon dioxide (30 to 50 percent). Self-assembled methanogenic ("methane-generating") microbial communities generate biogas as they degrade organic matter in the absence of oxygen. These communities live inside the anaerobic digesters present at many waste treatment facilities. Within these reactors, oxygen is excluded, and methane, a poorly soluble molecule, bubbles out of liquid solution into the gas phase, where it is collected and either flared or burned for energy. Release of methane to the atmosphere must be avoided because it is a potent greenhouse gas approximately 21 times greater than carbon dioxide. If biogas is routed into a moist aerobic environment, communities of methanotrophic ("methane-eating") bacteria will naturally assemble. These microorganisms consume methane and can produce PHB. But not all methanotrophs can produce PHB. As demonstrated in this research, the capability to produce PHB appears to be restricted to the so-called Type II methanotrophs (class Alphaproteobacteria). These bacteria must compete for

methane, oxygen, and nutrients with Type I methanotrophic bacteria (class Gammaproteobacteria) that do not produce PHB. Consequently, stable production of PHB in methane-fed communities requires conditions favorable for the growth of Type II methanotrophs. This research also demonstrates that PHB-producing methanotrophs use PHB in a manner that differs from PHB-producing non-methanotrophs. Most bacteria use PHB as a source of both carbon and energy, but Type I methanotrophic bacteria appear to use PHB as an energy source only. This suggests that PHB-producing methanotrophs will be favored by "energy shortages" that favor rapid growth of those methanotrophs that have previously stored PHB. Tests with dispersed cells and biofilms confirmed that PHB-producing methanotrophs are favored when methane is delivered intermittently and at low levels and when forms of nitrogen are supplied that require significant energy expenditures for their uptake (ammonium or N_2 gas). PHB production is also favored at lower pH levels (4-5) and at low copper levels.

This research establishes that PHB-producing methanotrophic communities produce PHB of high molecular weight (~1 million daltons). This is an attractive property for many applications. On the other hand, PHB is also brittle, and its processing window (the temperature range between its melting point and thermal decomposition) is narrow. These limitations can potentially be overcome by fabricating copolymers with other acyl groups, such as 4-hydroxybutyrate, 3-hydroxyvalerate, and 3-hydroxyhexanoate. Additional research is needed to explore these possibilities.

Use of PHBV, a copolymer of PHB and poly-3-hydroxyvalerate (PHV), was investigated for fabrication of foams and biocomposites. The 3-hydroxybutyrate (HB) monomers of PHB confer stiffness, while 3-hydroxyvalerate (HV) monomers of PHV add flexibility. Biocomposites and foams were evaluated using this matrix and various additives and chemical treatments. Addition of oak wood flour (sawdust) increased stiffness. Silane- and maleic anhydride-treated composites improved mechanical properties and resistance to water uptake. Rapid quenching of PHBV foam with sodium bicarbonate achieved high cell density. Addition of silica nanoparticles stabilized foam cells, enabling production of lighter foams and more uniform bubbles. At end-of-life, these biocomposites and foams are biodegradable to methane under anaerobic conditions.

This work also gives insight into the stoichiometry of PHB production. Conversion yields for methane to PHB vary, depending upon the bacterial species and growth conditions, but a conversion yield of 0.49 g PHB/g methane appears realistic. This value can be used to estimate an upper bound for PHB production. The State of California has the highest potential for biogas production of any state in the United States, with the potential for production of 1.1 million tons of methane per year from wastewater, landfills, animal manure, and industrial, institutional, and commercial organic waste streams.[2] Assuming a conversion yield of 0.49 g PHB/g methane, with which 75 percent is used for bioplastic and

25 percent for energy, approximately 400,000 tons of PHB could theoretically be produced per year. The current price of sugar-derived PHB is $4,000 to $5,000 per ton, suggesting the possibility of significant revenues. Use of biogas for PHB production has the potential to decrease PHB cost from more than $4 per kilogram to levels competitive with PLA and petrochemical-based plastics, at approximately $2 per kilogram. These costs are sensitive to scale, with costs at larger facilities dominated by the cost of energy and costs at smaller facilities dominated by labor costs. Estimates of cost and environmental impacts are also sensitive to assumptions regarding PHB separation and purification. Further analyses and technology development are needed to address these issues.

Other significant findings from this work relate to the potential for molecular-scale recycling of PLA through enzymatic and thermal degradation. Several microbial genes for novel PLA depolymerases are identified and expressed. These results are important because PLA is persistent in seawater and in compost and, as shown in this work, degrades slowly under anaerobic conditions. The discovery of microbial genes that encode PLA depolymerase activity suggests that PLA depolymerization can be enhanced in environments where it currently persists. Again, further technology development is needed to investigate and exploit these opportunities. Finally, this work establishes that PLA is readily depolymerized to lactide under a vacuum at relatively low temperature (190^{o} to 200^{o} C) with a tin (II) catalyst. This suggests that recovery of lactide from recycled PLA is technically feasible. Recycling through the lactide monomer followed by repolymerization would yield PLA with properties like those of the parent material, thus avoiding downcycling. Such a process could potentially be deployed in the near term at a significant scale.

1. Introduction

Currently, the vast majority of synthetic organic materials are produced from fossil carbon using processes that are unsustainable and not based on principles of green chemistry. Including both the material and energy inputs used to make plastics, conventional plastics consume nearly 10 percent of the oil and gas produced and imported in the United States.[1] This market is expected to grow at a rate of 15 percent per year.[2] But petroleum resources are increasingly difficult to access, are often located in politically volatile regions, and their use for production of plastics can result in significant greenhouse gas emissions (1.5 to >3 kg CO_2 eq/kg resin produced[2]). The products themselves may contain toxic additives or contaminants acquired in use and are often persistent, so end-of-service disposal can be problematic, especially in urban environments where landfill space is limited[3] (landfills contain about 20 percent plastic by volume) and incineration would release dioxins and other pollutants.[4,5] Persistence also leads

to unintended consequences during production and use, including release of harmful chemicals into food, water, and air, and littering of vast regions of the ocean with plastic debris.[6,7] Even when recycled, traditional polymers and conventional recycling methods do not provide a sustainable path. Five of the "big six" polymers (high- and low-density polyethylene, polyvinyl chloride, polystyrene, and polypropylene) can be reclaimed when properly collected and separated, but are typically downcycled in a single cycle to lower-value products. Society needs materials with excellent in-use performance that are renewable over shorter time periods (**Figure 1.1**) and can be managed in sustainable systems. While many polymers are biodegradable (**Table 1.1**), materials are needed that are recyclable over time scales short enough to avoid accumulation in the environment and the potential for adverse impacts on ecosystem health.

Figure 1.1: Time scales for fossil carbon plastics compared to renewable bio-based materials

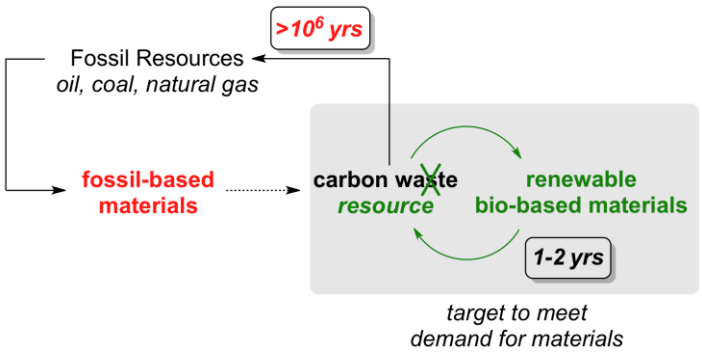

Table 1.1: Classification of biodegradable polymers

"New" carbon biomass			Fossil carbon	
Recovered plant polymers	**Recovered feedstock**	**Microbial polymerization**	**Extracted feedstock**	**Microbial polymerization**
polysaccharides	simple sugars	PHAs	natural gas methane	PHB
fats	purified oils	PHAs		**Chemical polymerization**
polysaccharides, fats, proteins	volatile fatty acids	PHAs	Components of crude oil	polycaprolactones
	biogas methane	PHB	Components of crude oil	polyesteramides
		Chemical polymerization	Components of crude oil	aliphatic copolyesters
polysaccharides	lactic acid, lactide	PLA	Components of crude oil	aromatic copolyesters
recovered plant polymers				

Pure poly (3-hydroxybutyrate) PHB is a biodegradable and biocompatible biopolyester within the broad family of polyhydroxyalkanoates (PHAs). Under growth-limiting conditions, many microorganisms produce PHAs as intracellular storage granules made of one or more PHA polymers.[8,9] PHA polymers consist of long polyester chains containing 100 to 30,000 repeated monomer units. More than 100 such monomer units have been identified.[10] This structure confers thermoplastic properties needed for molding and extrusion, making PHAs suitable replacement options for synthetic plastics in many applications.[11,12] Details of the properties of specific PHAs are well documented.[3,6,8,13] Different

microorganisms can produce different types of PHA, and the nature of the carbon feedstock affects the type of PHA produced.[3, 8,13] PHA resins degrade rapidly compared to most oil-based resins in soil, sludge, and seawater[16] with aerobic mineralization to carbon dioxide and anaerobic biodegradation to biogas. As shown in this work, both PHAs and biocomposites containing PHA rapidly degrade to biogas in anaerobic environments.[17, 18]

The market for PHAs has expanded from initial applications in packaging[19] (Griffin, 1994) to industrial and agricultural applications[20] to medical applications, where they are now marketed at low volume and high price as premium biocompatible bioplastics.[21] Further expansion of the market is limited by production cost.[3,8] Major factors affecting production cost are the use of cultivated feedstock, such as corn and sugar cane, and the associated water, chemicals, and energy required for growth, harvesting, and transport. Other costs include the energy and resources required to produce and purify the feedstock (typically glucose), as well as the energy and chemical costs of PHA synthesis, extraction, and purification.[21,22] According to one report, the cost of cultivated PHA feedstock accounts for 40 to 50 percent of total production costs.[23] The volatile and increasing price of crude oil[24, 25] and increasing awareness of the adverse environmental impacts of petrochemical-based plastics have revitalized research in PHA production.[21]

The potential use of organic waste as a feedstock opens the door to new methods of production that do not rely upon cultivated feedstock and imported energy. **Figure 1.2** illustrates a cradle-to-cradle cycle that is explored in detail in this report. The cycle begins with anaerobic digestion of organic waste streams. Anaerobic microbial communities that are naturally present in anaerobic digesters cleave the carbon-carbon and ester bonds of biopolymers present in a wide range of organic waste streams (such as carbohydrates, fats, proteins, and PHB) and funnel the carbon and electrons into single carbon compounds, carbon dioxide, and methane. The methane produced is poorly soluble and readily exits the aqueous phase, concentrating in the gas phase at concentrations of 50 to 70 percent methane by volume. Through these naturally occurring processes, a complex input of organic waste is efficiently converted into a biogas—a concentrated, nearly pure carbon feedstock that is also an energy-rich substrate for polymer production.

Biogas methane can be converted aerobically into PHB by some species of methanotrophic bacteria. Bacteria grown under “balanced” growth conditions, i.e., with sufficient carbon, nitrogen, and nutrients for cell replication, are induced for production of PHB by incubation under unbalanced growth conditions, where one or more nutrients limits cell replication, triggering storage of biopolymer as intracellular granules.[26] After extraction of the granules from the cell and PHB purification, the resulting resin may be used as is, mixed with other biopolymers to create blends, or combined with plant fibers to create biocomposites. Bioplastic products, such as toys, insulating foams, and shampoo bottles, can be

made by injection and blow molding. Biocomposites, such as pallets or furniture elements, can be made by injection molding and hot pressing. These bioproducts can incorporate inexpensive and biodegradable natural fibers for added tensile strength, improving properties for high-strength applications without compromising biodegradability. At end of life, they can ideally be recycled or collected and returned to a controlled anaerobic environment, such as an anaerobic digestion facility, for efficient biogas recovery. In such environments, waste products containing PHB are degraded back to methane, creating a cradle-to-cradle cycle.

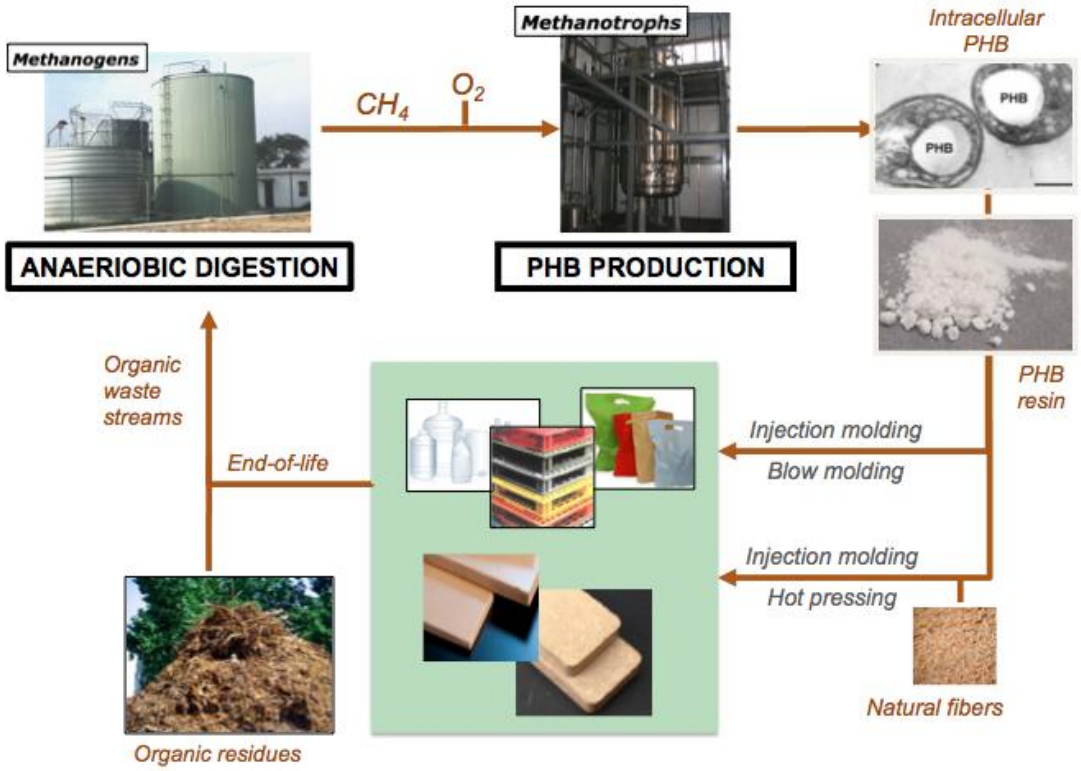

Figure 1.2: Cycle for production and degradation of poly (3-hydroxybutyrate) (PHB) via methane

This cycle of methane to PHB and PHB to methane can be used as the platform for a wider range of applications, with single carbon (C1) compounds CH_4 and CO_2 serving as feedstock and final degradation products. **Figure 1.3** illustrates the range of processes evaluated in this study. In addition to recycling and anaerobic degradation, the ester linkages in PHB can be cleaved chemically or enzymatically, releasing hydroxybutyrate. Aerobic, heterotrophic bacteria can use this monomer to reassemble virgin PHB. PHB can also be degraded thermally or hydrolytically to crotonic acid, a feedstock for polycrotonic acid, a class of polymers that are functionally similar to polyacrylates such as Plexiglas. These

polymers are known for their resistance to breakage, high melting point, and transparency, but end-of-life options will require additional research.

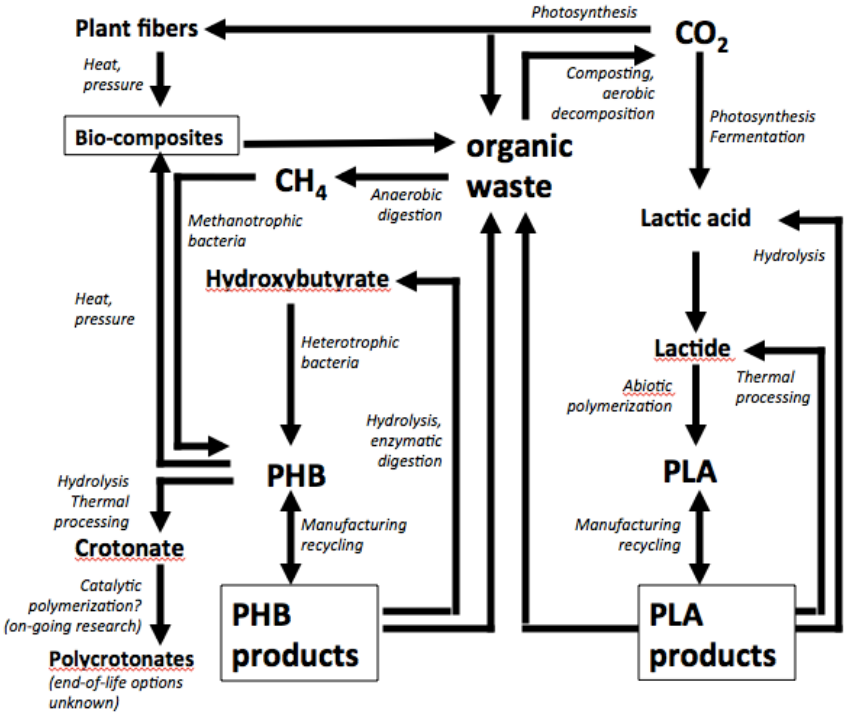

Figure 1.3: Cycles for production and degradation of PHB, PLA, and other high-value polymers

As shown in **Figure 1.3,** the suite of technologies for carbon cycling during production and consumption of PHB are complemented by a set of technologies useful for processing of the commercially established polymer polylactic acid (PLA). In aerobic environments, such as compost, PLA is recycled via carbon dioxide. The carbon dioxide is captured through photosynthesis as sugar. The sugar is fermented to lactic acid, and the lactic acid is dehydrated to lactide. Catalytic polymerization of lactide yields PLA. The PLA can be hydrolyzed to lactic acid and recycled. In this work, two additional PLA depolymerization routes are investigated: enzymatic digestion and thermal depolymerization. Enzymatic digestion may facilitate recycling through lactate. Thermal processing under vacuum depolymerizes PLA to lactide, which can be repolymerized to PLA.

Report overview

Chapters 2, 3, 4, and 5 of this report concern conversion of methane by methanotrophic (methane-oxidizing) bacteria to intracellular PHB. Existing literature on these bacteria fails to adequately describe which methanotrophic bacteria produce PHB and which do not.

Chapter 2 provides evidence that this capacity is limited to methanotrophs that assimilate carbon via the serine pathway, a metabolic mechanism to convert methane into PHB. In the literature, these bacteria are referred to as Type II methanotrophs. This result is used as the basis for an evaluation of conditions that favor growth of PHB-producing Type II methanotrophs over other methanotrophs.

In **Chapter 3**, the kinetics (rates of chemical reactions) and stoichiometry (types and amounts of matter used and produced during chemical reactions) of growth and PHB production for two model Type II methanotrophs are evaluated. Significant stoichiometric differences are observed for pure cultures of *Methylosinus trichosporium* OB3b and *Methylocystis parvus* OBBP grown under varying conditions. The results underscore the impact of microbial physiology and growth conditions on polymer yields.

Chapter 4 describes two studies of *Methylocystis parvus* OBBP. In the first study, a novel system is described for high-throughput screening of growth rates and PHB production across numerous strains and growth conditions. This technology is used to conduct an optimization of PHB production, with manipulation of nutrient concentrations in the growth medium resulting in a fivefold increase in total PHB production. In the second study, PHB-rich cultures of *M. parvus* OBBP are analyzed under varying conditions to determine under what circumstances PHB is consumed and for what metabolic purpose. PHB was consumed only in the presence of methane, with consumption inhibited by addition of formate. This is evidence that methanotrophs use PHB as a source of reducing equivalents (fuel for reductive reactions) and not used as a sole growth substrate (as previously assumed).

Chapter 5 focuses on medium- to long-term operation of methanotrophic bioreactors containing mixed or enrichment cultures. Conditions are evaluated for selection against methanotrophs that do not produce PHB and in favor of Type II methanotrophs that do produce PHB. These conditions are then implemented to enable PHB production in mixed culture methanotrophic communities without the need to operate under aseptic conditions. This is a departure from strategies based upon use of pure cultures and genetic engineering methods, and requires control over community ecology through reactor operating conditions. Use of a fluidized bed reactor is examined as an alternative to conventional completely mixed fermentation. The use of PHB as a source of reducing equivalents is harnessed to create a cyclic regime that is favorable for PHB production. This regime is combined with Type II selective conditions and the effectiveness of the combined cycle tested over time.

Methods for PHB extraction are evaluated in **Chapter 6**. A combination of surfactant-induced lysis followed by hypochlorite oxidation is used to extract polymer efficiently without use of added solvents. The molecular weight of methanotrophic PHB is found to exceed $1x10^6$ Da.

Chapter 7 describes PHA characterization for use in biocomposite materials and foams.

Options for end-of-life are evaluated in **Chapters 8, 9, and 10**.

Chapter 8 describes anaerobic biodegradation of PHB, polylactic acid (PLA), and PHBV-biocomposites. PHB and PHBV-biocomposites are found to be readily biodegradable under anaerobic conditions, but PLA degrades slowly. **Chapter 9** provides data on base-catalyzed hydrolysis of PHB to hydroxybutyrate and crotonate, and on microbial polymerization of hydroxybutyrate (HB) to PHB. An enrichment of aerobic heterotrophic microorganisms is shown to recycle HB back to PHB. **Chapter 10** describes the potential for enzyme-mediated hydrolysis of PLA and for low-temperature thermal depolymerization to lactide. Several microbial genes for novel PLA depolymerases are identified and expressed. These results are important because PLA is persistent in seawater, in compost and, as shown in this work, degrades slowly under anaerobic conditions. The finding that PLA is readily depolymerized to lactide under a vacuum at relatively low temperature (190^{o} to 200^{o} C) with a tin (II) catalyst is also significant. The process appears to be functional even in the presence of significant additive, suggesting that recovery of lactide from recycled PLA is technically feasible.

Chapter 11 provides a life cycle analysis for production of PHB and for PHA biocomposites. The major adverse impacts due to PHB production from biogas methane are energy inputs for aeration and chemical inputs during recovery. Adverse energy impacts could be mitigated by routing 18 percent to 26 percent of the biogas methane to energy and the remainder to PHB production. Such a strategy would eliminate the need for grid-sourced electricity and its associated environmental impacts.

Chapter 12 provides an economic analysis of PHB production from biogas methane. The analysis shows that methane in biogas or natural gas can be a cost-effective feedstock for PHB production, and could economically displace glucose or other cultivated feedstock. The analysis also shows that, in general, the value of PHB produced from a unit of methane exceeds the value of electricity generated from a unit mass of methane. The cost of PHB production with biogas is shown to be attractive at facilities producing more than 5,000 tonnes PHB per year. Costs of PHB production at this scale could compete with PLA- and petroleum-based plastic resins. At a small scale, labor costs are critical. Such costs might be reduced with effective labor management and training of the existing staff. At a large scale, energy efficiency becomes critical. At all scales of operation, chemical costs, especially for extraction and purification of PHB, are important. Some chemicals may be recycled. The PHB conversion yield has a large impact on production costs. Selection of high performing cultures and maintenance of cultures that can produce high levels of PHB are critical. The efficiency of PHB recovery in the extraction process also has a significant impact on production costs; thus, advances in extraction technology are needed. Pilot- and full-scale studies are critically needed to

assess the stoichiometry and kinetics of PHB production at a realistic scale and to accurately assess capital and operational costs.

Chapter 13 summarizes the major outputs from this research, including major findings, peer-reviewed publications, patent filings, and the formation of a start-up company led by former doctoral students who worked on this research.

2. Screening of Methanotrophic Bacteria for Polyhydroxybutyrate (PHB) Production

2.1 Executive summary

Methanotrophic bacteria are known to produce the biodegradable biopolymer poly-3-hydroxybutyrate (PHB), but there has been conflicting evidence in the literature as to which strains produce PHB. Understanding which methanotrophs produce PHB is crucial to the development of strategies that select for PHB production from methane feedstock. A variety of pure culture strains were screened for the *phaC*, a gene that encodes PHB synthase (a key enzyme required for PHB production) and enables PHB under nutrient-limited conditions. This analysis was complemented by a literature review and an analysis of key metabolic pathways. The combined evidence indicates that Type II methanotrophs produce PHB while other methanotrophs do not. This finding corrects a significant misconception in the literature.

Conditions allowing selective growth of Type II methanotrophs were investigated to determine which conditions reliably favor PHB-producing microorganisms in enrichment culture. Four conditions selected for PHB production from an activated sludge inoculum with PHB constituting up to 46 percent by dry cell weight. These selective conditions include low pH, low copper, dilute medium (all constituents added at 10 percent of the standard media), and nitrogen-fixing conditions.

Key publication:

Pieja, A.J., K.H. Rostkowski, and C.S. Criddle, 2011. Distribution and selection of poly-3-hydroxybutyrate production capacity in methanotrophic proteobacteria. Microbial Ecology 62:564-573. [3]

2.2 Motivation

Wild-type methanotrophic bacteria produce PHB when supplied with methane under nutrient-limited conditions, raising the possibility of cultivation in open systems without the need for aseptic cultivation techniques (e.g., media sterilization). Cultivation of methanotrophic PHB-producing communities under such conditions would decrease capital and operating costs by eliminating the need for media sterilization. With the proper selection conditions, such systems could potentially select for enhanced PHB production. To achieve these results, however, it is critical to understand the distribution of PHB production across methanotrophic genera. This knowledge would allow conditions to be tailored to

exclude organisms that do not produce PHB and to enhance the growth of those that do.

2.3 Classification of methanotrophs

Methanotrophic bacteria comprise a diverse group of organisms united by the capacity to use methane as a sole carbon and energy source. This diversity is broadly divided into three major groups: the Gamaproteobacteria methanotrophs (Type I and Type X), Alphaproteobacteria (Type II) methanotrophs, and methanotrophs in the recently discovered phylum Verrucomicrobia. The Verrucomicrobia are extremophiles (pH 2-2.5, T=60°C) and are not reported to produce PHB. Accordingly, the focus of this study was the capacity for PHB production among the methanotrophic Gamaproteobacteria (Type I and Type X) and Alphaproteobacteria (Type II). **Table 2.1** summarizes the most important differences between these groups with regard to biotechnological applications. The critical difference is the carbon uptake mechanism: Type I and Type X methanotrophs assimilate carbon via the RuMP pathway; Type II methanotrophs exclusively assimilate carbon via the serine cycle. Nearly all methanotrophs use the particulate methane monooxygenase (pMMO) enzyme to oxidize methane to methanol (the sole exception appears to be *Methylocella)*, but Type II methanotrophs can also use a soluble methane monooxygenase (sMMO). This enzyme is less specific for methane and results in slower growth, but, unlike pMMO, does not require copper and therefore allows growth under copper-limiting conditions. Another important metabolic difference is that both Type II and Type X methanotrophs possess the ability to fix atmospheric N_2 (convert N_2 into the amino acids for microbial growth and reproduction); but this ability is limited to a subset of Type I methanotrophs.

Understanding these differences is important to determining the distribution of PHB production in methanotrophic bacteria and understanding the implications of this distribution. PHB production has been reported for all methanotroph types, but further investigation of the primary data in these reports reveals that PHB production has only been experimentally confirmed for Type II strains. Citations identifying PHB production in Type I organisms have relied upon either unconfirmed visual evidence or use of Type II organisms that were mischaracterized as Type I methanotrophs (Table 2.1). Therefore, further analysis is required to determine the true distribution of PHB production in methanotrophs.

2.4 Physiology of PHB production

The metabolic relationships between methane oxidation, carbon assimilation, PHB production, and energy production are well characterized in serine cycle organisms. These pathways as currently understood are illustrated in **Figure 2.1.**

Methane is oxidized to methanol by methane monooxygenases (MMO) and then further oxidized to formaldehyde. Single-carbon formaldehyde is bound with the 2-carbon compound glycine to form serine in the critical carbon uptake reaction. Glycine used in this process is regenerated via the intermediate malyl-CoA, which can also be cleaved to form acetyl-CoA. Acetyl-CoA is used to regenerate glycine and also serves as the primary input to the catabolic and anabolic pathways of the TCA cycle. Acetyl-CoA is easily polymerized and stored as PHB and can be rapidly produced from stored PHB through depolymerization.

Table 2.1: Key differences between methanotrophic alphaproteobacteria (Type II) and gammaproteobacteria (Types I and X)

Characteristic	Type I Methanotrophs	Type X Methanotrophs	Type II Methanotrophs
Phylogenetic group	*Gammaproteobacteria*	*Gammaproteobacteria*	*Alphaproteobacteria*
Included genera	*Methylosphaera* *Methylobacter* *Methylomicrobium* *Methylomonas*	*Methylococcus* *Methylocaldum*	*Methylosinus* *Methylocystis* *Methylocapsa* *Methylocella*
Carbon assimilation pathway	RuMP cycle	Mixed	Serine cycle
PHB production cited in literature	Yes	Yes	Yes (confirmed in this study)
PHB production verified experimentally	No	No	Yes
Soluble methane monooxygenase	No	No	Yes
Particulate methane monooxygenase	Yes	Yes	Genus specific
Nitrogen fixation	Some	Yes	Yes

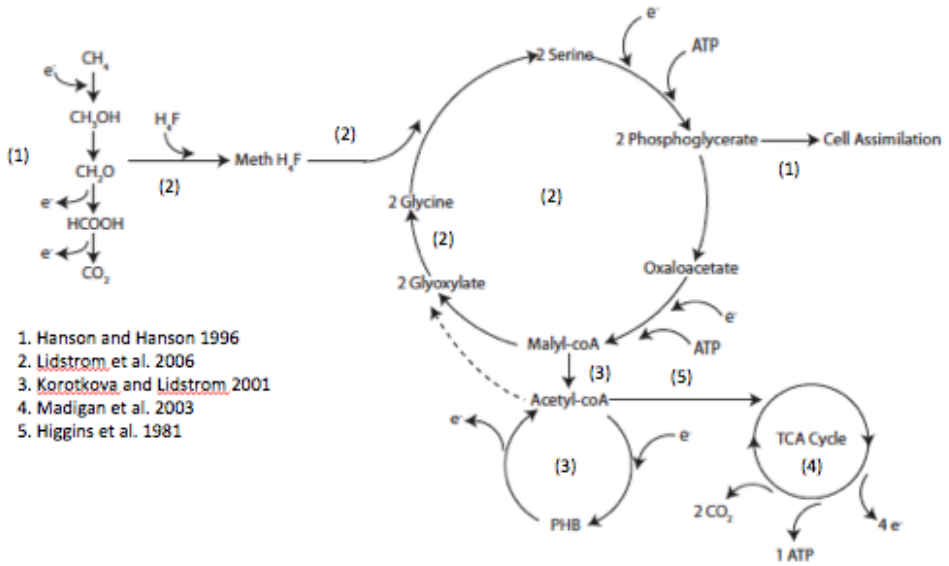

Figure 2.1: Pathways for metabolism of PHB in serine-cycle methanotrophic bacteria. Complete citations for the references supporting this pathway reconstruction are available in reference 27 of the Literature Cited.

2.5 Screening methanotrophs for PHB production

Screening of pure culture methanotrophs was conducted to determine whether methanotrophic PHB production is limited to Type II methanotrophs. Twelve strains from six genera were grown to exponential phase and transferred to nitrogen-free media to test for PHB production. All Type I strains tested negative for PHB production while all Type II strains tested positive for PHB production (**Table 2.2**). Extracted DNA from the same strains was tested by polymerase chain reaction (PCR) for the presence of the *pha*C gene product, a component of the PHA synthase that assembles PHB from acetyl CoA. All Type II strains tested positive for the *pha*C, while no Type I or Type X strain possessed that gene. When coupled with the lack of prior experimental evidence demonstrating PHB production in Type I organisms and the lack of a proposed mechanism for PHB production via the RuMP cycle, it appears that PHB production in wild-type methanotrophs is limited to Type II methanotrophs, and perhaps some Type X methanotrophs that have elements of the serine cycle. This finding clarifies the subset of organisms that should be considered as candidates for methanotrophic PHB production.

Table 2.2: Screening results for PHB production and presence of the *pha*C gene in 12 pure culture methanotrophic strains

Strain	Type	Carbon assimilation pathway	%PHB±std. dev.[a]	Presence/absence (+/−) of *pha*C
Methylocaldum O11a	I	RuMP	0±0	−
Methylomicrobium album BG8	I	RuMP	0 (range=0)	−
Methylomonas LW13	I	RuMP	0±0	−
Methylococcus capsulatus str. Bath	X(I)	RuMP	0 (range=0)	−
Methylocapsa acidiphila	II	Serine	n/a[b]	+
Methylocystis 42/22	II	Serine	25±7	+
Methylocystis hirsuta CSC1	II	Serine	7±2	+
Methylocystis parvus OBBP	II	Serine	36±8	+
Methylocystis rosea SV99	II	Serine	9±1	+
Methylocystis SC2	II	Serine	30±13	+
Methylocystis strain M	II	Serine	14[a] (range: 7–21)	+
Methylosinus sp. LW4	II	Serine	10±2	+
Methylosinus sporium	II	Serine	9	+
Methylosinus trichosporium OB3b	II	Serine	38±4	+

[a] Range is reported for duplicates; standard deviation for triplicates

[b] Not available; culture did not grow to sufficient density

2.6 Conditions selective for Type II methanotrophs

Given that PHB production appears to be largely or exclusively limited to Type II methanotrophs, maintaining conditions selective for them is essential to maintaining PHB production in enrichment cultures. Invasion of a PHB-producing culture by Type I methanotrophs would prevent PHB production. The concept of selective conditions for PHB-producing methanotrophs was evaluated by enrichment of methanotrophs from a wastewater biosolids inoculum under conditions expected to select for Type II methanotrophs. Conditions tested were based on previous research and reported characteristics of Type II methanotrophs. Results are summarized in **Table 2.3.**

Table 2.3: Detected genera and PHB production in methanotrophic cultures enriched from activated sludge under varying conditions. PHB production was detected in some communities where Type II methanotrophs were not detected. It is possible that Type II methanotrophs were present at levels too low to detect or that non-methanotrophic members of the community produced PHB.

Variable	Modification of growth medium	%PHB	Type I genera detected*	Type II genera detected*
Concentrations of trace Cu and mineral salts	[Cu]=5 μM, mineral salts=100%	1, 0		*Methylomicrobium*(+,−)
	[Cu]=5 μM, mineral salts=10%	25, 0	*Methylomonas/Methylobacter* (+,−), *Methylomicrobium* (+)	*Methylocystis/Methylosinus*(+)
	[Cu]=0 μM, mineral salts=100%	0, 0, 0	*Methylomicrobium, Methylocaldum/ Methylococcus, Methylobacter*	*Methylocystis/Methylosinus*
	[Cu]=0 μM, mineral salts=10%	7, 15, 17		*Methylocystis/Methylosinus*
Nitrogen source	Nitrate	2, 2, 3	*Methylobacter, Methylomicrobium*	
	N_2	43, 43, 46	*Methylocaldum/Methylococcus*	*Methylosinus trichosporium, Methylocystis/Methylosinus, Methylosinus*
pH and added carbonate	pH 4, added carbonate=1 mM	4, 11, 12		*Methylocystis/Methylosinus*
	pH 5, added carbonate=1 mM	14, 0, 0	*Methylobacter*(+), *Methylomonas*(+,−)	*Methylocystis/Methylosinus*(+)
	pH 6, added carbonate=1 mM	0, 0, 0	*Methylomonas*	
	pH 7, added carbonate=1 mM	0, 0, 0	*Methylomonas, Methylobacter*	
	pH 8, added carbonate=10 mM	0, 0, 0	*Methylomonas, Methylobacter*	
	pH 4, added carbonate=10 mM	0, 0, 0	*Methylomonas*	
	pH 5, added carbonate=10 mM	4, 6		*Methylocystis/Methylosinus*
	pH 6, added carbonate=10 mM	0, 0, 0	*Methylomonas*	
	pH 7, added carbonate=10 mM	0, 0, 0	*Methylomonas*	*Methylocystis/Methylosinus*
	pH 8, added carbonate=10 mM	0, 0, 0	*Methylomonas*	

Unless otherwise indicated, medium was prepared at pH 7 with 10 mM nitrate and 5 μM Cu. Phylogenetic analyses were based on T-RFLP analysis of *pmo*A. A slash sign'/'indicates that the indicated genera were not distinguished by T-RFLP. When both PHB-positive and PHB-negative enrichments were present, the symbol in parentheses indicates whether the indicated genus was present in PHB-positive (+) or negative (−) enrichments

Growth with low copper, pH 4-5, dilute medium (standard media diluted by a factor of ten) and growth under nitrogen-fixation conditions selected for PHB production. Growth in mesophilic (30° to 35° C) conditions in a medium of nitrate and mineral salts selected for Type I methanotrophs lacking the capacity for PHB production. Imposition of selection conditions favoring Type II PHB-producing methanotrophs is thus critical to PHB production in enrichment cultures. High concentrations of PHB are achievable in enrichment culture under selective conditions. PHB production of up to 46 percent was observed in enrichments grown with nitrogen gas as the sole nitrogen source.

2.7 Ammonium-based selection

The conditions listed in **Table 2.3** were effective selectors and demonstrate the importance of selective conditions for PHB production in enrichment culture. However, these conditions are difficult to implement at scale due to negative impacts on growth rates and final culture density. Copper limitation limits growth rates, likely due to reliance upon the slower sMMO enzyme. Dilute media limits final culture density due to the absence of sufficient nitrogen. Low pH results in slower growth rates for all organisms. Nitrogen fixation requires additional energy inputs. In Chapter 5, growth with ammonium as the sole nitrogen source is evaluated and found to select for PHB-producing methanotrophs in enrichment culture. This selection is maintained over repeated cycles of PHB production and consumption without seriously compromising growth rates or densities.

2.8 Key findings

The results of this work are significant because they establish that PHB production capabilities are likely limited to Type II methanotrophs and that environmental conditions can be manipulated to select for PHB production. Specific conclusions include the following:

1. PHB production is likely limited to Type II methanotrophs.
2. All Type II methanotrophs tested were capable of PHB production.
3. Type I strains outcompete Type II strains under standard growth conditions.
4. Type II-selective conditions can be applied to achieve PHB production in open mixed culture communities.
5. Conditions favoring PHB production included:
    a. Low copper

b. Dilute medium

c. Low pH

d. Nitrogen fixation

6. PHB production of up to 46 percent by cell weight can be achieved in methanotrophic enrichments inoculated with activated sludge and grown under selective conditions.

3. Growth Stoichiometry and Kinetics of PHB Production in Type II Methanotroph Pure Cultures: *Methylocystis parvus* OBBP and *Methylosinus trichosporium* OB3b

3.1 Executive summary

Understanding the stoichiometry and kinetics of methanotrophic PHB production is necessary to assess process environmental and economic impacts (Chapters 11 and 12). The quantity of methane consumed per unit of PHB produced is of particular importance. This value can be heavily influenced by strain selection and growth conditions. An understanding of the effects of these variables is therefore required to develop an accurate stoichiometric model and to predict volumetric PHB production rates. Modeling methane utilization is complicated by the initial step in methane oxidation – attack to methane monooxygenase – a reaction in which both oxygen and reducing equivalents are required reactants. Modeling of this step was accomplished using well-established reaction stoichiometry for methane monooxygenase (one mole of methane per mole of O_2), where the reducing equivalents required for the initial oxidative attack are generated by methane oxidation.

In this chapter, stoichiometric and kinetic factors are modeled and analyzed in two pure culture Type II methanotrophs: *Methylocystis parvus* OBBP and *Methylosinus trichosporium* OB3b. Kinetic and stoichiometric parameters are obtained for three nitrogen sources: nitrate, ammonium, and nitrogen gas, and for a variety of headspace gas concentrations (methane and oxygen). In both strains, the highest cellular yields of approximately 1g of volatile suspended solids (VSS) produced/g methane consumed were measured during growth on ammonium with high oxygen concentrations. Strain OB3b produced the most PHB (29% by dry weight) during growth on nitrate, while strain OBBP produced more during growth on ammonium. Analysis of growth under these conditions reveals a requirement of 4.77 g methane/g PHB produced in strain OB3b and 2.05 g methane/g PHB produced in strain OBBP. The value for OBBP is significantly better than the value of 5.3 g methane/g PHB used for the life cycle assessment in Chapter 11 and demonstrates the value of optimizing strains and growth conditions.

Key publication:

Rostkowski, K., A. Pfluger, and C. Criddle. 2013. Stoichiometry and kinetics of the PHB-producing Type II methanotrophs Methylosinus trichosporium OB3b and Methylocystis parvus OBBP. Bioresour. Technol. 132:71-77.[4]

3.2 Stoichiometry of methanotrophic growth

In order for methanotrophic bacteria to grow on methane, they must first activate methane by partially oxidizing it to methanol. This energy-intensive step is mediated by methane monooxygenase (MMO) enzymes and requires both oxygen and electrons as reactants. The methanol produced is a source of reducing equivalents for energy generation and carbon for cell synthesis. **Figure 3.1** illustrates the model used in this study to calculate stoichiometric parameters for methanotrophic bacteria. The model accounts for methane and oxygen required to produce methanol and partitions the methanol produced from a quarter mole of methane into a fraction for energy f_e and a fraction for synthesis f_s of biomass.

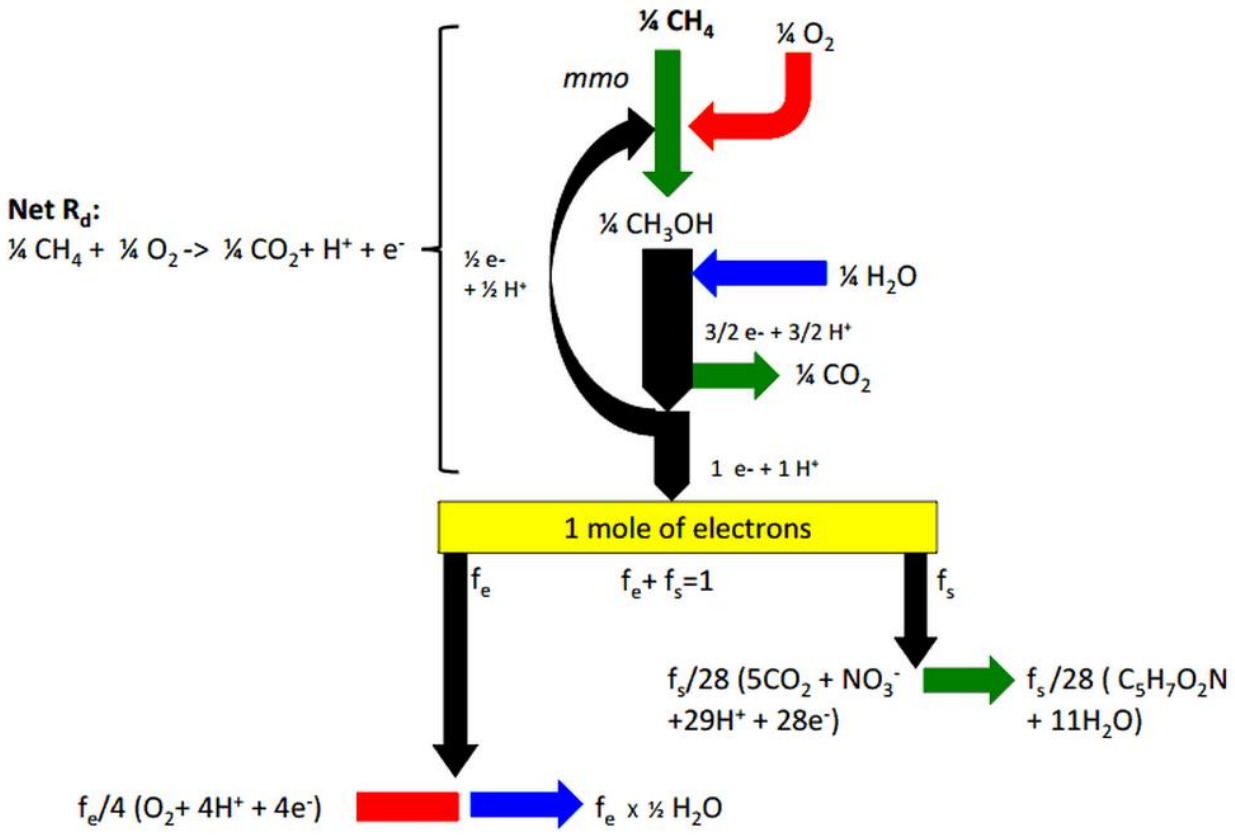

Figure 3.1: Stoichiometry of methanotrophic growth including initial inputs for methane oxidation. The example shown is for nitrate as the nitrogen source.

The stoichiometry illustrated in Figure 3.1 is for balanced growth on methane with nitrate as the N source. The complete reaction is given by $R_d + f_e R_a + f_s R_c$, where $f_s + f_e = 1$, and:

R_d: ¼ CH_4 + ¼ O_2 = ¼ CO_2 + H^+ + e^-

$f_e R_a$: f_e [¼ (O_2+4H^++4e^-) = ½ H_2O]

$f_s R_c$: f_s [1/28 (5 CO_2 + NO_3^- + 29 H^+ + 28 e^-) = f_s 1/28 ($C_5H_7O_2N$ + 11 H_2O)]

The above stoichiometry applies for the period of cell growth when the assumed empirical formula for biomass is $C_5H_7O_2N$. The same approach can be applied to the PHB production phase, where the product is PHB, with the empirical formula $C_4H_6O_2$ and the relevant whole reaction is:

$CH_4 + (1 + f_e)\ O_2 = (1 - 8f_s/9)\ CO_2 + (2f_e + 4f_s/3)\ H_2O + (f_s/9)\ C_4H_6O_2$

In this case, f_e and f_s refer to the fraction of methane used for energy and PHB production during the unbalanced growth phase, when nitrogen is absent.

Other nitrogen sources were evaluated in the same manner. For ammonia, the balanced whole reaction is: $CH_4 + (1 + f_e)\ O_2 + (f_s/5)\ NH_3 = (1 - f_s)\ CO_2 + (2f_e + 8f_s/5)\ H_2O + (f_s/5)\ C_5H_7O_2N$

3.3 Experimental setup

To determine stoichiometric parameters (i.e., f_e and f_s for each growth phase) and kinetic parameters for Type II methanotrophs, growth and PHB production were determined for *Methylocystis parvus* OBBP and *Methylosinus trichosporium* OB3b. Batch growth studies were carried out in closed serum bottles with controlled atmospheres of methane, oxygen, and nitrogen gas. Production of PHB was induced in the exponential phase by centrifuging cells and resuspending them in a nitrogen-free medium. Gas concentrations were monitored, along with biomass concentrations and PHB production. **Figure 3.2** illustrates a time course for gas consumption and biomass production in closed serum bottles. Growth in both strains was tested at initial oxygen concentrations ranging from 0.10 to 0.40 atm, with three nitrogen sources: nitrate, ammonium, and nitrogen gas. Growth curves for balanced growth and unbalanced growth with PHB production were modeled to obtain best estimates for f_e and f_s.

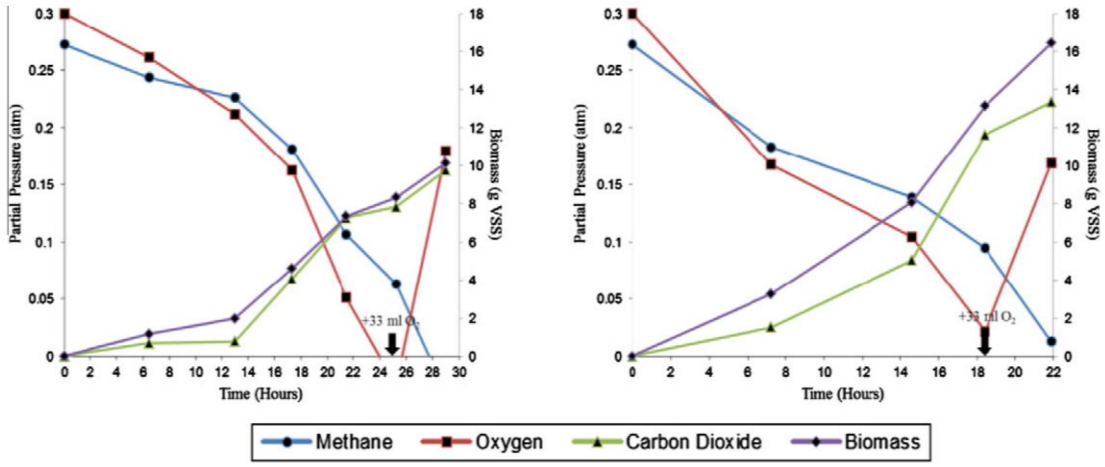

Figure 3.2: Methane consumption, oxygen consumption, carbon dioxide production, and biomass production as measured in *Methylocystis trichosporium* OB3b during growth with nitrate (left) and *Methylocystis parvus* OBBP during growth with ammonium (right)

3.4 Stoichiometric parameters

Table 3.1 summarizes stoichiometric parameters for varying oxygen concentrations and nitrogen sources. Biomass yields (Y_X, in units of biomass per unit mass of methane consumed) were most consistent for nitrate replicates in both strains, while values for ammonium and nitrogen gas replicates were highly variable. Y_X values for strain OB3b were on balance highest for nitrate replicates, while in strain OBBP, values were consistently higher for ammonium replicates. In both cases, maximum observed yield was approximately 1g VSS produced/g methane consumed. For strain OB3b, PHB production was consistently higher for cells grown on nitrate and N_2 gas; for strain OBBP, PHB production was higher for cells grown on ammonium. For strain OBBP, a maximum PHB production of 60 percent by dry cell weight was observed when cells were grown at 0.30atm oxygen. For strain OB3b, a maximum of 45 percent was observed during growth on N_2 gas; a value of 29 percent was observed during growth on nitrate at 0.30atm oxygen.

A key stoichiometric parameter for economic and environmental analyses is the total methane required per unit of PHB produced, including methane required for production of non-PHB biomass. The reciprocal of this value is the conversion yield: the grams of PHB produced per gram of methane. These values were calculated using stoichiometric parameters and final PHB production values at optimal experimental conditions. For strain OB3b grown with nitrate at 0.3atm oxygen, 4.77 grams of methane were required to produce one gram of PHB, a conversion yield of 0.21 g PHB/g methane. For strain OBBP grown with

ammonium at 0.3atm oxygen, only 2.05 grams of methane were required, representing a conversion yield of 0.49 g PHB/g methane. The value for OBBP is substantially lower than the assumption of 4.72 grams of methane per gram of PHB used to develop the life cycle analysis in Chapter 11. This suggests a significant potential for optimization of strains and growth conditions and underscores the importance of strain selection in process design and life cycle assessment.

Table 3.1: Substrate partitioning parameters (f_e, f_s), cellular yield (Y_X), and percent PHB production by cell dry weight for each strain as measured under varying oxygen partial pressure and nitrogen sources.

Strain	Oxygen partial pressure (atm)	f_e			f_s			Y_x (g VSS/g methane)			% PHB after nitrogen limitation[a] (cell dry weight)		
		Nitrate (NO_3^-)	Ammonium (NH_4^+)	Nitrogen gas (N_2)	Nitrate (NO_3^-)	Ammonium (NH_4^+)	Nitrogen gas (N_2)	Nitrate (NO_3^-)	Ammonium (NH_4^+)	Nitrogen gas (N_2)	Nitrate (NO_3^-)	Ammonium (NH_4^+)	Nitrogen gas (N_2)
OB3b	0.10	0.31	0.57	0.15	0.69	0.43	0.85	0.69	0.53	0.96	22	14	20
	0.15	0.34	0.59	0.64	0.66	0.41	0.36	0.66	0.51	0.41	22	13	28
	0.20	0.31	0.34	0.71	0.69	0.66	0.29	0.69	0.82	0.32	20	9	45
	0.30	0.38	0.50	N/A	0.62	0.50	N/A	0.63	0.61	N/A	29	12	N/A
	0.40	0.36	0.19	N/A	0.64	0.81	N/A	0.66	0.99	N/A	24	13	N/A
Av ± St Dv		0.34 ± 0.03	0.44 ± 0.17	N/A	0.66 ± 0.03	0.56 ± 0.17	N/A	0.66 ± 0.03	0.69 ± 0.21	N/A	24 ± 4	11 ± 4	29 ± 11
OBBP	0.10	0.41	0.39	N/A	0.59	0.61	N/A	0.59	0.75	N/A	19	50	N/A
	0.15	0.46	0.56	N/A	0.54	0.44	N/A	0.55	0.54	N/A	11	41	N/A
	0.20	0.48	0.44	N/A	0.52	0.56	N/A	0.53	0.69	N/A	8	37	N/A
	0.30	0.44	0.41	N/A	0.56	0.59	N/A	0.57	0.73	N/A	14	60	N/A
	0.40	0.47	0.15	N/A	0.53	0.85	N/A	0.53	1.05	N/A	6	42	N/A
Av ± St Dv		0.45 ± 0.03	0.39 ± 0.15	N/A	0.55 ± 0.03	0.61 ± 0.15	N/A	0.55 ± 0.03	0.75 ± 0.19	N/A	14 ± 8	46 ± 8	N/A

N/A: Not applicable because the cultures did not show significant growth.
[a] PHB production was induced by incubation with 1:1 methane:oxygen in the absence of nitrogen.

3.5 Kinetic parameters

Kinetic parameters measured in closed serum bottles are shown in **Table 3.2**. Growth rates generally mirrored yield values, with faster growth observed for OB3b during growth on nitrate and for OBBP during growth on ammonium. In general, maximum specific growth rates for the methanotrophic strains conform with values in the literature, with doubling times ranging from 2 to 11 hours. Specific growth rates were fairly consistent for the two strains. Differences in the growth rates were more due to variation in nitrogen sources than to variation in strains. As with stoichiometric parameters, strain selection is important, and the strain chosen must be paired with an optimal nitrogen source to ensure rapid growth.

Table 3.2: Microbial kinetic parameters, maximum specific growth rate (μ_{max}), and maximum specific rate of substrate utilization (q_{max}) of each strain as measured under varying oxygen partial pressure and nitrogen sources.

Strain	Oxygen partial pressure (atm)	μ_{max} (d^{-1})			q_{max} (mg methane/mg VSS d^{-1})		
		Nitrate (NO_3^-)	Ammonium (NH_4^+)	Nitrogen gas (N_2)	Nitrate (NO_3^-)	Ammonium (NH_4^+)	Nitrogen gas (N_2)
OB3b	0.10	5.94	3.11	5.83	8.57	5.86	6.08
	0.15	4.32	2.60	1.67	6.52	5.13	4.07
	0.20	4.99	7.18	1.50	7.22	8.81	4.66
	0.30	3.36	3.92	N/A	5.35	6.39	N/A
	0.40	4.96	6.06	N/A	7.67	6.11	N/A
Av ± St Dev		3.93 ± 2.10	4.57 ± 1.97	3.00 ± 2.45	7.07 ± 1.21	6.46 ± 1.39	4.94 ± 1.04
OBBP	0.10	2.92	4.21	N/A	4.93	5.63	N/A
	0.15	2.71	2.63	N/A	4.98	4.88	N/A
	0.20	2.28	4.25	N/A	4.31	6.16	N/A
	0.30	2.16	3.67	N/A	3.81	5.05	N/A
	0.40	5.55	5.94	N/A	3.07	5.67	N/A
Av ± St Dev		2.63 ± 0.40	4.14 ± 1.20	N/A	4.72 ± 0.67	5.48 ± 0.51	N/A

N/A: Not applicable because the cultures did not show significant growth.

3.6 Key findings

1. Methane oxidation and subsequent methanol oxidation and assimilation are best modeled as separate steps, with methane oxidation requiring inputs of both methane and oxygen.
2. Methane required for per unit of PHB produced is highly strain-specific and dependent on growth conditions, and these conductions were also strain dependent.
3. Depending on the strain and growth conditions, as little as two grams of methane may be required per gram of PHB produced. This is equivalent to a conversion yield of 0.5 g PHB/g methane.
4. Growth rates vary with yield and are highly dependent upon the nitrogen source. Highest biomass yields were obtained with nitrate as N source.
5. Total methane required per unit of PHB produced in *M. parvus* OBBP was far lower than the equivalent value for *M. trichosporium* OB3b, illustrating the effect of strain selection on process efficiency.

4. PHB Production in *Methylocystis parvus* OBBP

4.1 Executive summary

PHB production is heavily influenced by growth conditions, including nutrient concentrations, salinity, temperature, pH, gas composition, and the nature of the limiting nutrient (nitrogen, phosphorus, or trace nutrients) used to induce PHB production. Current culture techniques are insufficient for optimization of conditions due to the vast number of relevant variables and because the relative importance of these variables is largely unknown. To address this issue, a high throughput microplate growth system was developed and used to analyze growth rates and PHB production in *M. parvus* OBBP across hundreds of culture conditions. Through optimization, final PHB production was improved from 0.65g/L in the control condition to 3.43g/L in the optimized condition, demonstrating the effectiveness of the system and the importance of effectively optimizing growth conditions.

In addition to understanding the effect of growth conditions on PHB production, understanding the evolutionary basis behind PHB production is necessary for the development of conditions that select for increased production over time. While production of PHB can be understood as a carbon storage mechanism, it is the ultimate use of that PHB and not simply its production that defines its evolutionary purpose. Consumption of PHB in *M. parvus* OBBP under variable conditions was therefore analyzed to determine under what conditions PHB is consumed and for what purpose. No PHB was consumed in these experiments in the absence of methane even when all other required nutrients were present in sufficiency. PHB consumption was also slower in the presence of added formate, a compound used solely as a source of reducing power (electrons made available for reductive biochemical steps by oxidation) by methanotrophic cells. This result indicates that PHB is used as a source of reducing equivalents and not as a sole growth substrate. Selective regimes in which stored reducing equivalents are required for survival and growth should therefore select for increased PHB production over time.

Key publications:

Pieja, A.J., E.R. Sundstrom, and C.S. Criddle, 2011. Poly-3-hydroxybutyrate metabolism in the Type II methanotroph Methylocystis parvus OBBP. Applied Environ. Microbiol. 77(17): 6012-6019.[5]

Sundstrom, E.R. 2013. Ph.D. thesis: "Selection and optimization strategies for production of polyhydroxybutyrate in methanotrophic bacteria." Department of Civil and Environmental Engineering, Stanford University, Stanford, CA.[6]

4.2 Motivation

Factors affecting PHB production in methanotrophs are poorly understood. Existing studies have generally examined the effect of a variety of limiting nutrients on final PHB production and molecular weight. Other factors that may affect growth rates and PHB production include pH, gas composition, temperature, salinity, and trace mineral concentrations, but these effects are poorly understood at present. Analysis of the vast array of relevant growth factors is impractical due to the limited throughput of existing growth and analysis techniques. Growth in serum bottles requires cleaning bottles, adding media, adding inoculum, customizing growth conditions, capping, vacuuming, and injecting gas. Further manipulations are required for analysis of PHB content via gas chromatography. Conversion of these individual manipulations to parallel processes is a necessary precursor to effective optimization of growth conditions.

Optimization of growth conditions for increased PHB production can be complemented by the application of cyclic regimes that increase PHB production over time through selection. Such regimes have been applied for heterotrophic organisms, with periods of substrate excess inducing PHB production followed by periods of substrate absence during which stored PHB is consumed for reproduction. Replication of this strategy in methanotrophs could be achieved by inducing PHB production through nutrient limitation and subsequently providing nitrogen in the absence of methane to induce reproduction using stored PHB as the growth substrate. The effectiveness of this strategy is contingent upon reproduction in the absence of methane. The conditions under which PHB is consumed in methanotrophs are currently unknown, and further study was therefore required to determine if such a selective regime is possible or if modification is needed to better suit the metabolism of methanotrophic bacteria.

4.3.1 Microbioreactors

Commercialization of emerging biotechnological advances requires successive levels of scale-up, starting with proof of concept at the small batch scale and moving through bench scale and pilot-scale systems to demonstrate technical and economic viability (**Table 4.1**). Optimization of conditions in microscale reactors can complement this process by allowing for hundreds or thousands of experimental replicates with minimal effort. Effective microscale reactors must mimic the conditions found in full-scale systems, ensuring that optimized conditions will succeed at full scale. In addition, analysis methods must be tailored for small volumes and high throughput. With regard to methanotrophs, an effective microbioreactor system must be completely mixed, allow for temperature control, and allow for control of gas concentrations. Such a system must also be coupled with high-throughput analysis of biomass and PHB concentrations.

4.3.2 Miniaturized growth system

The miniaturized growth system developed for methanotrophic applications consists of 96-well microplates containing 250µL of methanotrophic culture and capped by gas-permeable plate covers (Enyzscreen). The plate covers allow diffusion of methane, oxygen, and carbon dioxide while preventing excessive evaporation and cross-contamination between wells. Covered microplates are clamped inside a gastight box and agitated at high RPM to achieve complete mixing within each well (**Figure 4.1**). Gas is supplied continuously via computer-controlled mass flow controllers, allowing customizable atmospheres within each gastight box. Temperature is controlled via a heating element beneath each box. This system allows 600-800 replicates per box and can easily be scaled to thousands of replicates. Use of standard 96-well microplates ensures compatibility with optical plate readers and existing high-throughput liquid processing equipment.

Table 4.1: Comparison of bioreactors across scale

Scale	Size	Effective Uses
Full scale 	–	Commercial production
Pilot scale 	100L+	Scale-up
Bench scale 	1-10L	Long-term operation
Small-batch scale 	20-100mL	Batch experiments
Microscale 	<1mL	Optimizing conditions, screening isolates

4.3.3 Microplate analysis

Growth in aerated microplates is coupled with two forms of high-throughput analysis: optical density and Nile Red fluorescence (**Figure 4.2**). Optical density readings can be obtained using an optical plate reader and provide a useful proxy for total biomass. Because this technique is non-destructive, growth rates can be determined by comparing optical density measurements over time. PHB content can be determined by staining with Nile Red, a fluorescent dye that segregates to the lipid phase and fluoresces only when suspended in lipid

inclusions. Fluorescence of the resulting cultures can be measured in aggregate using a fluorescent plate reader or on a cell-by-cell basis through the use of high-throughput flow cytometry. Use of flow cytometry has the additional benefit of determining the distribution of PHB content within the culture, as shown in **Figure 4.3**.

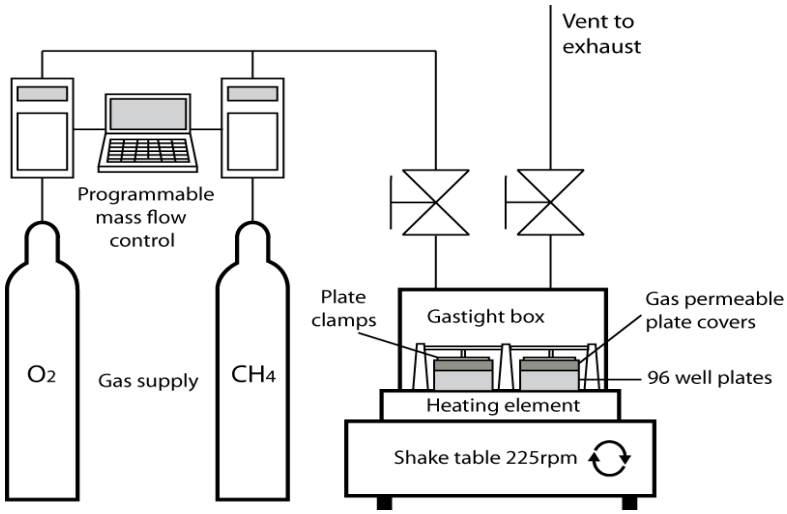

Figure 4.1: Schematic of the microplate growth system

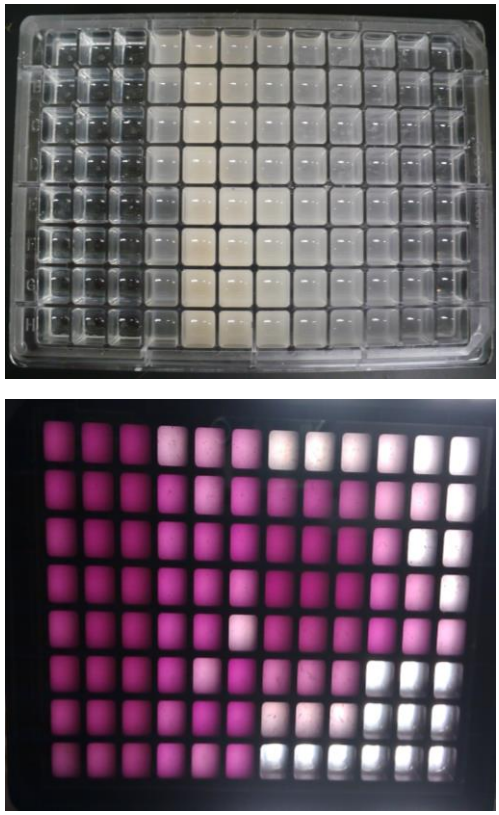

Figure 4.2: Methanotrophic cultures grown in microplates. Unstained cells for optical density analysis are shown above, and Nile Red stained cells prepared for fluorescence analysis are shown below.

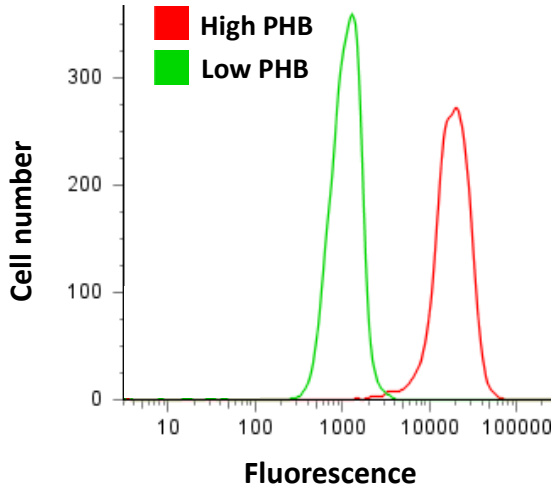

Figure 4.3: Fluorescence distribution of Nile Red-stained cells containing high and low PHB concentration as measured by flow cytometry

4.3.4 Media optimization

The effectiveness of the combined high-throughput growth and analysis system was evaluated by optimization of growth medium to increase PHB production in *M. parvus* OBBP. Microplates were created containing a control medium modified with gradients of eight nutrients: ammonium, nitrate, potassium, phosphorus, magnesium, sulfur, calcium, and copper. These plates were inoculated with *M. parvus* OBBP in exponential phase and incubated until cells entered the stationary phase. Optical density was measured periodically, and fluorescence of stained cells was monitored by flow cytometry.

Fluorescence values were multiplied by final optical density as a proxy for total PHB concentration in g/L. Distinct peaks in PHB content were observed at specific concentrations for four of the nutrients tested: potassium, phosphorus, calcium, and copper (**Figure 4.4**). Lower levels of potassium and phosphorus showed promise as alternative limiting nutrients (as compared to nitrogen limitation in the control medium). Copper is required for methane oxidation by particulate methane monooxygenase (pMMO) but is toxic at high concentrations. Low calcium concentrations favored PHB production, but the underlying mechanism is unknown. Faster growth was observed for three of the four conditions, with only the phosphorus-optimized condition growing more slowly than the control (**Figure 4.5**). Given these apparent benefits, these four conditions were subjected to further quantitative analysis.

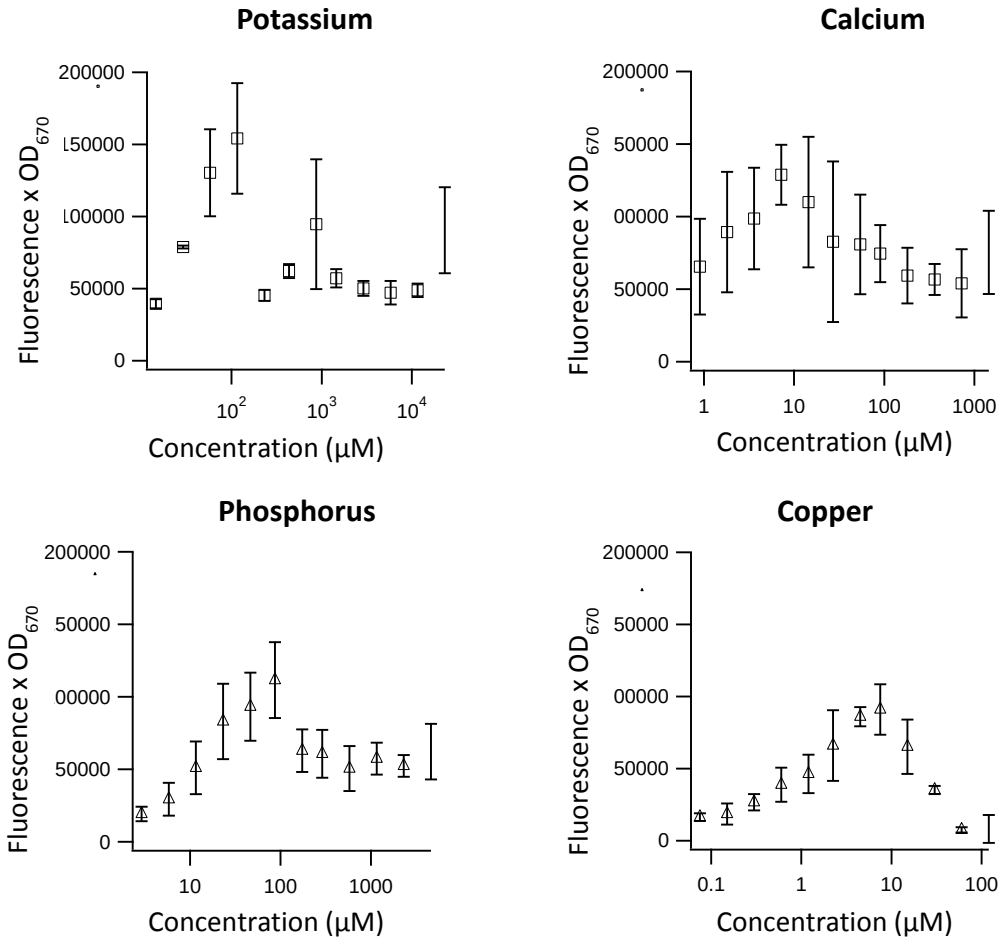

Figure 4.4: Optical density adjusted fluorescence for pure culture *M. parvus* OBBP grown on gradients of potassium, calcium, phosphorus, and copper

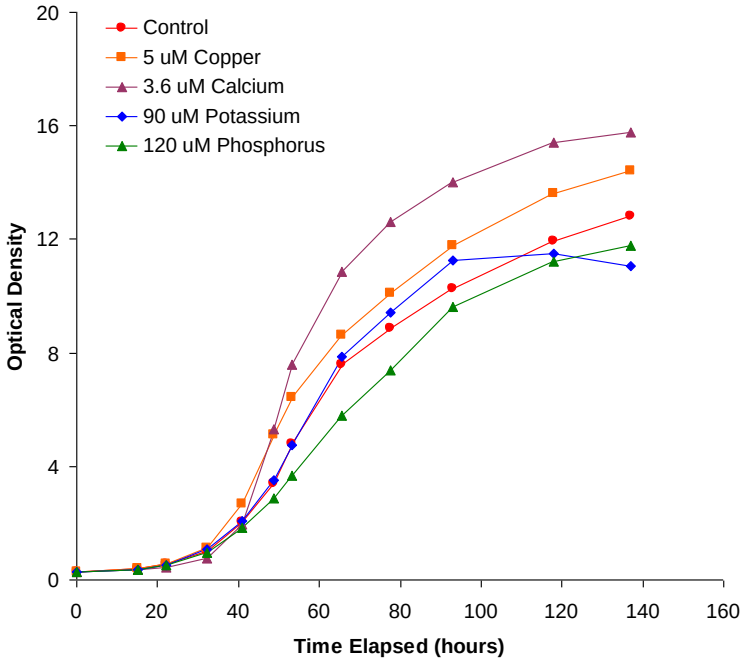

Figure 4.5: Relative growth rates of pure culture *M. parvus* OBBP grown in microplates with four optimized nutrient concentrations

4.3.5 Gas chromatographic verification

To determine levels of PHB produced by *M. parvus* OBBP when grown with optimized levels of phosphorus, potassium, calcium, and copper, plates were created containing 24 replicates for each condition. The control medium and a combined calcium-copper optimization were also assayed. Replicates were aggregated to allow direct measurement of PHB via gas chromatography and total suspended solids were measured by vacuum filtration. In each case the optimized conditions resulted in improved performance, with the combined copper-calcium condition achieving the best results (**Figure 4.6**). PHB content as a percentage of biomass increased from 18 percent in the control to 49 percent in the copper-calcium condition, and the concentration of PHB produced increased from 0.65 g/L to 3.43 g/L. These results confirm the effectiveness of the high-throughput system for identification of optimal growth conditions and highlight the importance of media composition for PHB production.

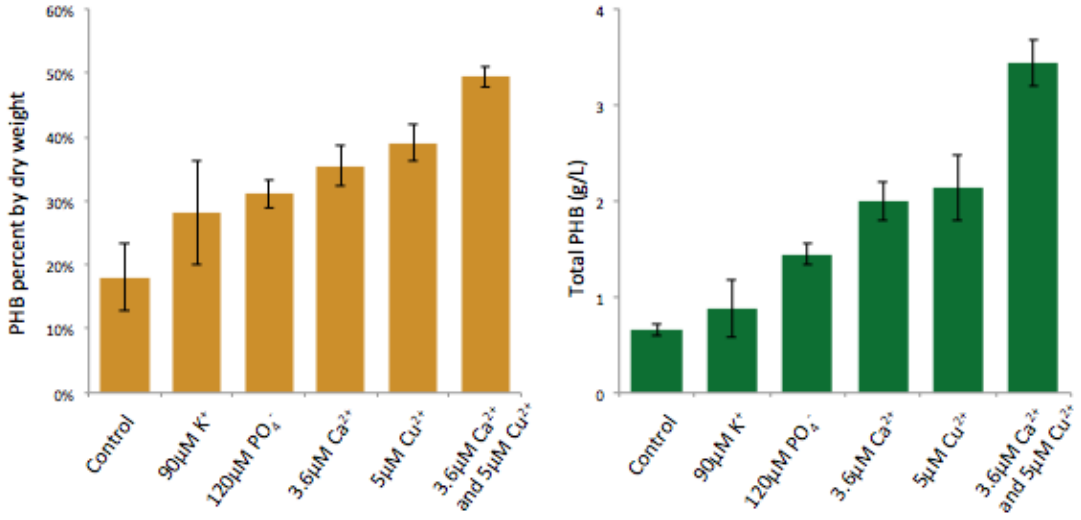

Figure 4.6: PHB concentration and total PHB production in M. parvus OBBP grown with optimized concentrations of phosphorus, potassium, calcium, and copper

4.4.1 Metabolic function of methanotrophic PHB

In addition to optimizing production of PHB, consumption of PHB was analyzed in *M. parvus* OBBP to determine the metabolic purpose or function of PHB in methanotrophic bacteria. In heterotrophic bacteria, PHB and other PHAs are stored under conditions of substrate excess, with polymer production used for rapid storage of available substrate. This stored polymer is then used for reproduction in the absence of substrate. Strains capable of high rates of substrate uptake and polymer production are at a competitive advantage under alternating conditions of substrate excess and substrate absence.

Consumption of PHB in methanotrophic organisms has been linked to long-term survival in the absence of substrate. Stored PHB also serves as a source of reducing power, and has been linked to increased rates of cometabolism of toxic substances. Consumption of PHB as a sole carbon source for growth and reproduction has not been demonstrated experimentally.

4.4.2 PHB consumption in M. parvus OBBP

To determine under what conditions PHB is consumed in strain OBBP, cells were grown to exponential phase and transitioned to PHB production phase by centrifugation and removal of available nitrogen. The resulting PHB-rich cells

were subjected to four conditions: methane addition with nitrate addition, methane addition with no nitrate addition, absence of methane with nitrate addition, and absence of methane with no nitrate addition (**Figure 4.7**). When methane was supplied in the absence of nitrogen, PHB production continued as expected. Cultures receiving no methane or nitrogen remained relatively stable without significant PHB production. Cultures receiving nitrogen in the absence of methane did not reproduce or consume significant quantities of stored PHB despite the presence of all nutrients needed for growth. This is unlike the case for other PHB-producing microorganisms, where growth on stored PHB is observed under such conditions. This result suggests that PHB sustains survival of bacteria in nitrogen-rich but methane-limited environments. Unexpectedly, cultures receiving both methane and nitrogen grew exponentially while consuming PHB. This indicates use of PHB as a source of reducing equivalents ("fuel") enabling more rapid utilization of available methane.

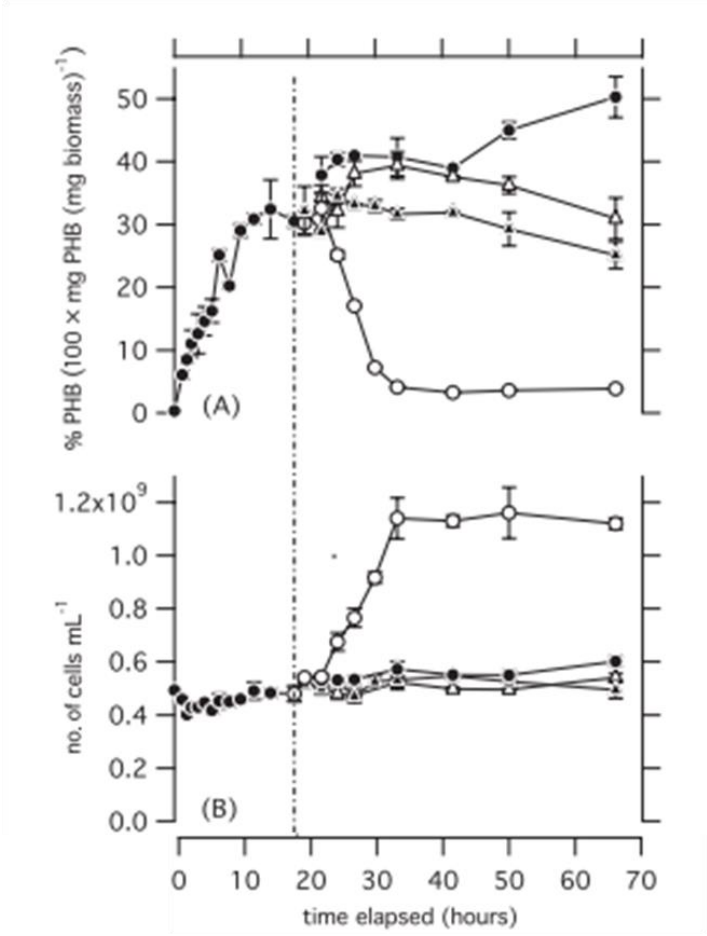

Figure 4.7: Percent PHB (A) and concentration of cells (B) over time for cultures of *M. parvus* OBBP incubated with methane and no nitrogen and transferred at 18 hours to a set of four conditions: methane and no nitrogen (black circles),

methane and nitrogen (white circles), no methane and nitrogen (black triangles), and no methane and no nitrogen (white triangles).

4.4.3 Effect of formate and glyoxylate on PHB consumption

Consumption of PHB was evaluated in the presence and absence of formate to determine whether PHB is a source of reducing equivalents during exponential growth (**Figure 4.8**). Formate is oxidized to CO_2 by methanotrophs, but is not incorporated into cell biomass, and therefore can only serve as a source of reducing equivalents. Addition of formate decreased the rate of PHB consumption. This is consistent with the hypothesis that PHB is used as a source of reducing equivalents.

Consumption of PHB was also evaluated in the presence of glyoxylate. Glyoxylate regeneration is critical to operation of the carbon-assimilating serine cycle in Type II methanotrophs. If consumption of PHB regenerates glyoxylate, cell reproduction should be enabled in the absence of methane. This was not observed.

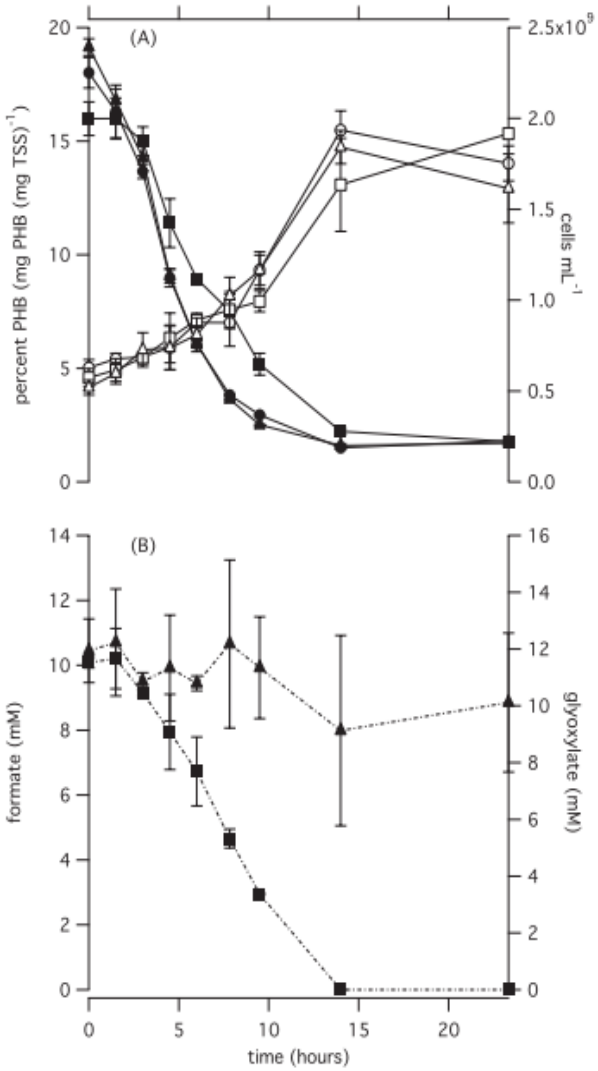

Figure 4.8: Concentrations of PHB, formate, glyoxylate, and total cells for PHB-rich cultures of *M. parvus* OBBP supplied with methane and nitrogen. PHB concentration is shown for cultures with methane only (black circles), methane and formate (black squares), and methane and glyoxylate (black triangles) in the upper panel. Cell concentration is shown for cultures with methane only (white circles), methane and formate (white squares), and methane and glyoxylate (white triangles) in the upper panel. Formate (black squares) and glyoxylate (black triangles) consumption is shown in the lower panel.

Addition of formate decreased the rate of PHB consumption, indicating that formate and PHB mediate similar metabolic roles. During exponential growth of *M. parvus* OBBP, PHB was used concurrently with formate, and growth was rapid. This indicates that PHB likely serves as a source of electrons for the oxidation of methane to methanol and for assimilation of nitrate into cell biomass. Added glyoxylate did not allow reproduction in the absence of methane, perhaps because *M. parvus* OBBP was unable to transport glyoxylate into the cell. In any

case, these results suggest that strategies based on use of stored PHB for reproduction in the absence of methane are unlikely to lead to higher PHB production over time. Selection strategies in which stored reducing equivalents are essential to survival and growth must be explored instead. Such selection strategies are described in Chapter 5.

4.5 Key findings

The findings are significant because they present a high-throughput growth and analysis system that can be used to rapidly screen conditions. They also discern the function of PHB in methanotrophs, which is crucial for understanding how to best select for methanotrophs that produce high levels of PHB.

1. The high-throughput growth and analysis system resulted in an order of magnitude improvement in handling time and effective selection of conditions for increased PHB production.
2. Media composition has a dramatic effect on PHB production in *M. parvus* OBBP. Calcium and copper had significant impacts.
3. A PHB content of 3.43g/L was achieved in pure culture *M. parvus* OBBP (3.6 µM Ca, 5 µM Cu).
4. PHB was not used as a sole growth substrate in the absence of methane, even when all other required nutrients were present.
5. The likely function of PHB in methanotrophs is to serve as a source of reducing equivalents (fuel).
6. Selection strategies designed to increase PHB production over time must use conditions in which stored reducing equivalents are beneficial to survival and growth in the presence of methane.

5. PHB Production in Methanotrophic Bioreactors: Mixed Culture and Enrichments

5.1 Executive summary

Long-term reactor operation is a necessary precursor to implementation of methanotrophic PHB production at commercial scale. A successful operational regime must remain functionally stable over time, produce polymer of high and consistent quality, achieve rapid growth, and achieve high biomass density in suspended culture. This chapter focuses specifically on operation in open mixed culture, as the associated genetic diversity helps achieve functional redundancy within the community, providing greater resistance to disruption and eliminating the need for costly sterilization practices.

In this chapter, a series of long-term reactor studies is presented with cultures grown in known mixed culture and enrichment culture. The use of varying nitrogen sources for selection of PHB-producing methanotrophs in enrichment culture is developed and evaluated for long-term efficacy. A cycle alternating between growth on ammonium and growth on nitrate is found to select for PHB-producing methanotrophs while maintaining high growth rates and culture densities.

Cyclic methane limitation during PHB consumption is tested as a means of inducing higher PHB production over time in known mixed culture. Methane limitation is found to improve PHB production over time as compared to replicates receiving oxygen limitation or an excess supply of both gases. Methane limitation is then combined with nitrogen-based selection and evaluated for long-term operation in enrichment culture. PHB production remained stable through 37 days, while polymer produced maintained a consistent molecular weight near 1.0×10^6 Da. Instability was observed after 37 days, pointing toward potential drawbacks in the use of ammonium for growth of methanotrophs.

Density of biomass in reactor systems is a major determinant of capital and operating costs. High-density cultures enable smaller reactor volumes at lower capital cost. They also decrease time required for growth allowing more cycles of PHB production over time. A fluidized bed reactor (FBR) design was evaluated to achieve biomass density without use of pressurization. High concentrations of biomass were grown in biofilms attached to activated charcoal particles and suspended within a column of upward-flowing methane-rich media. Growth was maintained over a period

of 255 days, and community composition was effectively manipulated through the use of nitrogen fixation and low dissolved oxygen concentration. When coupled with the selective conditions described in this chapter, an FBR system could provide high concentrations of easily extractable methanotrophic biomass while requiring a fraction of the footprint required for suspended growth.

Key publications:

Sundstrom, E.R. 2013. Ph.D. thesis: "Selection and optimization strategies for production of polyhydroxybutyrate in methanotrophic bacteria." Department of Civil and Environmental Engineering, Stanford University, Stanford, CA.[7]

Pieja, A.J., E.R. Sundstrom, and C.S. Criddle. 2012. Cyclic, alternating methane and nitrogen limitation increases PHB production in a methanotrophic community. BioResource Technology 107:385–392.[8]

Pfluger, A., W. Wu, A. Pieja, J. Wan, K. Rostkowski, and C. Criddle. 2011. Selection of Type I and Type II methanotrophic proteobacteria in a fluidized bed reactor under non-sterile conditions. Bioresour. Technol. 102: 9919-9926.[9]

5.2.1 Ammonium-based selection: Motivation

As reported in Chapter 2, PHB production is only detected in Type II methanotrophs. Because Type I methanotrophs grow more rapidly under mesophilic conditions, growth conditions selective for Type II methanotrophs or inhibitory to Type I methanotrophs are necessary to maintain PHB production in open cultivation (i.e. when no provisions are made to prevent contamination). Four conditions were found to select for Type II methanotrophs: growth without copper, growth at low pH, growth under nitrogen fixation conditions, and growth in dilute media. Each of these conditions selected for PHB-producing methanotrophs in enrichment culture, but all four conditions were unreliable as long-term selection conditions or resulted in low growth rates and biomass density. Alternative selective conditions are therefore required to achieve selection without sacrificing overall productivity.

Manipulation of nitrogen sources was considered as an alternative to the selective conditions discussed in Chapter 2. In particular, it was hypothesized that growth on ammonium is selective for Type II methanotrophs, as explained in **Figure 5.1**. Growth on urea was also considered as a selector, as urea is cleaved by urease to form ammonium, potentially allowing for a more gradual addition of ammonium. Evidence in the literature regarding selectivity conveyed by these reduced nitrogen sources is mixed, with almost all studies focused on environmental

systems rather than biotechnological applications. Experiments were therefore conducted to evaluate the short- and long-term effects of ammonium on Type II selectivity, growth rates, and PHB production.

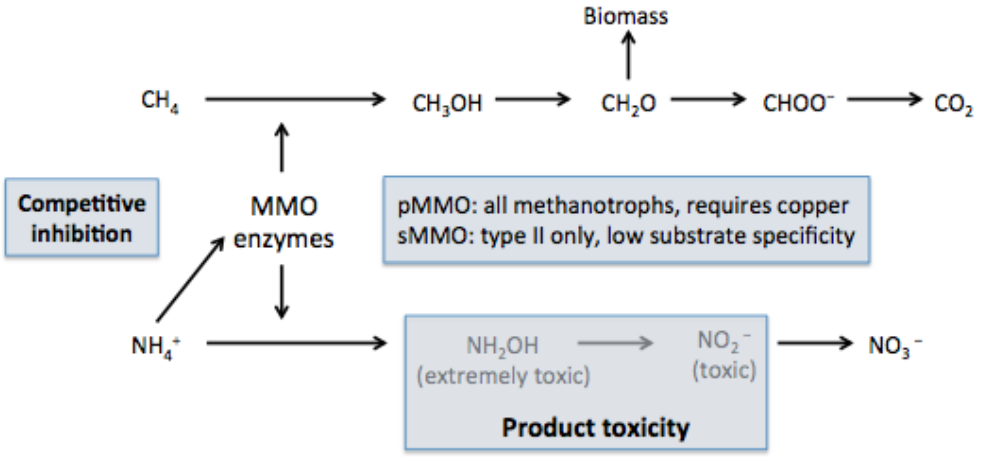

Figure 5.1: Methane and ammonium metabolism in methanotrophic bacteria. Both methane and ammonium are oxidized by methane monooxygenase (MMO); therefore, rates of methane and ammonium oxidation are not independently regulated. Ammonium may limit growth of methanotrophs in two ways: through competitive inhibition of MMO activity and through co-oxidation to form toxic hydroxylamine and nitrite. Type II methanotrophs possess the less-specific soluble methane monooxygenase (sMMO) and may therefore be particularly susceptible to co-oxidation of ammonium to hydroxylamine.

5.2.2 Experimental setup

Experiments with enrichment cultures were conducted using a 4-liter completely mixed batch reactor setup as shown in **Figure 5.2** and **Figure 5.3**. Methane and oxygen were supplied in excess via electronic mass flow controls. The reactors can be cycled manually or programmed to periodically empty into a waste container and refill from the nutrient reservoir. Gas flow was 50 percent oxygen and 50 percent methane unless otherwise specified. Activated sludge from the Palo Alto Regional Water Quality Control Plant (PARWQCP) was used to provide a diverse inoculum for enrichment cultures. Activated sludge was thoroughly washed and filtered to remove excess carbon and nitrogen.

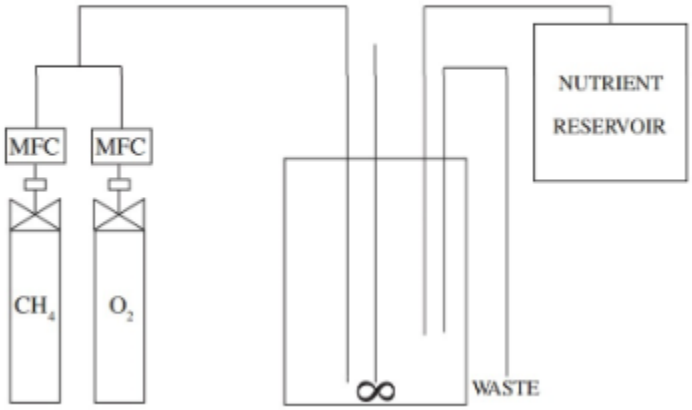

Figure 5.2: Schematic of the completely mixed 4-liter batch reactor system used

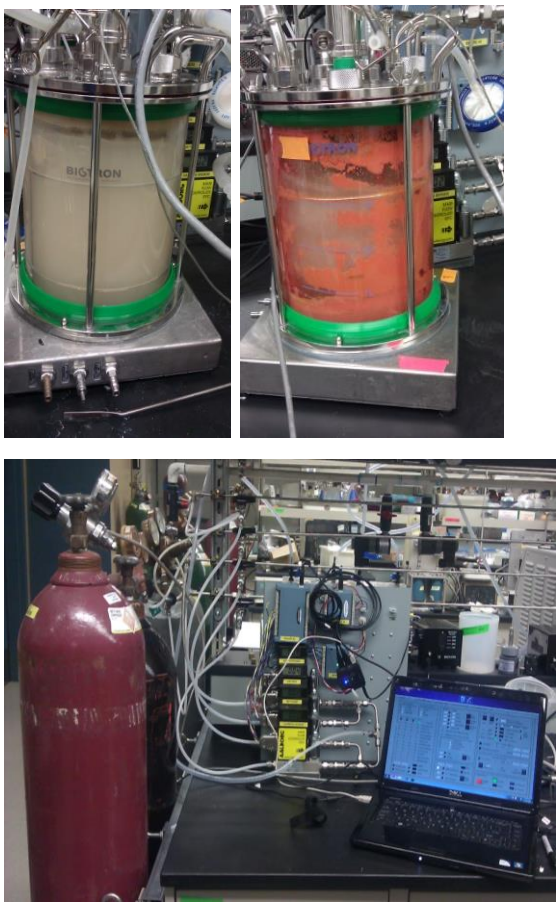

Figure 5.3: Photos of the 4-liter reactor system. Suspended growth of Type II methanotrophs is pictured on the upper left. A takeover event by non PHB-

producing methanotrophs is shown on the upper right panel (orange biofilm). The electronic gas supply system is pictured at the bottom.

5.2.3 Activated sludge enrichments

Activated sludge was enriched in 4-Liter reactors with varying nitrogen sources to determine if growth on ammonium or urea selects for PHB-producing methanotrophs. The results of these enrichments are shown in **Figure 5.4**. In all cases, growth on ammonium limited the final biomass density of the resulting enrichments, while growth on nitrate resulted in the production of high levels of biomass. No PHB production was observed in nitrate enrichments, while limited PHB production was observed in one replicate during growth on ammonium. Enrichments with both nitrate and varying ammonium levels increased biomass compared to enrichment with ammonium alone, and low levels of PHB were detected in two of the three replicates.

The best results were obtained when cultures enriched with ammonium alone were diluted and transferred to growth on nitrate. Biomass of approximately 3g/L was produced in all replicates, and PHB production of up to 10 percent by dry weight was observed. The biomass density of enrichments grown with ammonium alone was likely limited by buildup of toxic hydroxylamine and nitrite due to co-oxidation of ammonium. Dilution mitigated this limitation, and subsequent growth on nitrate allowed dense growth and PHB production. This approach combines the selectivity of growth on ammonium with the density obtained during growth on nitrate.

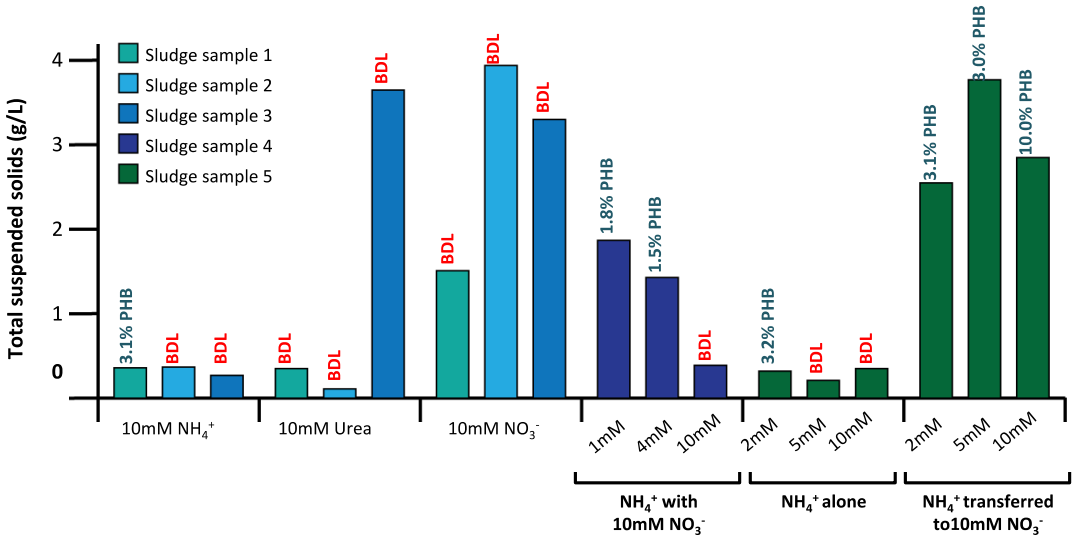

Figure 5.4: Biomass and PHB production for cultures enriched from five separate samples of activated sludge in the presence of methane, oxygen, and varying nitrogen sources. Total suspended solids measurements were taken after nine days of growth. Final PHB content is labeled for each replicate; “BDL” indicates PHB production below the detection limit. Sludge sample 4 was enriched with ammonium in the presence of 10mM nitrate; sludge sample 6 was enriched with ammonium and then transferred to three days of growth on nitrate.

5.2.4 Cycling nitrogen sources

Enrichment of activated sludge with ammonium followed by growth with nitrate resulted in a dense culture of PHB-producing organisms. The long-term effectiveness of this strategy was evaluated by exposing the enrichment to nitrogen cyclically, with 24 hours of growth on ammonium followed by 48 hours growth on nitrate. PHB production increased consistently over the course of nine days and remained stable for 27 days with no evidence of invasion by Type I methanotrophs. Selection therefore appeared to be robust. Biomass density was stable at 2-3g/L. A separate reactor was inoculated from the first after nine days, with urea replacing nitrate as a nitrogen source. Performance in this urea-fed reactor was indistinguishable from that of the nitrate-fed reactor. Given that urea is cleaved into ammonium more gradually by urease, urea may be preferred to nitrate as it may convey some Type II selectivity. Furthermore, unlike nitrate, urea does not require methane for reduction and incorporation into cell material, and may therefore improve yields.

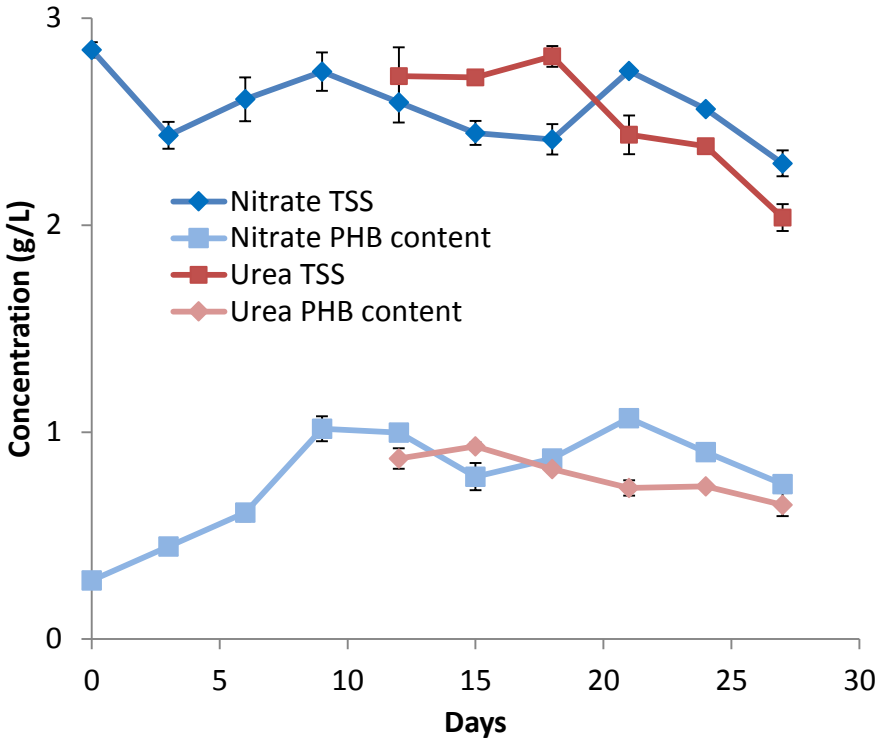

Figure 5.5: PHB production and total suspended solids (TSS) over time during cycling operation. Activated sludge was enriched with 10mM ammonium followed by 10mM nitrate as shown in Figure 3. This enrichment culture was diluted, grown for one day on 10mM ammonium, diluted, and grown for two days on 8mM nitrate after which PHB content was measured. Maximum PHB content of 1g/L was observed, with a maximum concentration of 39% PHB as a percentage of dry biomass.

5.3.1 Selecting for PHB production

The genetic diversity present in open communities can be harnessed to favor increased PHB production over time. This could conceivably enable improvements in fitness and PHB production at a fraction of the cost of metabolic engineering. To achieve such improvements, however, conditions must be set such that isolates with elevated PHB storage have increased fitness during periods of PHB consumption. Over numerous cycles of PHB production and consumption, strains and mutants with elevated PHB production should experience more rapid growth, enhancing performance.

Understanding the nature of PHB consumption in methanotrophic bacteria is central to establishing such selective conditions. PHB consumption in *Methylocystis parvus* OBBP is evaluated under varying conditions in

Chapter 4. PHB was not consumed in the absence of methane, even when all other nutrients were present, yet PHB was rapidly consumed in the presence of methane when the limiting nutrient (in this case, nitrogen) was replenished. This indicates that PHB is likely a source of reducing equivalents for methane activation/oxidation and for reduction of nitrogen present as nitrate or hydroxylamine (**Figure 5.1**). Limited methane availability during periods of PHB consumption may confer a competitive advantage on those methanotrophs that can generate one-carbon units for assimilation from methane while also oxidizing stored PHB and reducing nitrate or hydroxylamine.

5.3.2 Cyclic methane limitation as a selection condition

In methanotrophs, PHB is produced under unbalanced growth conditions, when methane is present and another nutrient required for cell replication is absent. PHB is not produced in the absence of methane, and is consumed slowly when methane is absent. To test the effects of cyclic methane limitation during PHB consumption, a known mixed culture of only Type-II methanotrophs was subjected to repeated cycles of PHB production and consumption under methane-limited, oxygen-limited, and control conditions. To begin the cycle, PHB-rich cells were inoculated into three identical reactors and amended with nitrate to encourage growth and PHB consumption. After eight hours of gas limitation, gases were supplied in excess for the next 16 hours; during this period, all nitrogen was consumed and PHB production resumed. Gas concentrations and cycle times for the 24-hour cycle are shown in **Figure 5.6**. Automatically cycling 4-liter reactors as described in section 5.2.2 were used for this experiment. The known mixed culture used consisted of *M. parvus* OBBP, *M. trichosporium* OB3b, and a methanotrophic community enriched from soil and known to produce PHB.

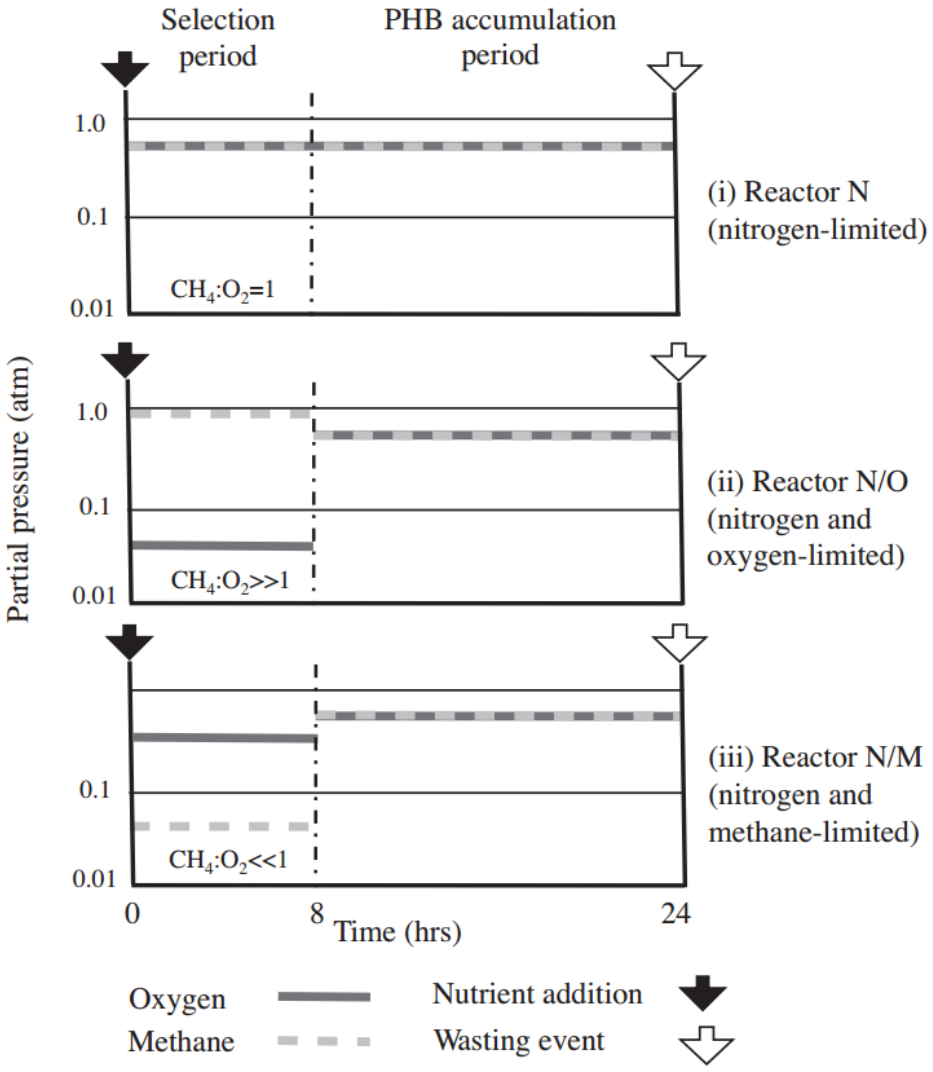

Figure 5.6: Gas flow rates for methane-limited, oxygen-limited, and control replicates. At the end of each 24-hour cycle, the reactors were diluted and refilled with fresh media. PHB concentration was measured at the end of each cycle. Off-line incubations were conducted at the end of each 24-hour cycle to measure final PHB content at the end of growth.

5.3.3 Effects of cyclic methane limitation

Concentrations of PHB were measured at the end of each 24-hour cycle and again for off-line incubations in which PHB production proceeded to completion. For both PHB assays, there was a significant upward trend over time in the methane-limited reactor; no such trend was observed in the oxygen-limited or control reactor (**Figure 5.7**). Final PHB

concentrations trended below 15 percent in the oxygen-limited and control reactors, while values above 20 percent were observed in the methane-limited reactor. These results are consistent with the hypothesis that methane limitation selects for enhanced PHB production.

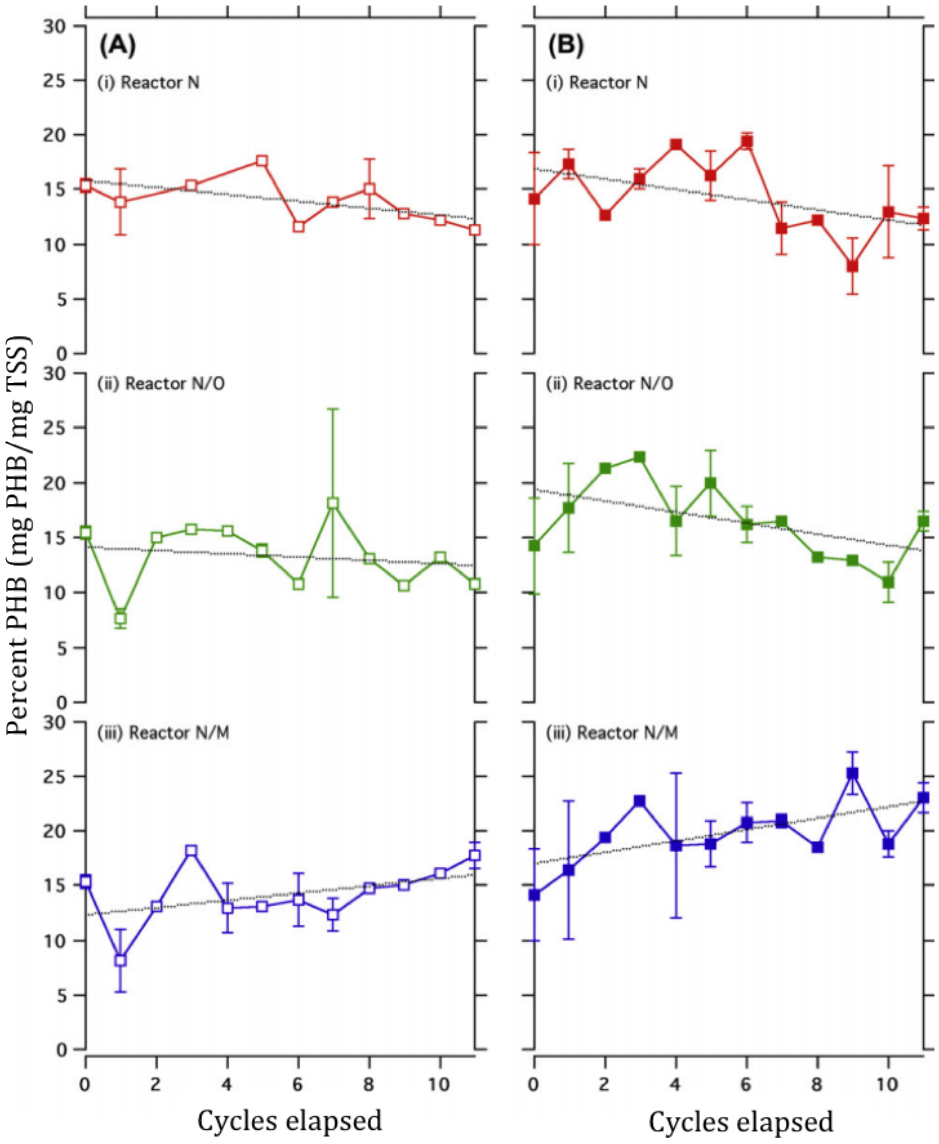

Figure 5.7: Final PHB production in the control (top), oxygen-limited (middle), and methane-limited (bottom) replicates. PHB production at the end of the 24-hour cycle is shown on the left, final PHB production after off-line incubation is shown on the right. All reactors were inoculated with an identical known mixed culture containing only PHB-producing strains.

5.3.4 Combining ammonium with methane limitation

Given the effectiveness of cyclic methane limitation for increasing PHB production in known mixed culture and the effectiveness of cycling nitrogen sources for selection of PHB-producing methanotrophs in enrichment culture, a combination of the two cycles may provide the benefits of both techniques. Operation in enrichment culture increases genetic diversity, increasing the potential for selection of highly fit PHB-producing methanotrophs and allowing long-term operation without the need for sterilization. A cycle in which cultures are exposed to ammonium with methane limitation during PHB consumption and nitrate with methane excess during PHB production could allow operation in enrichment culture with the added benefit of increased PHB production over time.

The long-term effects of a combined cycle were evaluated in two identical reactors. Both reactors were inoculated with PHB-rich cells and allowed to grow on ammonium for 12 hours. This was followed by dilution and 48 hours of growth on nitrate. During the ammonium growth phase, one reactor was subject to methane limitation while the second reactor received both methane and oxygen in excess. PHB production, total biomass, and molecular weight of extracted polymer were measured over time to assess operational stability and the effectiveness of the selective pressure applied.

5.3.5 Short-term cycling effects

During the ammonium growth phase of the initial cycle of reactor operation, the methane-limited reactor consumed more PHB (60 percent PHB consumption) than the control reactor (20 percent PHB consumption) while producing less biomass (**Figure 5.8**). The increase in PHB consumption indicates that PHB likely enabled more rapid and efficient use of the limited available methane for methane oxidation and cell growth. Methane limitation did not appreciably affect PHB production, with both reactors achieving similar performance following dilution and the addition of nitrate. Ammonium was consumed more slowly in the methane-limited reactor, however, and a small amount of nitrate was formed during growth on ammonium, indicating cometabolism of ammonium and hydroxylamine oxidation (**Figure 5.1**).

5.3.6 Long-term cycling effects

Over the first 37 days of operation, both reactors remained stable (Figure **5.9**). Biomass concentrations initially declined as a result of the formation of microbial films (biofilms) on the glass; biofilm removal at 20 days and 30 days reversed this decline. Total biomass remained at 2 to 3g/L while total PHB remained just below 1g/L. No notable increase in PHB production was

observed over time in either reactor, despite the increase in PHB consumption induced by methane limitation.

After 37 days the methane-limited reactor entered a period of instability, and washout was observed. This instability was likely due to protracted hydroxylamine exposure, with kinetics typical of cometabolic product toxicity. After resuspension in fresh media containing 10mM nitrate, biomass recovered but without accompanying PHB production, indicating that removal of ammonium led to a loss of Type II selectivity in this reactor.

Understanding the nature of the functional instability observed after day 37 remains the key to long-term operation of this combined cycling regime. Mitigation of prolonged hydroxylamine exposure may be possible, with solutions including reductions in ammonium concentration, increased dilution, and reductions in the number and duration of ammonium growth stages.

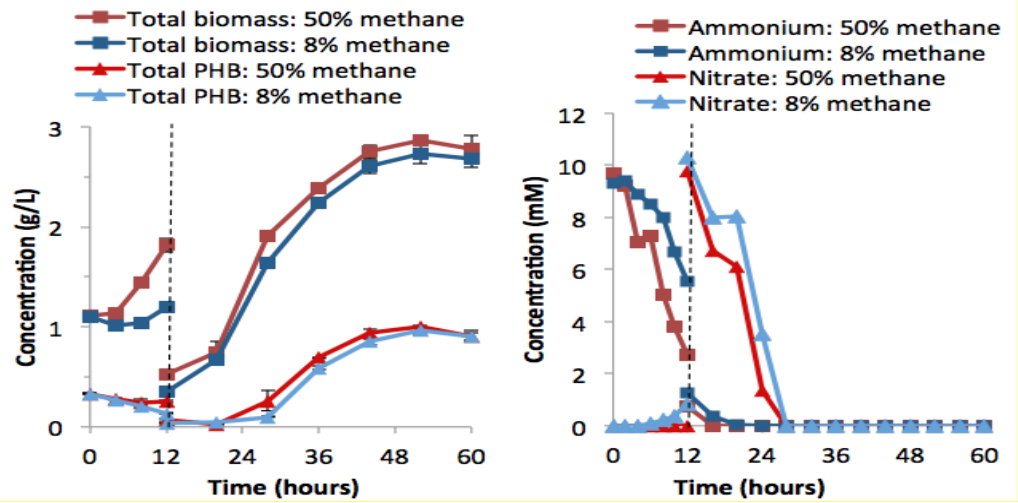

Figure 5.8: Total biomass, PHB, ammonium, and nitrate for reactors cycling between growth on ammonium and growth on nitrate with and without methane limitation. Data shown is for the first cycle of operation. Cultures received 8mM ammonium for 12 hours; the dashed line at 12 hours represents a dilution and addition of 8mM nitrate. Methane limitation was confined to the 12-hour ammonium growth period. Excess methane was supplied to both reactors during growth on nitrate. Both the control and methane-limited reactors were inoculated with a culture enriched from activated sludge in the presence of 10mM ammonium, then transferred to 8mM nitrate and allowed to accumulate PHB.

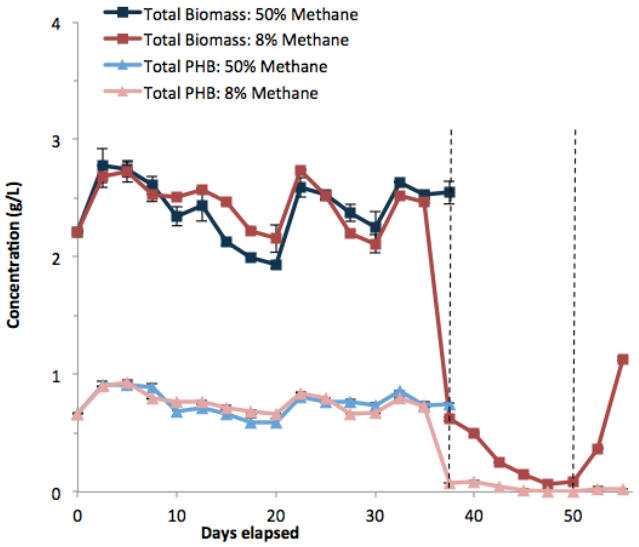

Figure 5.9: Biomass and PHB concentrations over time in the methane-limited and control reactors. Measurements were taken at the end of each cycle. After 37 days the control reactor was discontinued, while the methane-limited reactor was allowed to continue operation. After 50 days, the reactor contents were resuspended in fresh media containing 10mM nitrate, after which the cycles resumed as before.

5.3.7 Molecular weight of extracted polymer

High yields of PHB from methane are required for economic viability, but the quality of the polymer is equally important for commercial applications. Molecular weight must be high enough for diverse applications, and the molecular weight must remain constant to ensure a product of consistent quality. Using samples from the combined cycling reactor, molecular weight of extracted polymer was measured at five time points during the first 13 reactor cycles to evaluate stability over time. As shown in **Table 5.1**, measured molecular weight was highly stable in both the methane-limited and control reactors, ranging from 9.44×10^5 to 1.07×10^6. These values are in line with previously reported values for methanotrophic cultures and are higher than values observed in currently available commercial polymer. Consistency between time points and reactors indicates that production of stable molecular weight polymer may be achievable in mixed culture, despite reduced control over the composition of the microbial community.

Table 5.1: Molecular weight of polymer extracted from the cycling reactors at five time points. Polymer was extracted by first lysing the cells in a mixture of SDS (sodium dodecyl sulfate) and EDTA (ethylenediaminetetraacetic acid)

and then applying hypochlorite for oxidation of non-PHB biomass. This process is described in further in Chapter 6. Molecular weight was measured by GPC (gas permeation chromatography) and calibrated directly to polystyrene standards of known molecular weight. The polydispersivity index (PDI) is a measure of the distribution of molecular mass in a given polymer sample. Low values indicate little variation of molecular weight within the sample.

		Low methane			High methane		
Cycle number	**Days elapsed**	**Weight average M_w (Da)**	**Number average M_n (Da)**	**PDI**	**Weight average M_w (Da)**	**Number average M_n (Da)**	**PDI**
1	2.5	$9.85x10^5$	$5.04x10^5$	1.96	$9.70x10^5$	$4.80x10^5$	2.02
4	10	$9.99x10^5$	$5.14x10^5$	1.94	$9.69x10^5$	$4.87x10^5$	1.99
7	17.5	$1.07x10^6$	$5.58x10^5$	1.92	$1.06x10^6$	$5.18x10^5$	2.04
10	25	$9.44x10^5$	$4.85x10^5$	1.95	$1.01x10^6$	$4.95x10^5$	2.04
13	32.5	$1.06x10^6$	$5.02x10^5$	2.11	$1.05x10^6$	$4.88x10^5$	2.15

5.4.1 Fluidized bed reactors: Motivation

Dissolution of methane and oxygen for growth of methanotrophs is energy-intensive and limits biomass density achievable in suspended growth. Growth with low biomass density requires larger reactors, with associated capital costs. Handling large quantities of liquid growth medium requires energy, with additional energy inputs required for dewatering prior to extraction of polymer. Pressurized reactors can achieve high rates of gas dissolution, though such reactors are more costly and more dangerous than those operating at atmospheric pressure.

Growth of methanotrophs in a fluidized bed reactor (FBR) system is one possible means for achieving high biomass density without requiring pressurization. In such systems, biomass is grown on particles suspended within a column of upward-flowing liquid growth medium (**Figure 5.10**). The liquid media is continuously replenished, while available nutrients including methane and oxygen are constantly consumed by the suspended biomass. Gas contactors ensure that incoming media is saturated with methane and oxygen. In this way, extremely dense concentrations of biomass can be

achieved within the column due to the constant supply of fresh, gas-saturated media.

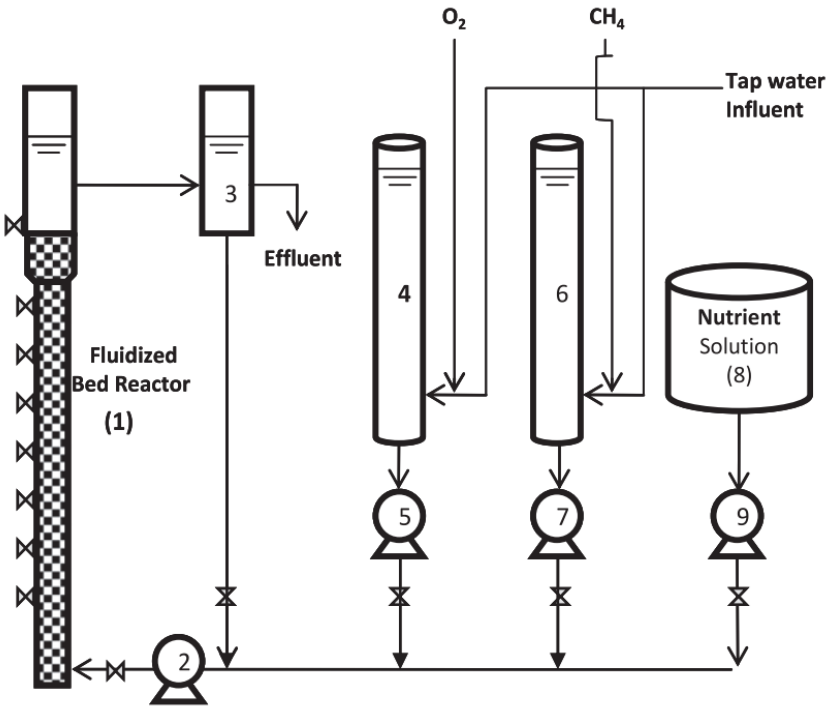

Figure 5.10: Schematic diagram of the FBR system for methanotrophic growth. (1) Fluidized bed with sampling ports, (2) fluidization pump, (3) effluent recycle reservoir, (4) dissolved O_2 contactor, (5) dissolved O_2 water feed pump, (6) dissolved CH_4 contactor, (7) dissolved CH_4 water feed pump, (8) nutrient solution tank, (9) nutrient solution feed pump.

5.4.2 Long-term FBR operation

An FBR was tested for growth of methanotrophs and operated for 255 days. The reactor was inoculated with known Type II cultures and operated under non-sterile conditions. Growth was initially quite robust but limited largely to Type I methanotrophs and therefore inappropriate for PHB production. During this phase influent dissolved oxygen (DO) was held at 9.3mg/L and nitrogen was supplied as dissolved nitrate. Growth of Type I methanotrophs (as verified by T-RFLP analysis) in the FBR column after 47 days of operation is shown in **Figure 5.11**.

Growth under nitrogen-fixation conditions, a known selection condition, was tested as a means of maintaining a community of Type II methanotrophs within the FBR. Ultimately, switching to dissolved nitrogen gas as a nitrogen source and reducing incoming DO to 1.9mg/L led to the

effective maintenance of a community of Type II methanotrophs within the reactor. The density of this community after 252 days of operation is shown in **Figure 5.11**. An FBR may therefore be effective for generating a high density of methanotroph biomass with a small footprint. This approach may be coupled with the selective conditions described elsewhere in this chapter to achieve effective selection for Type II methanotrophs coupled with high rates of PHB production with the FBR.

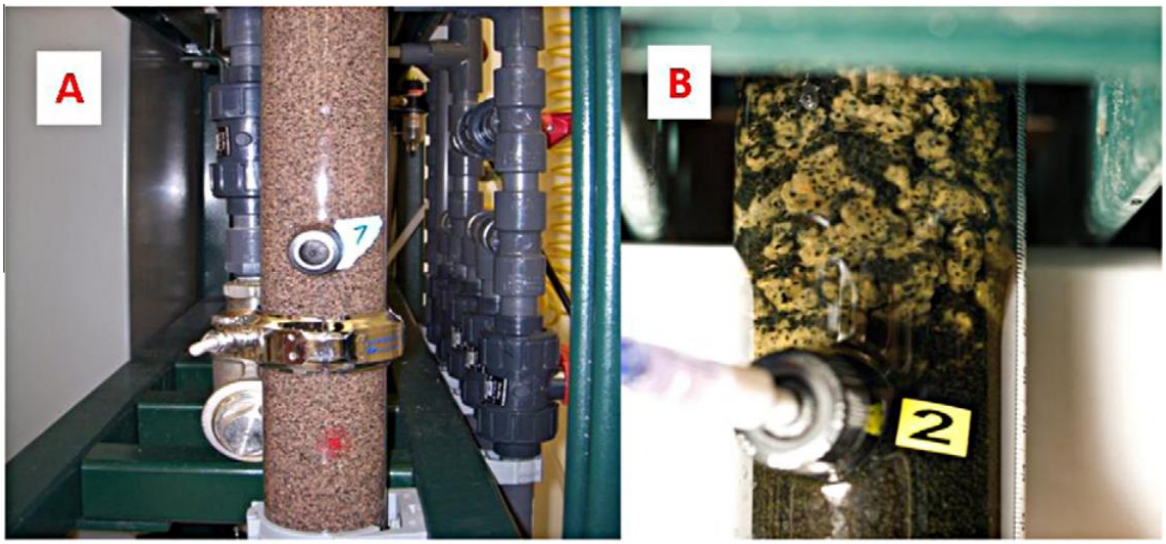

Figure 5.11: Growth of biomass suspended in the FBR column. Growth of pink-pigmented Type I methanotrophs after 47 days is shown at left. Growth of tan-pigmented Type II methanotrophs under selective conditions after 252 days is shown at right.

5.5 Summary of selection effects

Selection of Type II methanotrophs from a diverse inoculum and maintenance of such communities over time is achievable through the use of alternating nitrogen sources. This strategy allowed robust selection without compromising PHB production. Methane limitation during PHB consumption encouraged increased PHB production during subsequent reactor cycles. Combining these two approaches is possible but may induce long-term instability, though these concerns could likely be mitigated by decreasing ammonium exposure. Molecular weight of polymer produced during cyclic operation was high and consistent, and therefore promising for commercial applications. Use of a fluidized bed reactor allowed cultivation of Type II biomass at high density without pressurization and is therefore an interesting option for cultivation of Type II methanotrophs.

5.6 Key findings

1. Growth on ammonium selects for PHB-producing Type II methanotrophs.
2. Culture densities are limited during growth on ammonium, likely due to toxic products of ammonium co-oxidation.
3. Alternating between ammonium and nitrate maintains selection for PHB-producing methanotrophs in high-density culture, with observed PHB production up to 39 percent and 1g/L.
4. Methane limitation during PHB consumption leads to increased PHB production over time in known mixed culture.
5. Methane limitation can be combined with cycling nitrogen sources for long-term PHB production in enrichment culture but long-term exposure to high levels of ammonium appears to induce functional instability.
6. Molecular weight in enrichment cultures is consistent over time around 1.0×10^6 Da across reactors.
7. Growth of high-density methanotrophs is possible using a fluidized bed reactor (FBR).
8. Selection for Type II methanotrophs can be achieved in the FBR through application of nitrogen fixation conditions.

6. PHB Extraction and Characterization

6.1 Executive summary

When considering the complete process of PHB production from substrate to commercial polymer, extraction of pure PHB from bacterial biomass accounts for a significant fraction of overall cost (Chapter 12) and environmental impact (Chapter 11). In choosing an extraction technology, economic and environmental factors must be weighed against polymer quality to determine the ideal protocol. In this chapter, the technical merit of a number of extraction protocols is evaluated.

Selective dissolution in hot chloroform and subsequent precipitation has traditionally been used to extract polymer for analysis purposes, but this method proved ineffective for methanotrophic biomass. An initial lysis step using warm surfactant improved performance but did not mitigate the environmental consequences of solvent-based extraction. While hypochlorite extraction is likely preferable from an economic and technical standpoint, disposal of waste presents a new set of concerns. Use of scCO2 was not successful for the conditions evaluated. Further development of alternative oxidants and alternative extraction methods is needed for inexpensive extraction of polymer with low environmental impact.

Key publications:

Sundstrom, E.R. 2013. Ph.D. thesis: "Selection and optimization strategies for production of polyhydroxybutyrate in methanotrophic bacteria." Department of Civil and Environmental Engineering, Stanford University, Stanford, CA.[10]

Wright, Z.C. 2013. Poly(3-hydroxybutyrate-co-3-hydroxyvalerate) biodegradable foams: The effects of processing, nanoscale additives, and aging. Ph.D. thesis. Stanford University.[11]

6.2 PHB extraction

Polyhydroxyalkanoates are naturally stored within the cell as lipid inclusions, and cells must therefore be lysed to recover pure polymer. Following lysis, the nonlipid cellular biomass must be separated from the lipid biomass, yielding purified polymer. Any process used to extract and separate polymer must not affect the molecular weight of the polymer, as that would compromise its quality and value. Pure PHB is not soluble in water, and is suspended within the cell through the use of specialized proteins that maintain the solubility of the polymer within lipid inclusions. Pure PHB has low solubility in organic and chlorinated solvents, complicating extraction methods that use solvent dissolution.

A variety of protocols exist for achieving cell lysis and subsequent separation of PHB. Lysis techniques include use of chlorinated solvents, surfactants, sonication, and physical disruption. Separation techniques include dissolution in chlorinated solvents, selective oxidation of non-PHB biomass, dissolution of polymer or biomass in supercritical CO_2, exposure to high- and low-pH conditions, and density-based physical separation. Of these techniques, the most commonly used for analytical purposes is suspension of biomass in high-temperature chloroform, which performs the dual role of cell lysis and selective dissolution of PHB polymer. Dissolution in chloroform is followed by precipitation and drying, yielding polymer of high purity and preserving molecular weight if care is taken to minimize chloroform exposure time and temperature. This procedure has several drawbacks, with the high cost and adverse environmental impacts of chloroform use limiting its feasibility at commercial scale. Use of large quantities of chloroform is required for even small-scale extractions, and the use of a condenser or Soxhlet extraction limits throughput for analytical purposes. To address these issues, various combinations of surfactants and oxidants were investigated as an alternative to chloroform-based extraction.

6.3 Evaluation of extraction methods

To determine an optimal protocol for extraction of PHB from wild-type methanotrophs, biomass from a PHB-producing cycling bioreactor was aggregated, freeze-dried, and subjected to a variety of conditions. The initial PHB content of the freeze-dried biomass was 33% by dry cell weight. Extraction in chloroform was tested with and without a pretreatment with the surfactant sodium dodecyl sulfate (SDS). The surfactant pretreatment was intended to induce cell lysis. Use of hypochlorite and hydrogen peroxide to oxidize non-PHB biomass was also tested following SDS pretreatment. Varying durations of hypochlorite exposure were analyzed to determine the effects of exposure time on purity and molecular weight. Varying temperatures were tested for hydrogen peroxide exposure to determine if increased temperature would increase the effectiveness and oxidation. The purity and molecular weight of PHB extracted using these protocols is shown in **Table 6.1**. Purity was analyzed by gas chromatography, and molecular weight was analyzed by gel permeation chromatography.

Extraction in chloroform produced polymer of more than 90 percent purity, but yields were consistently low. For a variety of strains, chloroform extraction resulted in either no polymer recovery or barely sufficient polymer for molecular weight analysis. Pretreatment with SDS vastly improved yields without compromising molecular weight, which were consistent at ~1.15×10^6 Da. Higher purity of up to 98 percent was achieved through hypochlorite oxidation, and resulting molecular weight was similar

to the values observed for chloroform when hypochlorite exposure was 30 minutes or less. Treatment with hydrogen peroxide at 60˚C resulted in increased purity, with maximum observed purity at 69 percent. This process may be best used as an initial step prior to polishing with hypochlorite.

Purification of both commercial and cellular inclusions of PHB was also attempted with the use of supercritical CO_2 ($scCO_2$). Commercial PHB was used as received, and cell samples from a liquid media were freeze-dried after centrifugation. In a typical $scCO_2$ extraction, the reaction vessel was first filled to nearly 80% capacity by volume with pellets (~40 g). In the case of cellular material, in which there was limited material, the remaining volume would be filled with inert glass beads. Liquid CO_2 was pumped into the extraction vessel, which was set at 50°C, until a pressure of 4000 psi was reached. Following a 10-minute static soak at this temperature and pressure, the container was vented in to a glass vial through at 70°C restrictor valve. Carbon dioxide was allowed to flow through the vessel at 20 to 24 mL/min for several minutes until the solvent volume was exchanged approximately three times. Cycling of a static soak followed by dynamic flow was repeated up to three more times. In some cases, the pressure was increased in subsequent static/dynamic cycles. Much like the chloroform extraction, $scCO_2$ was efficient at purifying commercial PHB. Yellow liquids were observed in the glass vial after extraction at higher pressure (7500 psi), and the pellets in the extraction vessel turned white. This indicates that low molecular weight degradation products and/or additives are soluble in $scCO_2$ at the tested temperatures and pressures. There was an approximate 10% weight reduction in the pellets after five pressure cycles of increasing pressure from 4000 psi to 9000 psi. NMR peaks of the PHB have the desired three peaks in the correct ratio (1:2:3), but still contain some impurity peaks. However, they are significantly smaller than any of the PHB signatures, with the largest being approximately one-half the area of the smallest PHB peak. Longer extraction times would likely reduce these peaks further and result in a purer final product. Of the protocols tested, SDS pretreatment followed by 30 minutes of hypochlorite oxidation achieved the best combination of purity, molecular weight, simplicity, and cost. This method was therefore used for molecular weight analysis and bulk extraction of polymer from reactor biomass. An example of products made from this bulk polymer is shown in **Figure 6.1**.

Table 6.1: Purity, peak molecular weight, and dispersity index (PDI) of polymer extracted from methanotrophic biomass using a variety of protocols. Use of scCO2 was not successful for PHB extraction. Values were calibrated directly to a polystyrene standard. PDI indicates the distribution of individual molecular masses in a batch of polymers. As polymer chains approach uniform chain length, PDI approaches unity.

Extraction protocol	Purity	Weight average M_w (Da)	Number average M_n (Da)	Polydispersity Index (PDI)
SDS alone	49.9%	-	-	-
Chloroform alone	93.7%	$1.15x10^6$	$6.16x10^5$	1.87
37˚C SDS and chloroform	94.1%	$1.12x10^6$	$5.55x10^5$	2.02
60˚C SDS and chloroform	90.0%	$1.23x10^6$	$6.65x10^5$	1.85
120˚C SDS and chloroform	70.3%	$8.96x10^5$	$4.90x10^5$	1.83
60˚C SDS and 15 min hypochlorite	88.9%	$1.18x10^6$	$5.68x10^5$	2.07
60˚C SDS and 30 min hypochlorite	92.6%	$1.16x10^6$	$5.33x10^5$	2.18
60˚C SDS and 60 min hypochlorite	97.6%	$1.01x10^6$	$3.74x10^5$	2.69
60˚C SDS and 120 min hypochlorite	96.5%	$9.02x10^5$	$2.63x10^5$	3.43
60˚C SDS and 30˚C hydrogen peroxide	55.1%	-	-	-
60˚C SDS and 60˚C hydrogen peroxide	69.1%	$1.13x10^6$	$6.52x10^5$	1.74

Figure 6.1: Plastic coins extracted using a combined SDS and hypochlorite extraction protocol. The top two coins are commercial PHBV; the lower coins are PHB from methanotroph biomass.

6.4 Key findings

1. Extraction in chloroform alone or using supercritical CO_2 is ineffective, though both methods effectively removed impurities from extracted polymer.
2. Addition of surfactant to induce cell lysis increases surfactant efficiency.
3. Extraction in hypochlorite eliminates the need for solvent while preserving molecular weight.
4. Hydrogen peroxide provides oxidation of non-PHB biomass without producing chlorinated waste but does not produce high-purity polymer.
5. Hypochlorite extraction is a simple, inexpensive, and effective technique, but strategies are required for residuals management.

7. Biocomposites and Foams

7.1 Executive summary

The use of plastics and natural fiber-reinforced composites such as wood plastic composite (WPC) in construction has risen over the last few decades due to advantages such as low cost, high specific stiffness and strength, and lower maintenance requirements in comparison to wood and engineered wood materials. Widespread applicability is limited, however, because of persistent concerns over the long-term performance of biopolymers and natural fiber composites, especially in outdoor applications. Commercially available wood-plastic composites are typically

fabricated using a reinforcing natural fiber filler, such as wood flour, a waste byproduct of the wood manufacturing industry, in a matrix derived from hydrophobic thermoplastic polyolefins like polypropylene (PP), polyethylene (PE), or polyvinyl chloride (PVC).

Biopolymeric natural fiber composites are hygroscopic in nature and inevitably absorb moisture in high humidity and wet environments. Water transport in natural fiber composites is driven by the chemical potential gradient between the hydroxyls present in lignocellulose and the polarity of water molecules. Absorbed moisture causes swelling in individual wood fibers, which can lead to WPC dimensional instability, matrix cracking, mass loss, susceptibility to in-service biodeterioration, and a significant loss in structural integrity, namely reductions in mechanical stiffness and strength.

This research assesses the suitability of PHAs for use in plastic, foam, and natural-fiber composite materials. Targeted applications include construction materials as well as packaging materials. For composites, initial mechanical and physicochemical properties are addressed, as well as long-term durability related to accelerated weathering, physical aging, and moisture absorption. Results of environmental impact studies on biocomposite production are also presented. For biocomposite and foam testing, large quantities of PHB are required. Lab-scale production of PHB from methane could not provide sufficient material for testing. Accordingly, commercial sources of PHA were used for biocomposite and foam testing. These PHAs are sourced from sugar feedstock.

The ability to manufacture rigid foams out of biodegradable polymers can lead to replacement of nonrenewable resource-intensive polystyrene foams typically used for insulation alone or as part of structural insulation panels for single-family homes. Foams must have very low bulk density, high cell density, and uniformity of closed-cell microstructure in order to yield appropriate insulating properties. However, PHAs currently do not have the appropriate melt strength and thermal stability for foaming. Specifically, low viscosity of the PHAs leads to increased cell coalescence and high cell densities. Because PHAs thermally degrade close to the melting temperature, processing conditions must be carefully chosen to achieve proper viscosity and minimize decomposition. Because foaming is a challenging process, achievement of foams broadens the applications for which PHAs can be processed.

Various approaches to improving the foamability of PHBV are also explored from both materials and processing perspectives. PHBV is a copolymer of PHB and PHV: 3-hydroxybutyrate (HB) monomers confer stiffness while 3-hydroxyvalerate (HV) monomers confer flexibility.

Cellulose acetate butyrate, another biodegradable polymer with higher viscosity, was blended with PHBV in order to enhance the viscosity. More uniform closed-cell structure was achieved, and high cell density was achieved at higher blowing agent concentrations. The influence of gas solubility on the resulting foam was also investigated, where a method to predict gas solubility in PHBV was developed and provided insights into cell density. This study led to the use of carbon dioxide-generating blowing agents, which are predicted to have much higher solubility in PHBV. Addition of bicarbonate as a blowing agent significantly reduced bulk density.

Key publications:

Srubar III, W.V., S.L. Billington. 2013. "A Micromechanical Model for Moisture-Induced Deterioration in Fully Biorenewable Wood-Plastic Composites." Composites Part A: Applied Science and Manufacturing; 50: 81-92.[12]

Miller, S.A., M.D. Lepech, S.L. Billington. 2013. "Application of multi-criteria material selection techniques to constituent refinement in biobased composites." Materials and Design. 52: 1043-1051.[13]

Miller, S.A., S.L. Billington, M.D. Lepech. 2013. "Improvement in environmental performance of poly(β-hydroxybutyrate)-co-(β-hydroxyvalerate) composites through process modifications." Journal of Cleaner Production. 40:190-198.[14]

Michel, A.T., S.L. Billington. 2012. "Characterization of poly-hydroxybutyrate films and hemp fiber reinforced composites exposed to accelerated weathering." Polymer Degradation and Stability. 97(6): 870-878.[15]

Srubar III, W.V., Z.C. Wright,* A. Tsui, A.T. Michel, S.L. Billington, C.W. Frank. 2012. "Characterizing the Effects of Ambient Aging on the Mechanical and Physical Properties of Two Commercially Available Bacterial Thermoplastics." Polymer Degradation and Stability; 97(10): 1922-29. *equal contribution.*[16]

Srubar III, W.V., C.W. Frank, S.L. Billington. 2012. "Modeling the Kinetics of Water Transport and Hydroexpansion in a Lignocellulose-Reinforced Bacterial Copolyester." Polymer; 53(11): 2152-61.[17]

Srubar III, W.V., S. Pilla, Z.C. Wright, C.A. Ryan, J.P. Greene, C.W. Frank, S.L. Billington. 2012. "Mechanisms and Impact of Fiber-Matrix Compatibilization Techniques on the Material Characterization of PHBV/Oak Wood Flour Engineered Biobased Composites." Composites Science and Technology; 72(6): 708-15.[18]

Q. Liao, A. Tsui, S. Billington, and C.W. Frank. 2012. Extruded foams from microbial poly(3-hydroxybutyrate-co-3-hydroxyvalerate) and its blends with cellulose acetate butyrate. Polym. Eng. Sci. 52:7:1495-1508.[19]

Tsui, A., X. Hu, D.L. Kaplan, and C.W. Frank. 2013. Biodegradable films and foam of poly(3-hydroxybutyrate-co-3-hydroxyvalerate) blended with silk fibroin. Green Polymer 2, American Chemical Society, in press.[20]

Wright, Z.C. 2013. Poly(3-hydroxybutyrate-co-3-hydroxyvalerate) biodegradable foams: The effects of processing, nanoscale additives, and aging. Ph.D. thesis. Stanford University.[21]

Tsui, A., Z.C. Wright, and C.W. Frank. 2013. Prediction of gas solubility in poly(3-hydroxybutyrate-co-3-hydroxyvalerate) melt to inform process design and resulting foam microstructure. Submitted.[22]

Wright, Z.C. and C.W. Frank. 2013. Increasing cell homogeneity of semicrystalline, biodegradable polymer foams with a narrow processing window via rapid quenching. Submitted.[23]

7.2 Biocomposites: Mechanical properties

Fully biobased composite materials were fabricated using a natural, lignocellulosic filler, namely oak wood flour (OWF), as particle reinforcement in a matrix derived from poly(hydroxybutyrate)-co-poly(hydroxyvalerate) (PHBV) via an extrusion injection molding process. The mechanisms and effects of processing, filler volume percent (vol%), a silane coupling agent, and a maleic anhydride (MA) grafting technique (both intended to improve moisture resistance) on polymer and composite morphologies and tensile mechanical properties were investigated and substantiated through calorimetry testing and scanning electron microscopy. The addition of 46 vol% silane-treated OWF improved the tensile modulus of neat PHBV by 165 percent. Similarly, the tensile modulus of MA-grafted PHBV increased 170 percent over that of neat PHBV with a 28 vol% addition of untreated OWF. Incorporation of OWF reduced the overall degree of crystallinity of the matrix phase and induced embrittlement in the composites, which led to reductions in ultimate tensile stress for both treated and untreated specimens (**Figure 7.1**).

In addition to wood flour filled composites, PHBV reinforced with natural fiber woven textiles was examined. To form these composites, PHBV and the textiles were oriented in a lay-up process and then formed into composites using a hot press. Five types of woven textile were considered: virgin jute burlap (JB), virgin jute burlap processed without hydrocarbons (NJB), recycled jute burlap (RJB), virgin hemp burlap (HB), and a virgin

hemp linen (HL). The different fiber types and weaves allowed for assessment of the influence of fiber species as well as processing levels on composite behavior. The composites were examined at varying fiber volume fraction as well as under different processing conditions. It was found that for most of the composites analyzed, there was a peak in composite stiffness at approximately 40 percent fiber volume fraction. The tightly woven hemp linen textile provided composites with a higher ultimate tensile strength, but the lower-processed virgin jute burlap composites provided a similar stiffness to the high-processed hemp linen reinforced composites. Due to variations in weave properties for the warp (0°) and weft (90°) fibers, composites were tested in both directions. **Figure 7.2** displays stress-strain plots for the five types of fiber-reinforced composites for both the warp and weft directions.

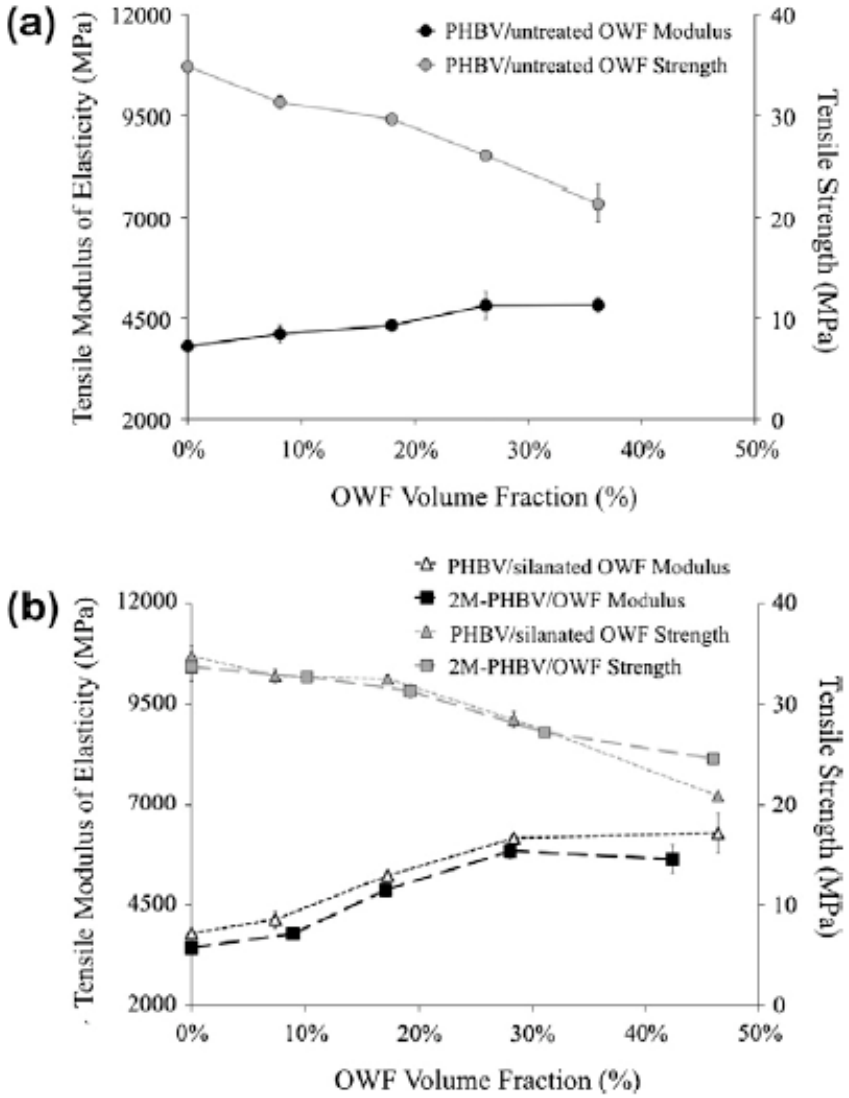

Figure 7.1. Effect of (a) fiber loading and (b) fiber loading and chemical compatibilization technique on tensile modulus and tensile strength of PHBV/ OWF composites. Each data point represents the average tensile properties of three (3) specimens. The error bars represent ± one standard deviation.

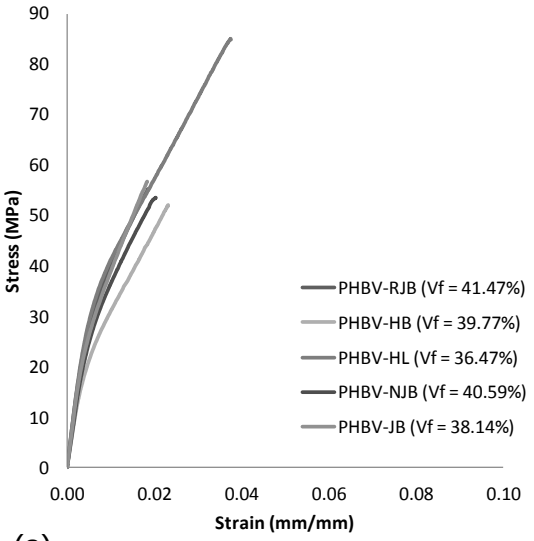

(a)

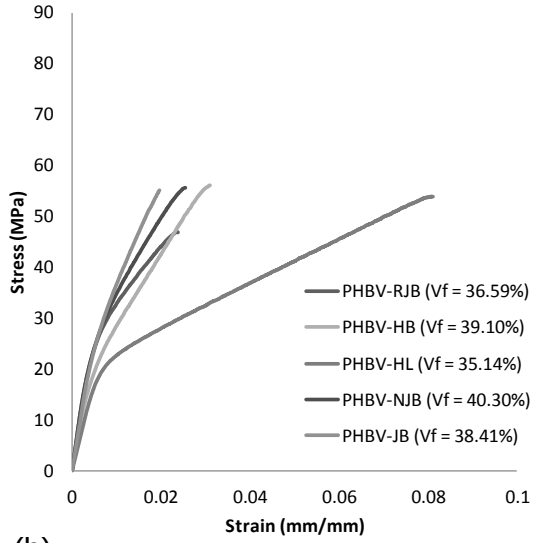

(b)

Figure 7.2: Tensile stress-strain diagrams for five biobased composites examined: (a) on-axis properties & (b) off-axis properties

A comparison of initial mechanical properties of PHBV-based natural fiber composites and other conventional construction materials is listed in **Table 7.1**.

Table 7.1. Mechanical properties of selected biobased composites, wood, and engineered wood products.

Material	Tensile Strength [MPa]	Tensile Modulus [Gpa]	Shear Strength [MPa]	Flexural Strength [MPa]	Flexural Modulus [Gpa]	Density [kg/m^3]
Hemp/CA	54	5.4	12	95	6.6	1300-1370
Hemp/PHB	56	5.5	10	65	6.5	1270-1310
Hemp/PHBV	54-83	4.0-7.4	-	66-88	4.1-5.8	1170-1250
Jute/PHBV	48-59	6.2-7.5	-	59-76	5.2-6.4	1160-1310
OWF/PHBV	20-38	3.6-5.2	-	40	4.0	1200-1310
Douglas-Fir*	-	-	7.8	85	13.4	480
Western Hemlock*	-	-	8.6	78	11.3	450
Ponderosa Pine*	-	-	7.8	65	8.9	400
Plywood•†	27	10.3	1	27	10.3	400-810
Oriented Strand Board •‡	-	-	1.2	21.2	5.3	490-810
Glulam *°	-	-	-	26-72	10.6	320-720

† Hurd MK. Formwork for concrete. Detroit: American Concrete Institute; 1995.

• *APA. Relative Lightness in Weight, APA-The Engineered Wood Association; 2011. http://www.performancepanels.com/index.cfm?content=app_pp_atr_weight [28.01.11]*

** Green DW, Winandy JE, Kretschmann DE. Mechanical properties of Wood. Wood handbook—Wood as an engineering material, Gen. Tech. Rep. FPL–GTR–113. Madison, WI: U.S. Department of Agriculture, Forest Service, Forest Products Laboratory; 1999.*

‡ Thomas WH. Concentrated load capacity and stiffness of oriented strand board: Calculation versus test. J Struct Eng 2002;128(7):908–12.

° Issa CA, Kmeid Z. Advanced wood engineering: Glulam beams. Constr Build Mater 2005;19(2):99–106.

7.3 Biocomposites: Durability

Renewable biobased polymers and composites have been shown to have suitable initial specific strength and stiffness for use in commercial applications. However, the long-term performance of these materials under variable environmental conditions is largely unknown. To investigate long-term durability, accelerated weathering testing was performed on PHB biopolymer films and PHB-hemp fiber reinforced composites. Simulated weathering conditions include exposure to cyclic ultraviolet (UV) light, heat, water spray, and elevated relative humidity. Two distinct weathering procedures are performed, one with cyclic elevated relative humidity and one without. Changes in the mechanical properties of ultimate stress, ultimate strain, and modulus of elasticity, as well as mass, cross-sectional area, molecular weight, and color were reported. It was found that neat PHB polymer films exhibit increased elastic modulus and decreased ultimate strength and strain with weathering exposure, while PHB-hemp fiber composites exhibit decreased ultimate strength and elastic modulus. Both the films and composites experienced mass loss and increased fading with weathering exposure. The molecular weight of the PHB polymer decreased steadily with increasing weathering. The observed changes in physical and mechanical properties are attributed to photo-oxidation and hydrolytic degradation of the PHB bio-polyester and cyclic hygrothermal expansion and contraction of the natural reinforcing fibers.

Physical aging of commercial PHB and PHBV were also investigated. Aging-related changes in mechanical properties and crystalline matrix morphology were characterized using mechanical tensile tests, gas chromatography, differential scanning calorimetry, and gel permeation chromatography. Both PHB and PHBV samples, which were verified to contain a heterogeneous mixture of processing additives, experienced significant embrittlement upon storage in a desiccated isothermal (15ºC) environment set moderately above their glass transition temperatures. Increases in the tensile modulus of elasticity (+40) were accompanied by decreases in ultimate strain (-60%); however, the aged samples exhibited no variation in ultimate tensile strength after 168 days. Melt extrusion and ambient aging did not lead to any significant reduction in polymer molecular weights. Calorimetry results suggested that aged samples exhibited only a slight

increase (+2%) in overall degree of crystallinity, and multiple melting peaks were observed, indicating the presence of crystals of multiple thermal stabilities. Upon aging, the major melting peaks shifted to lower melting temperatures in both PHB and PHBV. The results demonstrate that physical aging of the two industrial biopolyesters can induce substantial changes in physical and mechanical properties in PHB and PHBV when stored just above their respective glass transition temperatures, and that the governing mechanism for embrittlement in both biopolymers is restricted to the noncrystalline phase.

Moisture absorption is a primary deterioration mechanism for natural fiber composites. The governing kinetic behavior of water transport in a biopolymeric composite material derived from PHBV and wood flour were investigated along with the influence of temperature, wood flour content, and chemical modification (silane, maleic anhydride) on polymer and composite diffusivity. The water absorption process in both untreated and treated composites was found to follow the kinetics of Fickian diffusion theory. Diffusion coefficients for neat polymer and composite samples were experimentally determined, and the thermodynamics of diffusive water transport were observed to exhibit Arrhenius rate-law behavior. Isodiffusion plots (**Figure 7.3**) were developed to evaluate the effectiveness of chemical modifications. Both silane and maleic anhydride treatments were found to reduce the rates of water uptake.

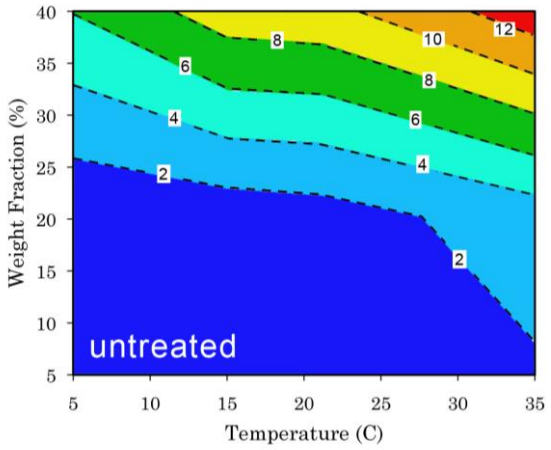

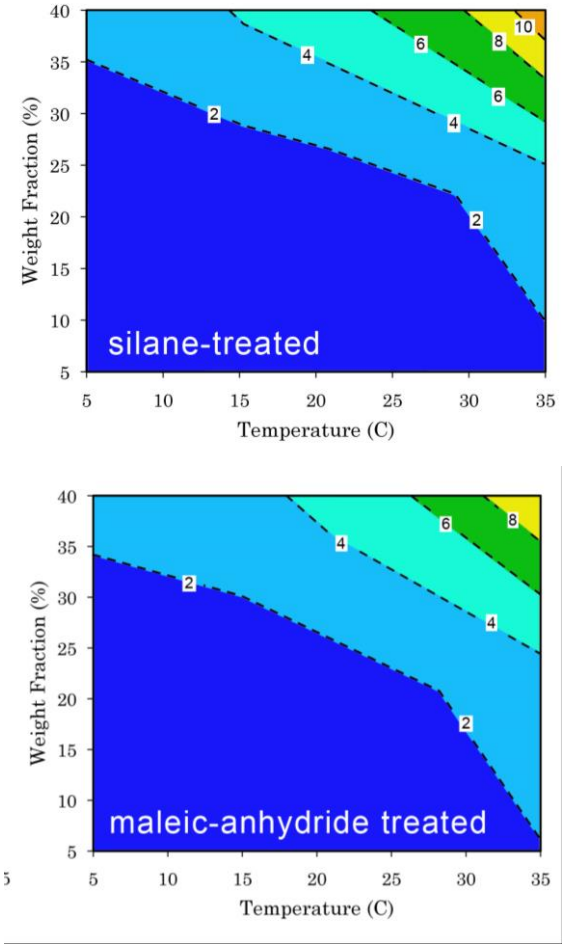

Figure 7.3: Isodiffusion plots showing the effect of wood fiber fraction, temperature, and chemical modification on PHBV/wood flour composite diffusivity

The influence of moisture on the morphological and flexural mechanical properties of PHBV/wood flour composites was also investigated. The effect of two fiber-matrix chemical modifications on enhancing composite durability in wet environments was assessed. Physicochemical changes to the matrix micro-structure were further investigated using gel permeation chromatography and differential scanning calorimetry. Flexural mechanical tests confirm that the addition of wood flour increases the flexural performance of PHBV in the immediate post-processing, dry condition. After being exposed to one complete saturation-drying cycle, the modulus of elasticity of PHBV increased, while the ultimate flexural strength decreased. The result of physicochemical investigations via calorimetry and chromatography conclude that the change in PHBV properties was due to an embrittlement phenomenon that involved hydrolytic degradation of the polymer matrix phase. In contrast, upon exposure to moisture, both the flexural mechanical stiffness and strength of the composites decreased, particularly in higher fiber volume fraction composite samples. The use of both a silane and maleic anhydride fiber-chemical modification resulted in negligible

improvements in moisture resistance and durability of the saturated and saturated-dry composites. Higher degrees of swelling, mass loss, and macroscopic surface cracking were also evident in composite samples with higher fiber volume fractions.

7.4 Foams: Motivation and approach

Production of polymeric foams not only reduces the material cost compared with an unfoamed case, but also leads to very low thermal conductivity useful for insulating materials. Common polymeric insulators, such as expanded polystyrene and polyurethane, are typically non-biodegradable and sourced from nonrenewable resources. Successful development of biodegradable foams would be an important step toward more complete energy-efficient “green” buildings and packaging systems. PHAs, and specifically PHBV, are biodegradable in many natural environments and are microbially derived, making them attractive, environmentally benign alternatives. However, PHBV has insufficient rheological properties to support foam microstructure and bubble, or cell, development and has a narrow thermal processing window due to a low thermal decomposition temperature. Specifically, low viscosity of the PHBV leads to increased cell coalescence and high cell densities (**Figure 7.4**). To overcome these challenges, we have investigated various techniques to improve material properties and optimize processing conditions. Here, we will discuss viscosity enhancement through blending with cellulose acetate butyrate (CAB), maximizing gas solubility through processing and blowing agent selection, and incorporating additives to promote cell nucleation and stability.

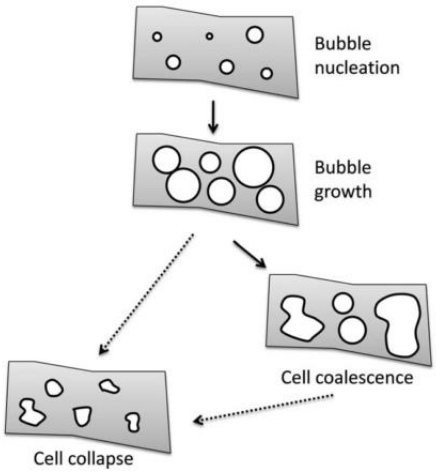

Figure 7.4: Simple schematic of bubble dynamics during foam expansion

7.5 Foams: Experimental setup

Foams were produced using a single-screw extruder (Brabender) equipped with a 2-inch horizontal flex-lip ribbon die, shown in **Figure 7.5**. The extruder barrel has four temperature zones; temperatures of each zone ranged from 140° to 170° C depending the materials used. The temperature is chosen to achieve melting, gas decomposition, and blending, while minimizing thermal decomposition. Screw speed of the die ranged from 25 rpm to 80 rpm to vary the pressure, pressure drop, and pressure drop rate across the die. A pressure transducer measures pressure in the barrel preceding the die. The gas for producing the foam was generated from chemical blowing agents, which were dry-blended with the polymer and chosen to thermally decompose in the extruder to release gas. Two types were used: azodicarbonamide (AZ), which generates mostly nitrogen, and sodium bicarbonate (SB), which generates carbon dioxide and water.

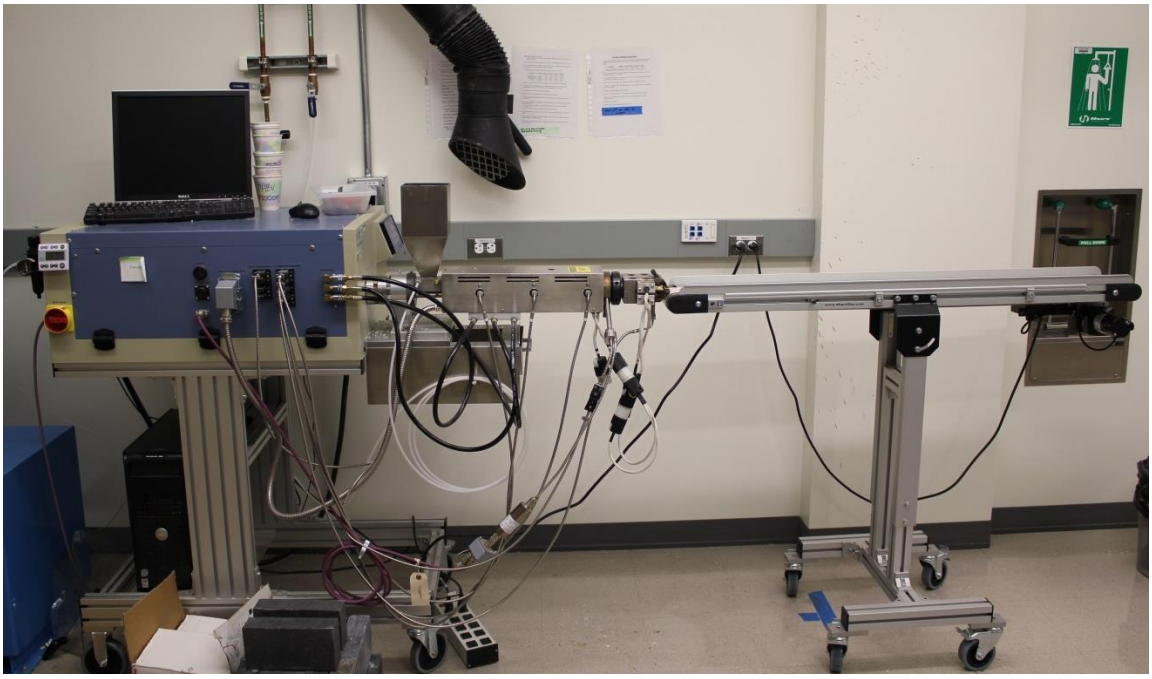

Figure 7.5: Lab-scale extrusion foaming setup

7.6 Foams: Viscosity enhancement through blending

Blending of polymers to achieve intermediate or even synergistic properties is a common practice. In order to increase the melt viscosity of PHBV to prevent cell coalescence and collapse, cellulose acetate butyrate, another biodegradable polymer with higher viscosity, was added at 20 wt% (P80C20) and 40 wt% (P60C40). **Figure 7.6** shows that the viscosity of the blends is enhanced above

that of neat PHBV by an order of magnitude. These blends were foamed and compared to near PHBV foams. As shown in **Figure 7.7**, a 40 percent density reduction and greater cell uniformity and homogeneity were achieved by using these blends, but only at higher blowing agent concentrations. However, the cell densities of the blends were significantly lower than that of neat PHBV foams, likely caused by the high viscosity, which would reduce cell nucleation and gas diffusivity. During these foaming experiments, the lowest screw speeds were used, so it is also possible that at blowing agent content above 2 phr, the pressure in the extruder was insufficient to maintain solubility leading to gas loss and higher bulk density. This observation led to further studies on the impact of gas solubility on foam microstructure.

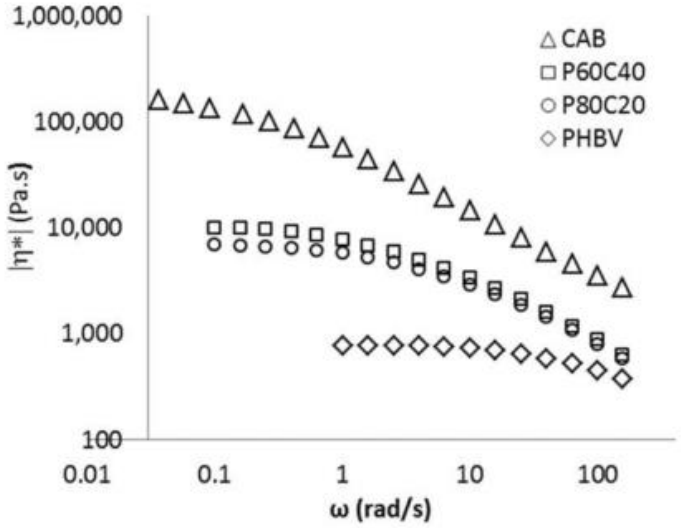

Figure 7.6: Representative complex shear viscosity curves of PHBV, CAB, and the blends as a function of oscillatory shear frequency (T = 140 °C)

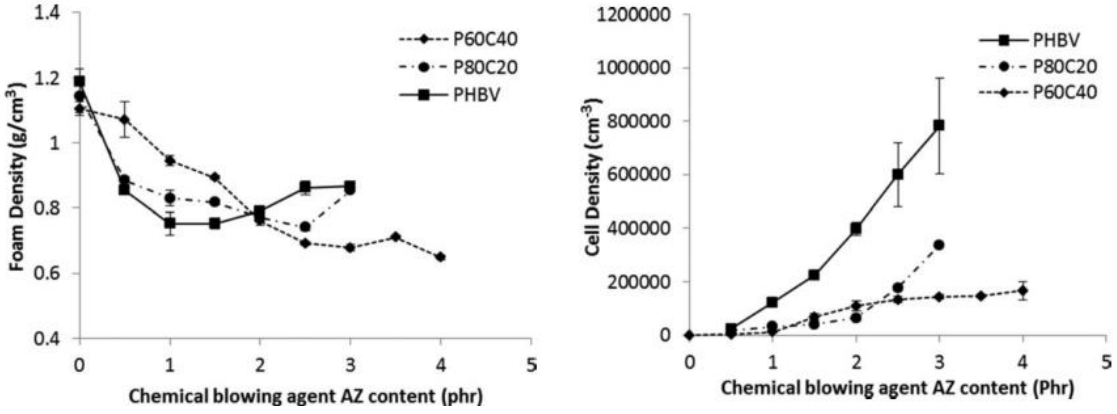

Figure 7.7: Bulk density (left) and cell density (right) of foams produced with varying amount of CAB and PHBV

7.7 Foams: Impact of solubility and processing

Understanding gas solubility

In the extruder barrel, the polymer melt and gas must form a homogeneous blend. This uniform distribution of gas allows uniform distribution of cell nuclei and even growth of cells. Foaming occurs due to the sudden pressure drop upon exiting the die, which causes phase separation of gas from polymer. If the pressure and temperature conditions in the die are not sufficient for complete gas solubility, early phase separation occurs, which has been known to lead to gas loss and the presence of large bubbles. It is therefore, important to understand what the solubility conditions must be for a given blowing agent content.

Direct means of determining gas solubility in a PHBV melt is not possible due to the relatively harsh measurement conditions for this thermally sensitive polymer. Applying methods developed by others for predicting gas solubility in polystyrene and polyethylene, gas solubility of nitrogen was calculated for PHBV. It was estimated that this predicted solubility had a 20 percent error. As shown in **Figure 7.8**, the prediction of the pressure threshold, above which the gas is soluble, aligns well with the observed step change in the cell density that occurs. Using these insights into improved foam processing, bulk density at AZ content above 2 phr was lower than previous foaming methods. However, overall bulk density was not improved and appeared to plateau. A gas with higher solubility could lead to more improved bulk densities.

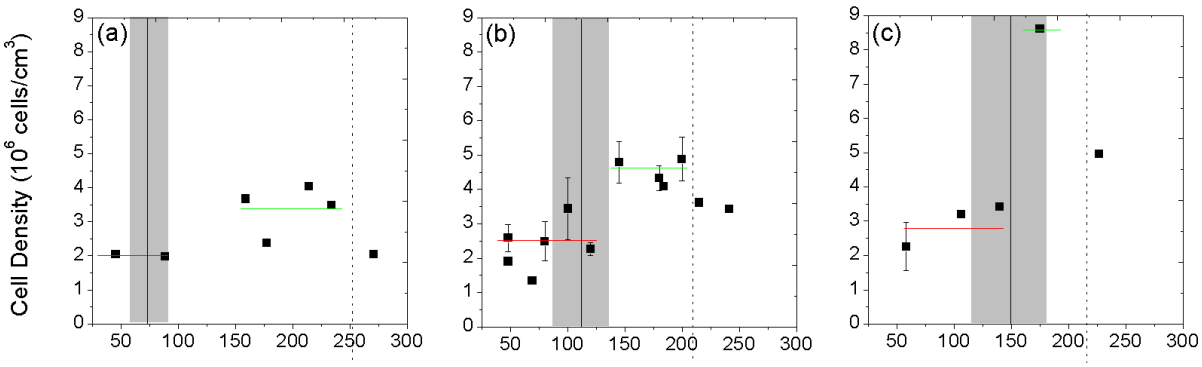

Figure 7.8: Cell density of (a) 2 phr, (b) 3 phr, and (c) 4 phr AZ content with increasing pressure. The lower (red) and upper (green) horizontal lines indicate the average cell density of the area of lower cell density that is dominated by large and irregular cells and the region of higher cell density, respectively. The dotted line separates the highest pressures attained, at which the cell density lowers again. Error bars indicate the standard deviation around the average cell density of multiple samples at the same processing conditions and same observed extruder pressure. The black vertical line indicates the predicted solubility pressure for the indicated blowing agent content and the gray area indicates a 20 percent error.

Foaming with carbon dioxide

SB was used to produce carbon dioxide, which was expected to have higher solubility in PHBV. As a result, bulk densities of SB foams were reduced significantly to 0.32 g/cm^3. However, the foam microstructure was very nonuniform; cells were particularly large in the center where the melt remained molten for longer than the edges and exhibited open cell structure. In order to improve the cell density and uniformity, water quenching was used on the extrudate. **Figure 7.9** shows the resulting change in cell density when water quenching is utilized. Cell density is significantly increased and a closed cell structure is observed. A downside of using SB is that water produced causes significant hydrolytic degradation of the polymer chains leading to lower molecular weight and poorer mechanical properties.

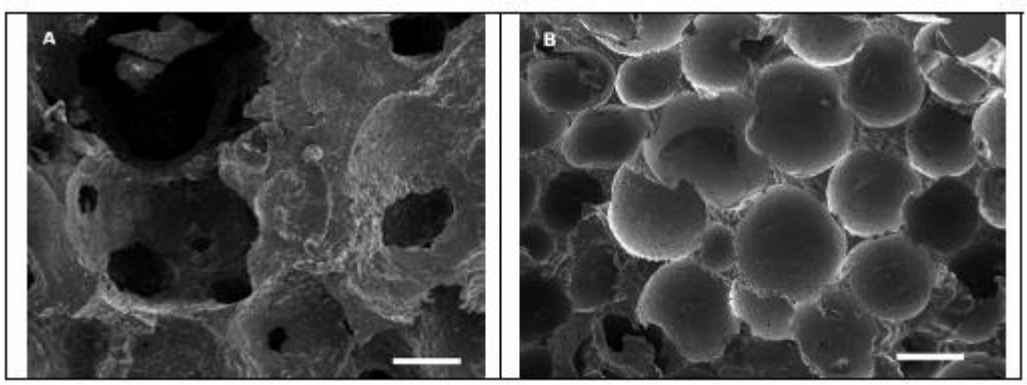

Figure 7.9: Extruded PHBV foams blown at 8 mL/g blowing agent potential of SB under (A) air cooling and (B) water cooling demonstrating open- and closed-cell structures respectively. Both scales are 200 microns

7.8 Foams: Process additives

Additives have long been added to foams to improve foam microstructure and lower the bulk density via heterogeneous cell nucleation or provide other benefits such as anti-oxidation or plasticization. We have studied the impact of both organic and inorganic additives with various particle sizes and surface energies.

Silk fibroin

Silk fibroin (SF) is a protein produced by silkworms that is known be biodegradable and have excellent mechanical properties. It was determined that SF and PHBV were immiscible, which could possibly promote bubble nucleation on the surface. However, the immiscibility led to unstable cell surfaces causing increased cell coalescence with increasing SF concentration. It is therefore important to use additives that can increase cell surface stability.

Silica nanoparticles

Nanoparticles can provide mechanical enhancement to growing bubbles, particularly if the particles are surface active at the gas/polymer interface. Here, silica nanoparticles were used due to the controlled geometry and ability to tune the surface chemistry. Because nanoparticles are prone to aggregation, the ability to properly disperse the particles is essential. **Figure 7.10** shows the results of three different methods of dispersion; sonication of the silica with PHBV proved to yield the most uniform microstructure. It is possible the bubbles were stabilized due to the earlier inducement of crystallization with the presence of silica.

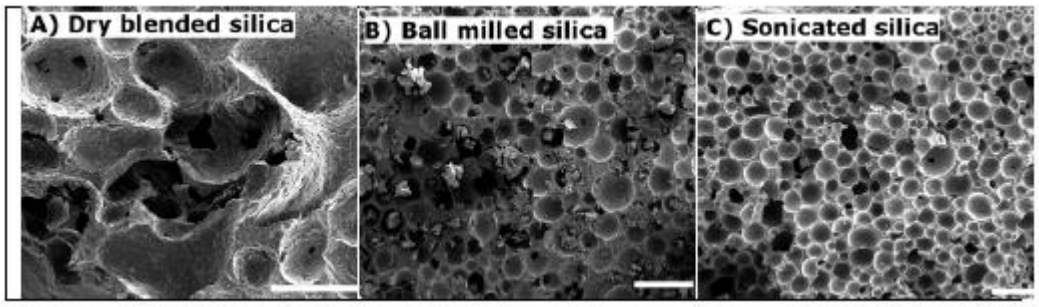

Figure 7.10: Scanning electron microscopy (SEM) images of foamed PHBV nanocomposites with 1 phr silica nanoparticles with (A) dry blending, (B) ball milling, or (C) sonication as the primary technique of silica dispersion in PHBV. Scale bars are 500 microns.

The amount of particle loading was also shown to affect the foam density. **Figure 7.11** shows the bulk density of foams produced with silica nanoparticles of various concentrations. Lower particle loading, such that aggregation was prevented, led to lower-density foams. To change to surface chemistry, a silane coupling agent, heptadecafluoro(1,1,2,2-tetrahydrodecyl)trimethoxysilane (HFTMS) was used. The HFTMS silica nanoparticles had much lower surface energy, which reduces the ability for PHBV to wet the surface.

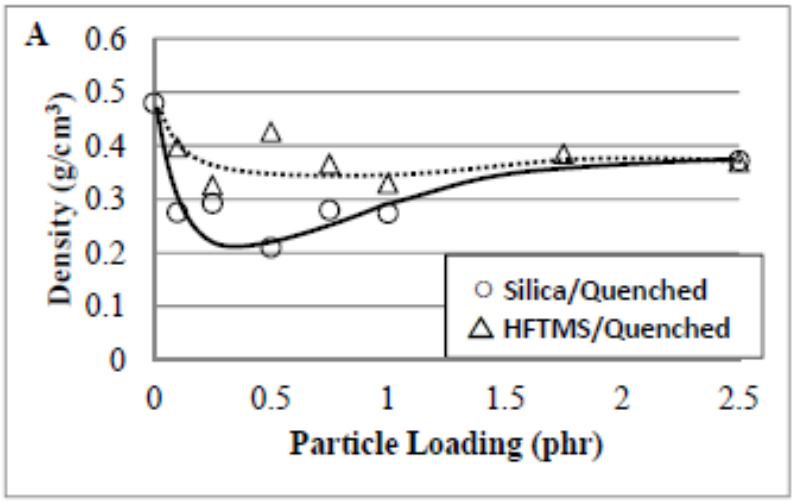

Figure 7.11: The bulk density of silica (circle) and HFTMS (triangle) nanocomposite PHBV foams blown with 5 phr SB and rapidly quenched with water are plotted as a function of particle content. Lines are to guide the eye.

7.9 Key findings

1. The density of PHBV is increased with addition of OWF due to the collapse or matrix infill of OWF during the injection molding process.
2. The introduction of OWF led to an increase in composite stiffness and to decreases in strength and elongation-to-break.
3. Both silane- and maleic anhydride-treated composites exhibited improved mechanical properties.
4. The crystallinity of neat PHBV decreased after MA-grafting via reactive extrusion, and the overall crystallinity of neat PHBV and MA-grafted PHBV decreased with the incorporation of OWF.
5. The initial modulus softening of MA-PHBV was overcome with as little as 17 vol% OWF.
6. The inclusion of natural textile woven reinforcement can double the initial stiffness of PHBV, and while different weave types lead to a change in ultimate tensile strength of the composites, most fibers examined resulted in similar tensile stiffness composites.
7. PHB polymer films exhibited mass loss, decreased molecular weight, decreased cross-sectional area, increased elastic modulus, and decreased ultimate strength and strain when exposed to moisture, heat, and UV.

8. PHB-hemp fiber composites exhibited mass loss, increased cross-sectional area, and decreased ultimate strength and modulus when exposed to moisture, heat, and UV, while ultimate strain increased in the presence of moisture and decreased otherwise.
9. Both the films and composites experienced increasing fading with weathering exposure. The presence of moisture generally exacerbated polymer and composite mechanical degradation, cracking, and fading.
10. During ambient storage, both PHB and PHBV polymer films exhibited significant increases in modulus and decreases in ultimate strain at break, while ultimate tensile strength remained relatively unchanged for both materials.
11. Results suggest that secondary crystallization does not make a significant contribution to physical aging. Rather, the amorphous regions undergo glassy aging in the rigid amorphous fraction over the span of months.
12. The absorption processes for all families of wood flour/PHBV composites were found to exhibit Fickian diffusion behavior.
13. Results suggested improved resistance to moisture uptake for the silane- and MA-treated wood flour/PHBV composites in contrast to the untreated samples.
14. Isodiffusion plots were developed to aid in the visualization of the dependence of OWF/PHBV composite diffusivity on temperature and fiber content.
15. After one saturation-dry cycle, the modulus of elasticity of PHBV increased, while the ultimate flexural strength decreased.
16. The change in PHBV properties was due to an embrittlement phenomenon that involved hydrolytic degradation of the polymer matrix phase.
17. Upon exposure to moisture, both the flexural mechanical stiffness and strength of the composites decreased, particularly in higher-fiber volume fraction composite samples.
18. Both a silane and maleic anhydride fiber-chemical modification resulted in negligible improvements in moisture-resistance and durability of the saturated and saturated-dry composites.
19. Blending PHBV with CAB increases its viscosity and results in foams that have lower bulk density and better cell uniformity. However, cell density is reduced.

20. Gas solubility in the extruder die must be maintained to avoid reductions in bulk density and cell density.
21. Using a gas with higher solubility, such as carbon dioxide, can lead to significant reductions in foam bulk density.
22. Rapid quenching with water is an effective method for cooling PHBV foamed with SB to maintain high cell density.
23. Low concentrations of silica nanoparticles can provide cell stabilization to promote lower bulk density and more uniform bubbles.

8. Anaerobic Biodegradation of PHB, PLA, and Biocomposites

8.1 Executive summary

Anaerobic biodegradation refers to microbial breakdown of organic matter to biogas, a mixture of methane and carbon dioxide, in the absence of oxygen. This process occurs naturally in landfills and anaerobic digesters. The biogas can be burned for heat or electricity or used to produce PHB. If not collected and allowed to enter the atmosphere, methane contributes significantly to greenhouse gas emissions and global warming. Anaerobic degradation summarized in this chapter confirms that polyhydroxyalkanoates (PHAs) and PHA-based biocomposites are rapidly biodegradable to biogas under anaerobic conditions. By contrast, polylactic acid (PLA) is only slowly biodegradable, and the extent of degradation was greater at higher temperatures. These observations suggest advantages for thermophilic degradation of PLA.

Key publications:

Morse, M.C. (2009). Anaerobic biodegradation of biocomposites for the building industry. Ph.D. Thesis. Stanford University, Stanford, CA.[24]

Ryan, C.A. (2014, Expected) Closed-loop life cycle engineering of biopolymer composites: end-of-life degradation and reuse. Ph.D. Thesis. Stanford University, Stanford, CA.[25]

Morse, M.C., Liao, Q., Criddle, C.S. and Frank, C.W. 2011. Anaerobic biodegradation of the microbial copolymer poly(3-hydroxybutyrate-co-3-hydroxyhexanoate): Effects of comonomer content, processing history, and semi-crystalline morphology. Polymer. 52, 2 (2011), 547–556.[26]

8.2 Introduction

Anaerobic biodegradation of an organic solid, such as a biopolymer or biocomposite, begins with microbial colonization of the solid surface. The attached microorganisms secrete enzymes that hydrolyze the solid, breaking it down into smaller molecules that can be taken up into the microbial cells. After uptake, these molecules are fermented into fatty acids and hydrogen. Longer-chain fatty acids are converted to acetic acid. Ultimately, acetate-utilizing methanogens cleave acetic acid, releasing methane and carbon dioxide, and hydrogen-oxidizing methanogens oxidize hydrogen while reducing carbon dioxide to methane. In the research summarized in this chapter, two primary

methods were used to assess biodegradability of PHB and PHBV biopolymers and biocomposites: In the first, test samples were incubated with anaerobic digester sludge and the volume of biogas generated is manually monitored over time; in the second, biogas was automatically monitored using the Automated Methane Potential Test Set-up. The AMPTS unit from Bioprocess Control accommodates samples of 0.5g allowing biodegradation of larger samples. Visual confirmation of biocomposite biodegradation was accomplished by scanning electron microscopy and by micro X-ray computed tomography (Micro-CT).

8.3 Anaerobic biodegradation of PHB and PHB-hemp biocomposites

Biocomposites were prepared using three different matrix materials—polyhydroxybutyrate (PHB), cellulose acetate (CA), and soybean oil (SO)—and reinforced with four layers of hemp fiber fabric (roughly a 40 percent fiber fraction by weight).[45] These samples were cut into 0.2g pieces, and incubated in anaerobic digester sludge at 37°C. Biogas volume produced was determined manually. As shown in Fig 8.1, the PHB-based biocomposite biodegraded significantly more quickly than biocomposites prepared with CA and SO.

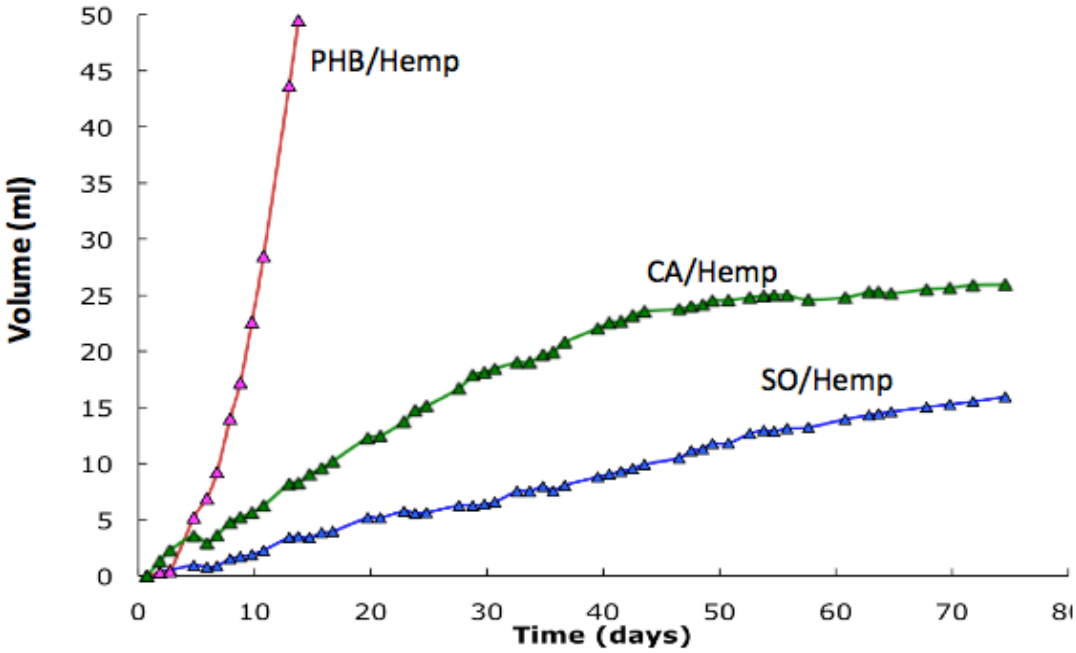

Figure 8.1: Gas production from biocomposites made with polyhydroxybutyrate (PHB), cellulose acetate (CA) and soybean oil (SO). All biocomposites were

reinforced with hemp fabric, weighed 0.2g and were immersed in anaerobic digester sludge at 37^{o}C.

Scanning electron microscopy (SEM) was used to investigate the sample surface of the PHB-based biocomposite. **Figure 8.2** illustrates the extent of biodegradation after one week of incubation: by this point, microorganisms had excavated much of the PHB matrix, exposing hemp fibers that protruded from the remaining matrix material.

Table 8.1 summarizes the extent of biodegradation of the biocomposites containing PHB, CA, and SO resins. The PHB-containing biocomposite degraded to a much greater degree than those prepared with CA or SO.

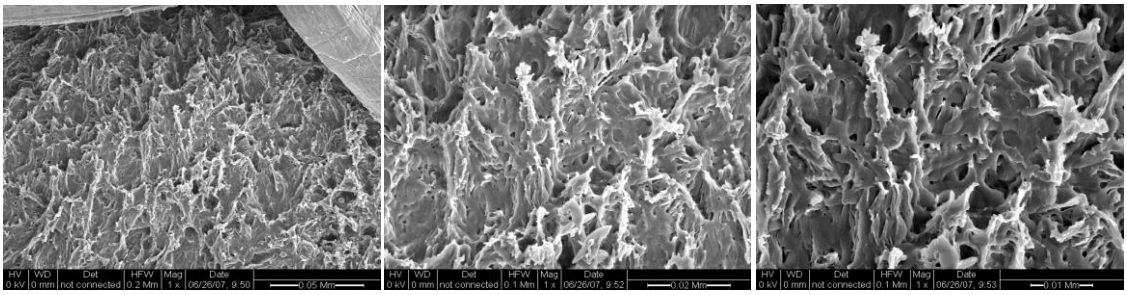

Figure 8.2: PHB-based biocomposite at three different magnifications. Samples with four layers of hemp were allowed to biodegrade for seven days and were

then washed with phosphate buffer. In the image at left, a hemp fiber is exposed. Microorganisms removed and excavated the surrounding PHB matrix.

Table 8.1: Biocomposite materials and biodegradation characteristics

Material	COD/Wt	Theoretical Biogas Production for 0.07g material	% Methane Recovered	% Mass Loss	Max Biogas/Day [ml/day]
Hemp	1.1	63	75	100	2
PHB Plastic	1.7	84	60	100	8
PHB/Hemp		75	65	90	5.2
SO Based Plastic (SOBP)	2.5	109	20	30	
SOBP/Hemp		90			0.2
CA Based Plastic (CABP)	1.4	74	20	30	0.9
CABP/Hemp		69	15	30	0.6

Figure 8.3 illustrates the pattern of biodegradation for PHB and hemp at 30°C to 37°C. For both materials, biodegradation was faster at 37°C, but increasing the temperature had more impact on PHB degradation than on hemp. The anaerobic seed material for this experiment originated in an anaerobic digester operated at roughly 37°C. Thus, the microorganisms in the seed were preselected for growth at 37°C. By lowering temperature, the microbial community was less efficient, and could not function as effectively.

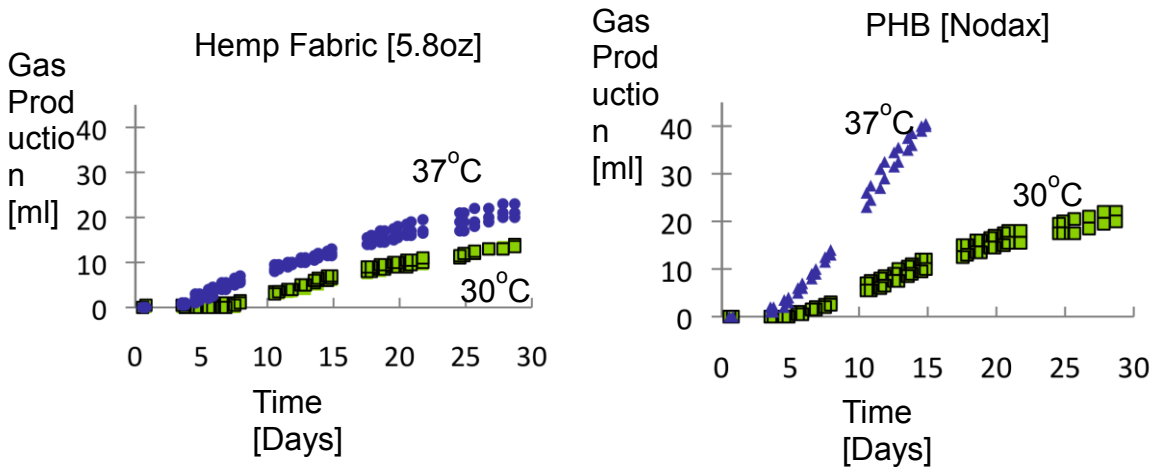

Figure 8.3: Effects of temperature on biogas production for hemp fabric and PHB

8.4 Anaerobic biodegradation of oak wood flour and PHBV biocomposites

The anaerobic biodegradability of a biobased composite consisting of oak wood flour (OWF) and poly(hydroxybutyrate)-*co*-poly(hydroxyvalerate) (PHBV) was evaluated to determine the effects of varying the weight percent of filler along with the silane fiber treatment and maleic anhydride graft.[46] To assay anaerobic biodegradability, two automated methane potential test systems from Bioprocess Control—AMPTS I and AMPTS II—were used **(Figure 8.4)**. This test measures methane generated from the composite samples while they degrade at 37°C under anaerobic conditions. Anaerobic digester sludge from the San Jose wastewater treatment plant was used as the inoculum. Gas chromatography (GC) was used to determine the percentage of CH_4 and CO_2 in the microcosm headspace.

Figure 8.5 shows methane production from different biocomposite samples. Samples investigated were PHBV with untreated oak wood flour, PHBV with silinated oak wood flour, and biocomposites with varying weight percent of OWF, plus 2 percent PHBV modified with a maleic anhydride. The composite geometry was a 31mm x 2mm x 6mm rectangular prism, and all samples were approximately 0.5g.

Figure 8.4: Automated methane potential test setups from Bioprocess Control: AMPTS I (left) and AMPTS II (right). Methane is collected from the anaerobic degradation of the biocomposites. T-valves near the gas headspace in the microcosm allow for the collection of gas composition samples, which were measured using gas chromatography. Microcosms are kept at 37°C.

To calculate the theoretical gas production expected for each sample, a control sample consisting of the anaerobic inoculum with no sample is subtracted from the gas measured on each sample channel. The gas generated is normalized by the mass of the composite sample.

The theoretical gas production in mL/g was calculated using the stoicheometry from the Buswell and Mueller equation:[27]

$$C_aH_bO_c + \left(\frac{4a-b-2c}{4}\right)H_2O \rightarrow \left(\frac{4a+b-2c}{8}\right)CH_4 + \left(\frac{4a-b+2c}{8}\right)CO_2$$

The Buswell and Mueller equation was used to compute gas production for PHBV and cellulose-based biocomposites, using the empirical formula for PHBV and assuming that approximately 45 percent of the weight of the oak wood flour is α-cellulose that can degrade anaerobically. Results from a positive control for α-cellulose was indicated that greater than 70 percent of the theoretical methane was produced, indicating sufficient inoculum activity for a valid test.

The percentage of theoretical methane produced in almost all of the composites exceeded 80 percent, indicating a high level of anaerobic degradability and establishing that fiber and polymer treatments did not have a negative impact. The composites typically reached 80 percent of the theoretical methane yield at four to six weeks. For higher weight fractions of oak wood flour in the treated composites, however, a slight retardation in rate was observed, with the sample

reaching 80 percent after six to eight weeks.

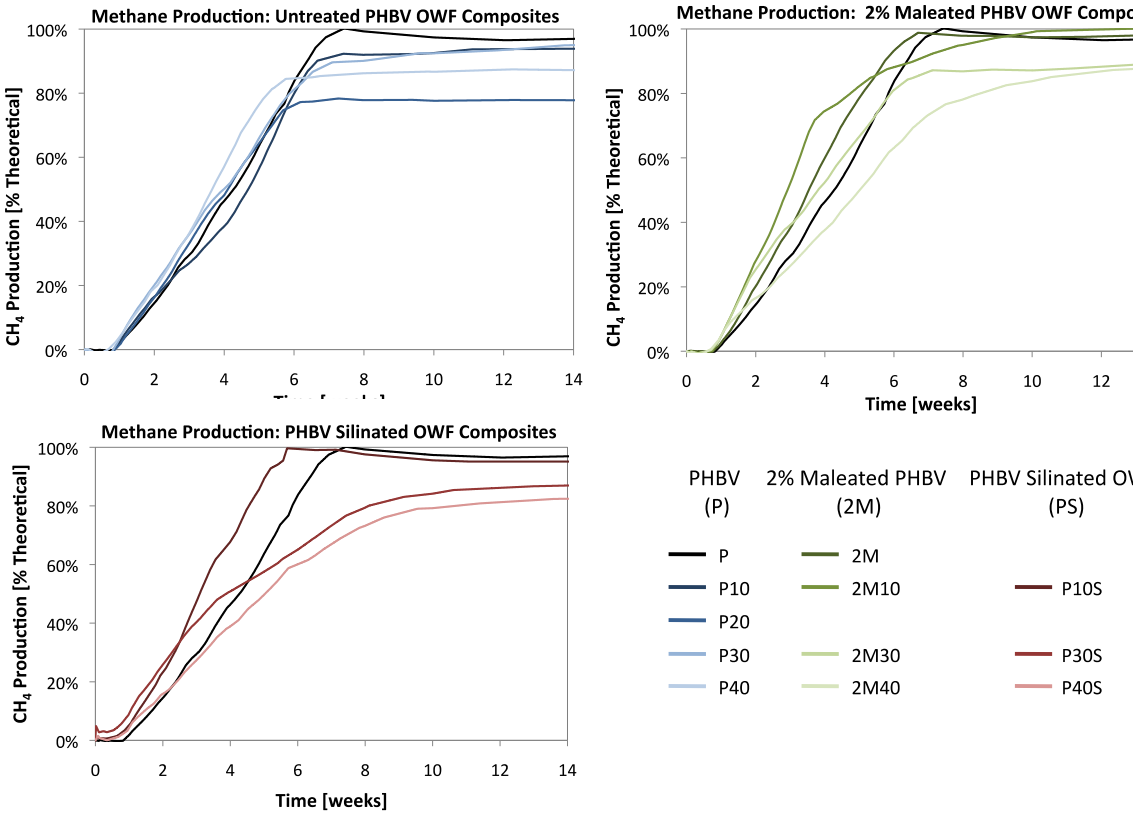

Figure 8.5: Methane produced from the anaerobic degradation of PHBV-biocomposites. Results are shown for PHBV with varying weight fractions of OWF and two treatments: silination of the OWF (PS) and the addition of a 2 percent fraction of PHBV with a maleic anhydride treatment (2M). These treatments are compared to untreated biocomposites (P). Samples P and 2M had no added oak flour. The weight percentages of oak flour for Samples P10, P20, P30, and P40 had oak floor added at 9.8, 21.5, 36.3, and 44.7 weight percent, respectively. Samples 2M10, 2M30, and 2M40 had oak floor added at 14.7, 38.6, and 39.4 percent, respectively. Samples P10S, P30S, and P40S had oak floor added at 14.9, 35.7, and 55.1 percent, respectively.

8.5 Anaerobic biodegradation of PHBV, P3HB-co-3HHx, and PLA

Adding copolymers of hydroxyvalerate (HV) and hydroxyhexanoate (HHx) to PHB is of interest because of their ability to influence processing temperatures and material ductility. Accordingly, we investigated the anaerobic biodegradability

of PHBV and P3HB-*co*-3HHx and compared the degradation of these polymers to PLA, the bioplastic that is most commonly used commercially.

Figure 8.6 illustrates biodegradation of 0.5g of Tianan PHBV Y1000P powder compared to Tianan PHBV pellets processed into a 0.5g, 31mm x 2mm x 6mm sample via injection molding. The rate of degradation increased for the powdered sample, but both samples ultimately achieved the same extent of biodegradability.

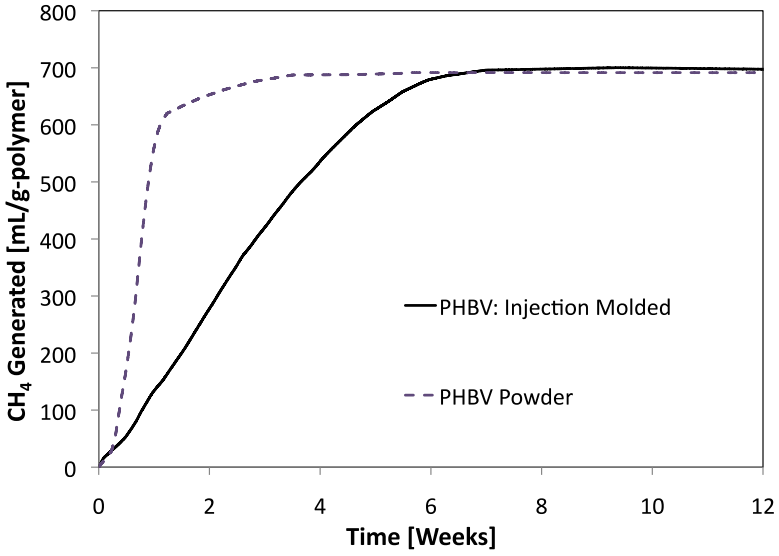

Figure 8.6: Anaerobic degradation of an injection-molded PHBV sample and PHBV powder as measured by the methane generated from each sample during degradation

Because of the interesting material properties obtained by adding HHx copolymer content to PHB, the anaerobic degradation of copolymers of P3HB-*co*-3HHx was investigated**.** Powders of P3HB-*co*-3HHx provided by Procter & Gamble were pressed into thin film specimens of approximately 0.3 mm thickness with the following molecular compositions:

Sample Name	Polymer	M_w ($x10^3$)	M_w/M_n
P3HB-co-3HHx3.8	Poly(3-hydroxybutyrate-co-3.8mol% 3-hydroxyhexanoate)	659	2.99

P3HB-co-3HHx4.6	Poly(3-hydroxybutyrate-co-4.6mol% 3-hydroxyhexanoate)	658	2.87
P3HB-co-3HHx6.9	Poly(3-hydroxybutyrate-co-6.9mol% 3-hydroxyhexanoate)	723	2.55
P3HB-co-3HHx10	Poly(3-hydroxybutyrate-co-10mol% 3-hydroxyhexanoate)	312	2.30

Anaerobic degradation of the copolymers of P3HB-*co*-3HHx was investigated using the test procedure outlined by Morse in reference 45. Figure 8.7 shows anaerobic degradation measured by mass loss for the different HHx comonomer contents.

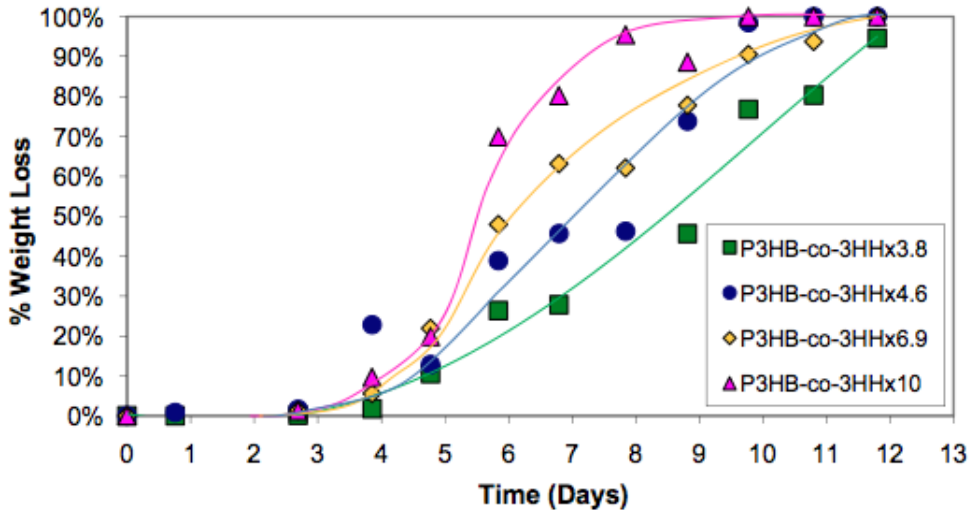

Figure 8.7: Anaerobic biodegradation of P3HB-*co*-3HHx samples. Weight loss was fastest for samples with the highest fraction of comonomer: HHx (P3HB-*co*-3HHx10). At 100% weight loss, no remaining sample could be collected.

The rate of microbial biodegradation of P3HB-*co*-3HHx was dependent upon the copolymer composition and processing history. Increasing the 3HHx fraction in P3HB-*co*-3HHx resulted in increased rates of biodegradation. This is likely due to decreased crystallinity, as confirmed by differential scanning calorimetry.

In order to investigate the potential for the anaerobic degradation of NatureWorks 2003D PLA, a test of anaerobic biodegradability was conducted at 37°C and 55°C, and compared to the results for Tianan PHBV Y1000P at 37°C. All samples were fabricated by hot pressing thick (~0.3mm) films of the plastic and trimming the samples into squares weighing approximately 0.05g. Anaerobic digester sludge from the San Jose wastewater treatment plant was used as an inoculum. The sludge for the PLA biodegradation tests was first added to digesters that were fed PLA from NatureWorks cups for two weeks, and maintained at the test temperature (37°C or 55°C) for three weeks to enable acclimation to the PLA and elevated temperature (55°C). The sludge for the PHBV test was kept at 37°C for one week with no additional feeding prior to initiating the test. The total biogas generated was collected and measured and compared to a negative control of the inoculum (following test procedure in reference 45). As shown in **Figure 8.8**, the biodegradation of the PHBV initiated quickly, within seven days. Biogas production from the PLA samples at both 37°C and 55°C initiated much more slowly, requiring approximately 30 days before appreciable biogas production exceeding that of the control was observable. The extent of the PLA degradation was also less than that of the PHBV. The Buswell and Mueller equation and the chemical formulas for PLA ($C_3H_4O_2$) and PHB ($C_4H_6O_2$) were used to calculate the theoretical amount of biogas for each plastic. Based on this calculation, the expected amount of biogas generated from PHBV should be 1.3 times the amount generated from PLA. As can be seen in **Figure 8.8**, the ratio was closer to three times. It is significant, though, that biogas production from PLA was observed. Further testing would be of interest as a potential method of material recycling PLA to biogas.

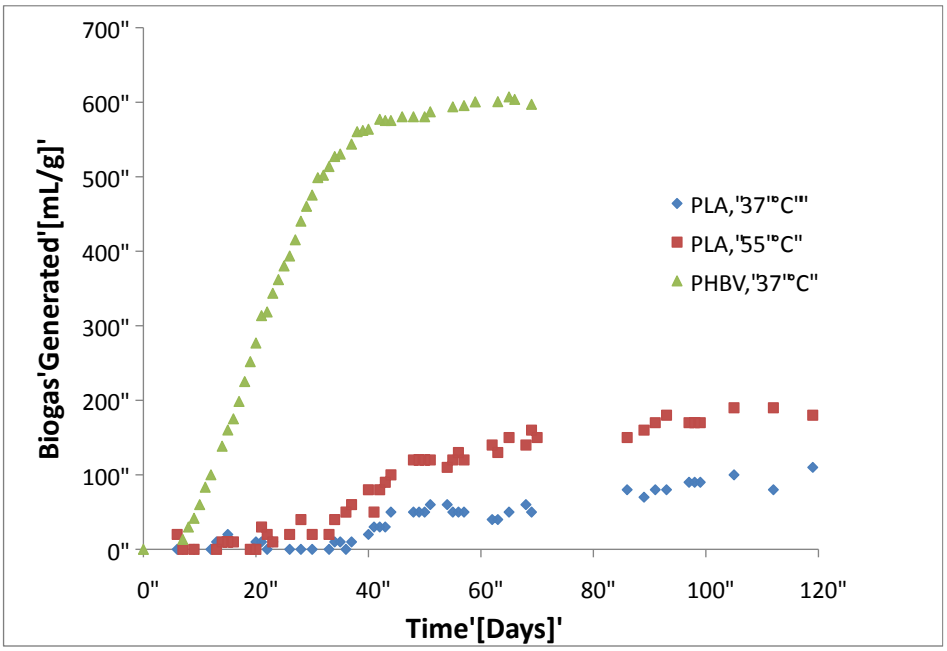

Figure 8.8: The biogas generated from PLA, tested at both 37 °C and 55 °C, and PHBV, tested at 37 °C. All samples have the gas generated from the negative control subtracted, and are normalized by the sample mass.

8.6 Key findings

1. Fully biobased composites exhibited a high level of anaerobic degradability; almost all of the composites produced 80 percent or greater of the theoretical methane expected based on stoichiometry.
2. PHB-based biocomposites biodegraded significantly faster, with biogas production 8 to 25 times faster than that observed with cellulose acetate and soybean oil-based biocomposites.
3. Almost all of the biobased samples, including those with fiber and matrix treatments (silination and maleation) reached 80 percent of theoretical degradation by four to six weeks. For the higher-weight fractions of oak wood flour in the treated composites, a slight retardation in rate was observed with samples reaching 80 percent around six to eight weeks.
4. When compared to PHBV, the rate of PLA degradation is slower, resulting in lower percent biodegradability over time. However, that biogas output from PLA was observed is interesting to note, as PLA is typically not considered for anaerobic degradation.
5. The microbial biodegradation rate of P3HB-*co*-3HHx depends on the copolymer composition and processing history. Increasing the 3HHx fraction in P3HB-*co*-3HHx resulted in increased rates of biodegradation that are likely due to the decreased crystallinity.

6. The amount of biogas generated at 55°C for PLA is approximately double that observed at 37°C, indicating that further testing of anaerobic biodegradability at 55°C is warranted.

9. Depolymerization and Re-polymerization of Polyhydroxyalkanoates (PHAs)

9.1 Executive summary

Thermal or chemical recycling of polymer products often leads to downcycling, in which polymer properties degrade with successive reuse. Depolymerizing polymer to recreate monomer units can circumvent this issue if the resulting monomer can be re-polymerized to form virgin material. In the case of polyhdroxybutyrate, base-catalyzed hydrolysis of polymer chains yields a mixture of hydroxybutyrate (HB) and crotonate monomer. For the copolymer polyhydroxybutyrate-co-hydroxyvalerate (PHBV), this mixture includes the hydroxyvalerate (HV), 2-pentanoate, crotonate, and pentanoate, respectively.

PHB can be degraded anaerobically to methane gas and reassembled into virgin material through the action of methanotrophic bacteria. The stoichiometry of such an approach is detailed in Chapter 11. Biological degradation is less efficient than chemical digestion, as carbon and energy are lost to microbial metabolism, production of biomass, and release of CO_2. A more direct approach involves chemical depolymerization of PHB to HB followed by biological reassembly of HB to form virgin PHB. To determine the feasibility of this process, a community of bacteria selected from activated sludge was fed HB in regular pulses to induce storage of PHB. When these cultures were then exposed to nitrogen-limited conditions, PHB production of up to 50 percent by dry weight was observed, verifying the efficacy of biological PHB repolymerization.

In addition to HB and HV monomer, depolymerization by hydrolysis can result in dehydration of HB and HV to crotonate and pentanoate, respectively. Crotonate is often viewed as a dead-end product. But crotonates are isomers of methacrylates, differing only on the point of attachment of the methyl group to the olefin (at the 2- and 1-positions, respectively). Poly(methacrylate)s are widely used with applications in construction, electronics, and medicine. The applications market for polymethyl methacrylate (PMMA), or Plexiglas, is expected to be worth $9.7 billion by 2017.[28] Like methacrylates, crotonate can be chemically polymerized to polycrotonates, a class of polymers with highly tunable properties and a high melting point. To date, however, this synthesis has proved challenging and often involves environmentally undesirable solvents and catalysts. Research in the lab of Professor Robert Waymouth (Dept. of Chemistry, Stanford) indicates that polymerization of crotonate is possible without harsh catalysts,

demonstrating potential for “upcycling” from methane to PHB to crotonate to high-value polycrotonates (James Flanagan, personal communication).

9.2 Hydrolysis of PHB and PHBV

PHB collected at end of life can be repurposed in numerous ways, including direct reuse, recycling of intact polymer, depolymerization, or anaerobic digestion. Due to degradation of polymer chains during recycling and metabolic inefficiencies inherent in anaerobic digestion, hydrolysis is an attractive option for monomer recovery followed by re-polymerization. Hydrolysis of PHB-rich biomass is also a potential alternative to extraction of intact polymer, if crotonate or HB are desired products.

Hydrolysis of PHB yields HB, which may undergo dehydration to crotonate. Under acidic conditions complete dehydration occurs, with only crotonate produced. Under basic conditions, a mixture of HB and crotonate is produced. Products produced by hydrolysis of PHV are unknown, but under basic conditions the carbon analogues hydoxyvalerate, 2-pentenoate, and 3-pentenoate are expected. These compounds are shown in **Figure 9.1.** Understanding and ultimately controlling the resulting hydrolysis products is a key determinant of available options for re-polymerization.

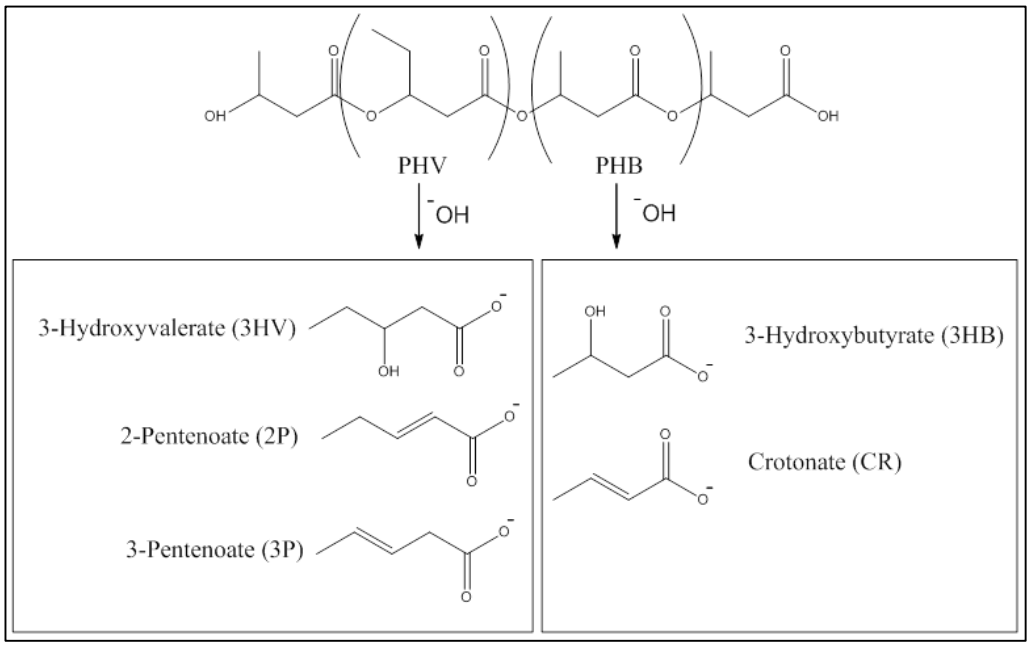

Figure 9.1: Products of PHB and PHV depolymerization. Products for PHB hydrolysis are known; products for PHV are proposed.

To determine the distribution of products produced during hydrolysis of PHBV, commercially available PHBV was hydrolyzed under basic

conditions at 60˚C with the resulting monomer distribution analyzed via gas chromatography. As expected under basic conditions, a mixture of HB and crotonate was produced, with the reaction slightly favoring production of HB. The total distribution of species produced is depicted in **Figure 9.2**. A similar pattern was reflected in the five carbon analogues as shown in **Figure 9.3**. Notably, the dehydration reaction produced 2-pentanoate exclusively, with no significant production of 3-pentanoate observed.

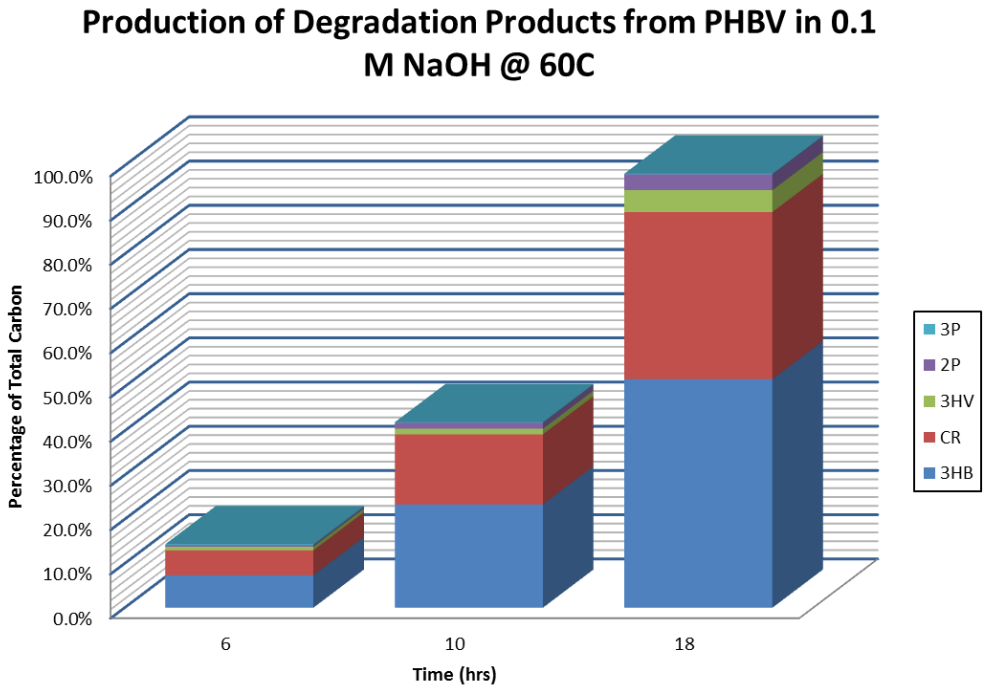

Figure 9.2: Distribution of product formation over time during hydrolysis of PHBV under basic conditions at 60˚C. Compounds observed are as follows: 3HB (hydroxybutyrate), CR (crotonate), 3HV (hydroxyvalerate), 2P (2-pentenoate), and 3P (3-pentanoate).

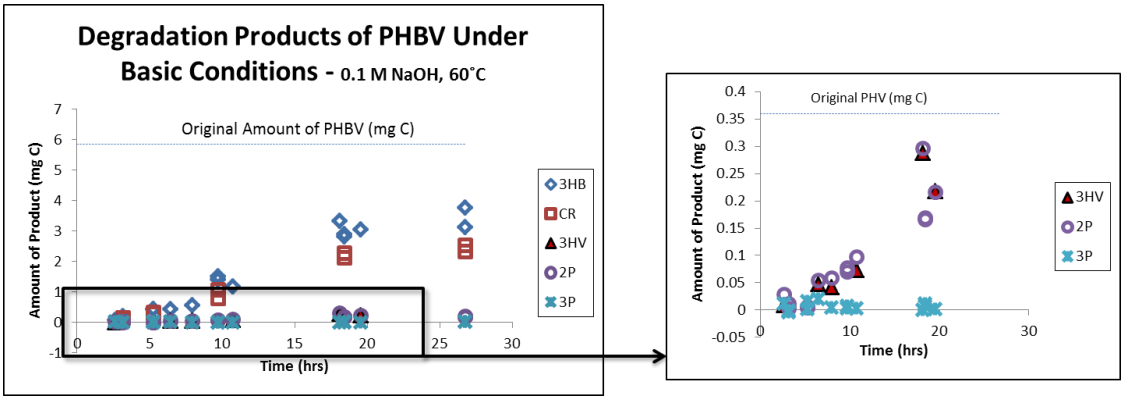

Figure 9.3: Rate of product formation over time during hydrolysis of PHBV under basic conditions at 60˚C. Compounds observed are as follows: 3HB (hydroxybutyrate), CR (crotonate), 3HV (hydroxyvalerate), 2P (2-pentenoate), and 3P (3-pentanoate). The total distribution is shown at left, with only the five-carbon compounds shown at right.

9.3 Biological repolymerization of hydroxybutyrate

Polymerization of HB to PHB is the final step in microbial PHB synthesis across known PHB-producing organisms. Use of HB as a sole substrate for growth and PHB production has not been evaluated previously due to the present lack of an inexpensive source of HB. Acetate-metabolizing organisms are known to accumulate PHB at concentrations of up to 90 percent during exposure to feast-famine conditions, in which acetate is supplied in periodic spikes. Organisms exposed to substrate excess are forced to store acetate as polymer, and later use stored polymer for reproduction after available substrate is exhausted. A similar approach should be practical for use with HB replacing acetate. Production in mixed culture eliminates the need for sterilization, and could yield a robust process practical for distributed operation.

To determine if HB can be used directly as a substrate for growth and PHB production in mixed culture cultivation, activated sludge was collected from the Palo Alto Regional Water Quality Control Plant (PARWQCP) to serve as a diverse inoculum. This sludge was oxygenated and spiked with fresh, HB-containing media on a 12-hour cycle. PHB production, nitrogen consumption, and HB consumption were monitored over time. Periodically, cells were removed for off-line incubation in nitrogen-free conditions to determine ultimate PHB production.

As expected, PHB production occurred for 1.5 hours after the addition of excess HB as organisms were incentivized to rapidly uptake available substrate. This PHB was consumed as cells reproduced over the remaining 10.5 hours of cycle time (**Figure 9.4**). All HB was consumed after eight hours, with nitrogen present throughout the cycle (**Figures 9.5 and 9.6**). Maximum PHB was measured by gas chromatography at the end of the no-nitrogen cycles. Values of up to 50.4 percent PHB by dry weight were recorded after 12 hours of off-line incubation without nitrogen.

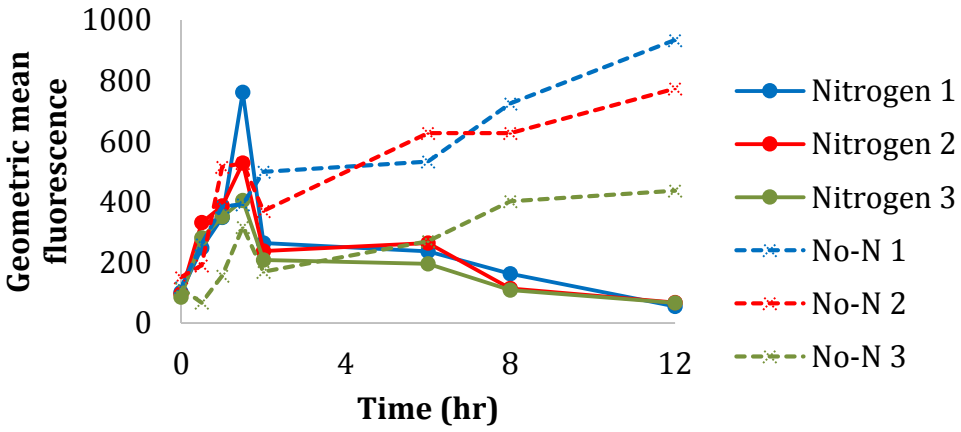

Figure 9.4: PHB content for enrichment cultures fed with pulses of HB in both the presence and absence of available nitrogen. Nile red fluorescence is used as a proxy for PHB content. Time courses for three independent replicates are plotted.

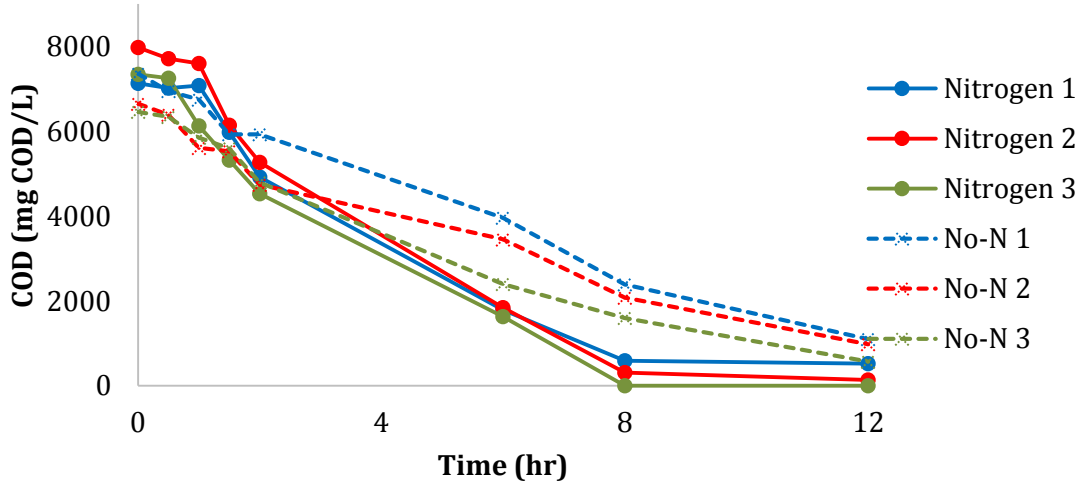

Figure 9.5: COD (chemical oxygen demand) oxidation for enrichment cultures fed with pulses of HB in both the presence and absence of available nitrogen. Time courses for three independent replicates are plotted.

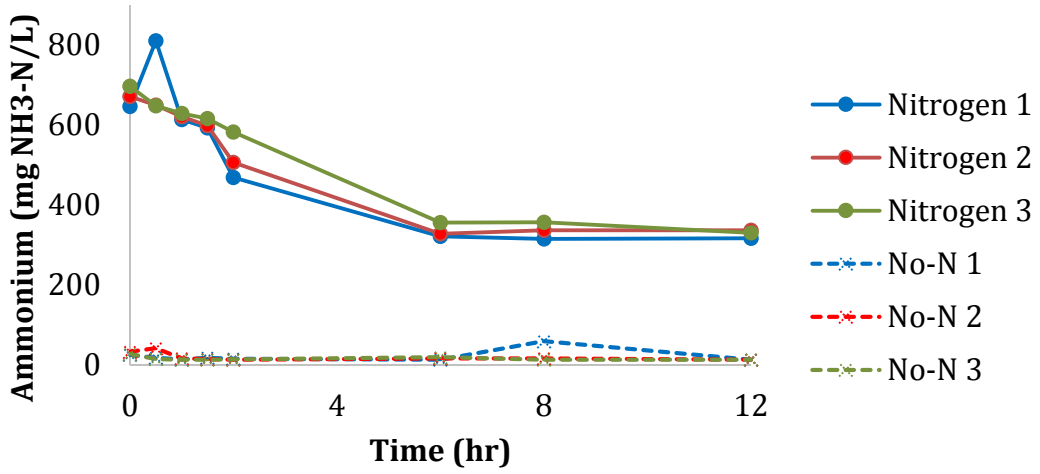

Figure 9.6: Nitrogen consumption for enrichment cultures fed with pulses of HB in both the presence and absence of available nitrogen. Time courses for three independent replicates are plotted.

9.4 Production of polycrotonates

Unsaturated carboxylic acids produced by hydrolysis of PHB and PHBV include crotonate and 2-pentenoate. Production of these compounds is promising due to their similarity to the unsaturated acids acrylate and methacrylate, both of which are precursors to commercially produced petrochemical plastics (**Figure 9.7**). Polycrotonate has previously been synthesized in small quantities, but commercial interest has been low as there is no current large-scale source of crotonate. Properties of polycrotonates are promising; modification of the ester group would allow for highly tunable properties, while the measured degradation temperature is close to 100˚C higher than the melting temperatures, leading to a large temperature window for manipulation. Hydrolysis of PHB under acidic conditions leads to complete dehydration of HB to form crotonate. Given the low cost of hydrolysis and the potential value of polycrotonates as alternatives to acrylates such as Plexiglas, production of pure crotonate could create a significant revenue stream for processing of recovered PHB.

Current methods for crotonate polymerization implemented at laboratory scale rely on harsh chemicals, including cadmium and mercury catalysts. Initial experiments with group transfer polymerization (GTP) using N-heterocyclic carbene (NHC) and Bronsted-acid catalysts have yielded promising results, with polymer of up to 9700 Da produced when using Bronsted-acid catalysis. Yields were approximately 10 percent and must be improved through further optimization. Once an efficient protocol has been determined, physical and chemical testing of the resulting polymer will be required to determine optimal

uses and applications for polycrotonates. Ultimately, manipulation of the ester group should allow tunability for use across a wide variety of applications.

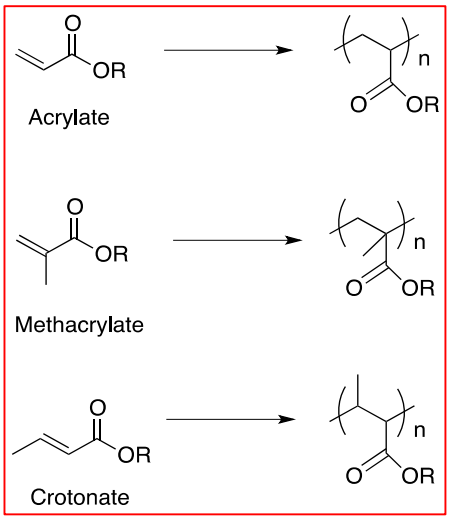

Figure 9.7: Polymerization of crotonate as compared to production of polyacrylate and polymethacrylate

9.5 Key findings

1. Chemical depolymerization of PHB can be used to rapidly recover HB and crotonate from PHB products at end of life.
2. Hydrolysis of PHBV yields both pentenoate and hydroxyvalerate.
3. Biological reassembly of HB monomer to PHB is feasible.
4. PHB production of up to 50 percent is observed in mixed cultures fed HB under feast-famine conditions.
5. Crotonate can be used as a feedstock for polycrotonates, a class of polymers with promising material properties, but end-of-life options require further investigation
6. Production of polycrotonates without the use of hazardous catalysts appears feasible, but yields must be improved.

10. PLA Depolymerization: Enzymatic Hydrolysis and Thermal Depolymerization

10.1 Executive summary

Polylactic acid (PLA) is a renewable thermoplastic and alternative to conventional petroleum-derived plastics because of its physicochemical properties. It is widely used, but issues of fate and recycling need to be resolved. In some environments (anaerobic digesters and seawater), PLA biodegradation rates are slow, and recycling options would be of value as another end of life option. Bench-scale studies suggest potentially viable solutions based on enzymatic hydrolysis and thermal depolymerization.

PLA is produced by production of lactic acid, lactic acid conversion to lactide, and catalytic polymerization of lactide. Because PLA is not produced naturally, enzymes that can depolymerize it do so fortuitously, having initially evolved for hydrolysis of other biopolymers that are produced naturally. Consequently, screening of existing hydrolase libraries is a potentially useful strategy for PLA depolymerase activity. Multiple protocols were developed to screen for PLA-degrading activities within banks of recombinant clones and purified proteins at the University of Toronto. Genes encoding PLA-degrading activity were identified, and the encoded enzymes were purified and characterized for hydrolytic activity. More than 22 novel PLA depolymerases were identified. These findings indicate that PLA depolymerase activity is present in a diverse range of microorganisms from different habitats. PLA depolymerase activity was detected for a marine gram-negative bacterium, and several hydrolases were identified that can function at low temperatures, a result of potential significance for the fate of PLA in marine environments.

Vacuum-heating of materials containing polylactide and a tin(II) catalyst at 190^{o} to 200^{o} C resulted in thermal depolymerization of the PLA and release of lactide vapors. Upon condensation, white lactide crystals were recovered. PLA-containing materials evaluated included PLA resin, commercial PLA cups, and blends containing PLA and different levels of poly(butylene adipate-*co*-terephthalate) (PBAT). Efficient recovery of lactide was achieved in all cases (up to 95-98%) except in the blend containing 50% PBAT where lactide recovery decreased due to catalyst inactivation. The crystals recovered contained high levels of lactide (96-99%) and a consistent isomer content: L-lactide (>88%), D-lactide (6%), and *meso*-lactide (<0.2%). The tin (II) catalyst (0.1%, w/w) was reusable for repeated (three times) thermal depolymerization.

Key publications:

Hajighasemi, M., A. Tchigvintsev, W. Wu, C.S. Criddle, E.A. Edwards, and A. F. Yakunin. 2013. Enzymatic degradation of polylactic Acid. In preparation.[29]

Wu, W.M., C. LaFeldt, J. Ren, Q. Wang , R, Narayan, and C. S. Criddle 2013. Recovery of lactide by thermal depolymerization of poly(lactic acid) materials. Submitted for publication.[30]

10.2 Motivation

The attractive physicochemical properties of PLA have led to its widespread commercial use, but its rate of biodegradation is slow in anaerobic digesters (Chapter 8), compost, and the marine environment. Methods of accelerating these activities are desirable. Also needed are efficient methods of recycling PLA without downcycling.

10.3 Enzymatic depolymerization

Enzymes that hydrolyze PLA can potentially be applied directly to post-consumer PLA plastic waste to produce lactic acid monomers suitable for re-polymerization into virgin polymer. PLA hydrolases might also be employed to increase the biodegradability of PLA products in environments where PLA currently degrades slowly, such as anaerobic digesters, compost, and the marine environment.

To identify PLA depolymerases, numerous *E. coli* hosts carrying gene fragments from environmental samples were screened for PLA degradation activity. Each recombinant bacterial cell produces a particular enzyme encoded by the inserted gene fragment. Each enzyme catalyzes a specific chemical reaction on different substrates. The key is to identify enzymes with activity toward PLA.

To identify PLA-degrading activity from different sources, multiple screening protocols were developed using recombinant clones and purified proteins already present within the University of Toronto enzyme characterization pipeline. Active phenotypes were initially characterized by inspecting for halos within a PLA substrate exposed to a candidate hydrolase (**Figure 10.1**). The genes responsible for this activity were identified for positive clones, manipulated for overexpression, and the encoded enzyme was purified. To further characterize purified enzymes biochemically, their hydrolytic activity was assayed against a set of defined PLA polymers (**Figures 10.2 and 10.3**) as well as soluble model substrates.

More than 22 carboxylesterases were highly active PLA depolymerases, capable of degrading different PLA substrates to differing degrees. The results indicate that diverse microorganisms from diverse habitats possess enzymes capable of PLA depolymerization: PLA depolymerase activity was detected for a marine gram-negative bacterium, and several hydrolases were identified that can

function at low temperatures, of potential significance for PLA fate in marine environments. Some enzymes exhibited the highest PLA depolymerase activity reported to date. Ultimately, the goal will be to incorporate such enzymatic activity into processes that enable efficient recycling of monomer back to polymer and to more rapid biodegradation of waste materials in both engineered and natural environments.

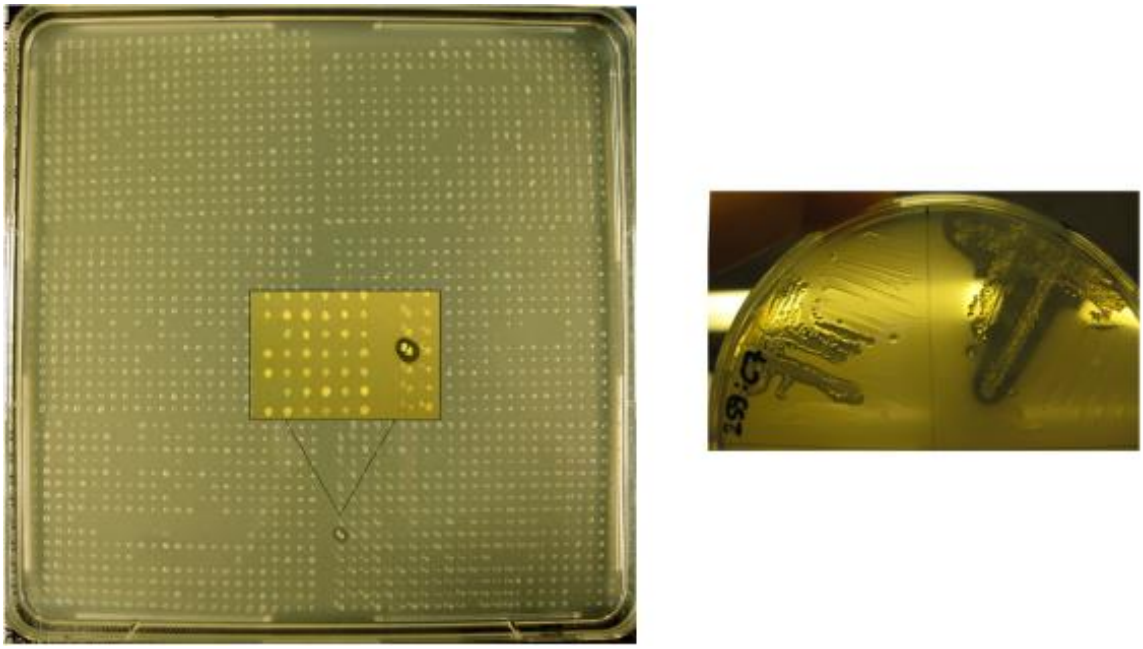

Figure 10.1: Functional screening of genome libraries: a clear halo around positive recombinant clones on double layer screening plates indicates a possible positive hit for a PLA-degrading enzyme.

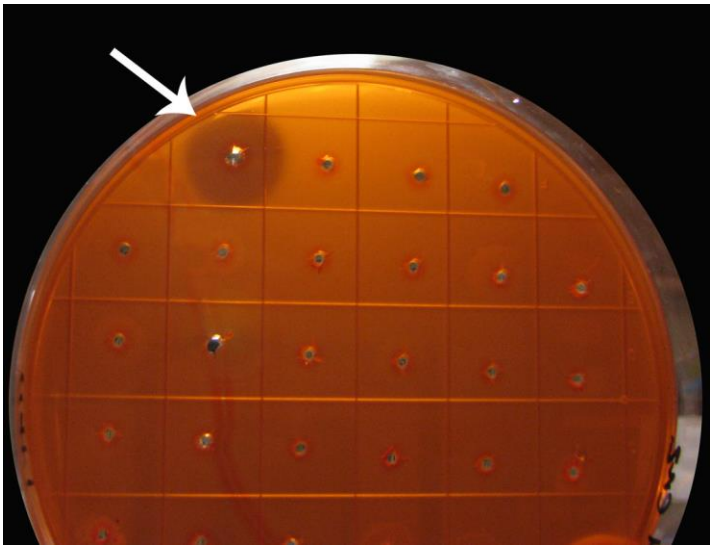

Figure 10.2: Agar-based PLA depolymerase assay emulsified PLA is the substrate (turbid). A clear halo around the well containing purified enzyme indicates substrate degradation (positive signal).

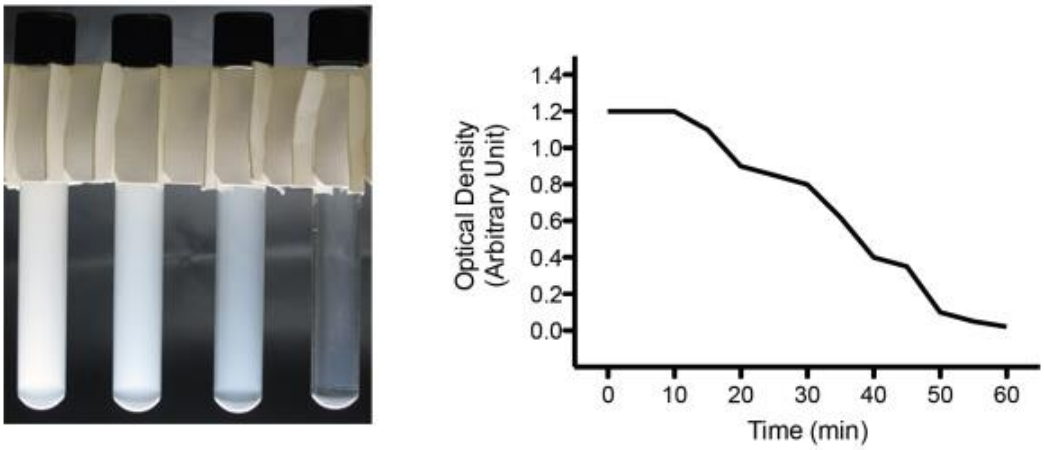

Figure 10.3: Liquid turbidometric enzyme assay. Emulsified PLA is the substrate (milky). The reaction mixture turns water clear within 60 minutes of incubation with purified PLA2-9 enzyme, indicating substrate degradation (positive signal).

10.4 Thermal depolymerization

PLA resins were obtained from NatureWorks LLC. Commercial PLA products tested were PLA cups (NatureWorks GC7) collected at a Stanford University cafe. The cups were cut into small pieces (about 0.4 x 1 cm) and placed inside

the reactor flask. The PLA/PBAT blend was obtained from BASF (Ludwigshafen, Germany) and contained 50 percent PLA and 50 percent Ecoflex, the trade name for PBAT. The PBAT is a compostable aliphatic-aromatic copolyester.

Tin(II)ethylhaxanoate, a catalyst for polymerization and depolymerization of PLA, was purchased from Aldrich. Reported purity was 95 percent, with 4.6 percent ethylhexanoic acid, 0.3-0.5 percent water, and less than 0.05 percent tert-butylcatechol (stabilizer). The catalyst was added directly to the PLA depolymerization reactor.

As shown in **Figure 10.4**, the experimental setup used to investigate the thermal depolymerization of PLA materials consisted of a depolymerization reactor consisting of a round-bottom glass flask (100 mL in volume), a heater, a silicone oil bath (170^{o} to 200^{o} C), a lactide collector consisting of two glass flasks (100 ml in volume) in series, a glass vapor trap, and a vacuum pump (Robinair 15500 VacuMaster). Heating tape with a timer was used to ensure that the collection tube temperature was maintained above the melting point of L-lactide (96 ^{o}C) so that lactide would condense as a liquid and flow into the lactide collector. To protect the vacuum pump from lactide vapors and particulates, an icebox-enclosed glass vapor trap was installed in the vacuum line connecting the vacuum pump to the lactide collector.

Test material (10 or 20 g) was weighed, transferred to the depolymerization reactor, and mixed with tin(II) ethylhexanoate as catalyst (0.1%, w/w). Melting was observed at 170° 175° C and depolymerization at 180° to 200° C. Tests were also conducted to evaluate lactide recovery from PLA/PBAT blends. To assess the effects of PBAT mass fraction on lactide recovery, additional PLA resin was added to the PLA/PBAT blend to achieve of PLA:PBAT mass ratios of 50:50, 75:25, and 90:10.

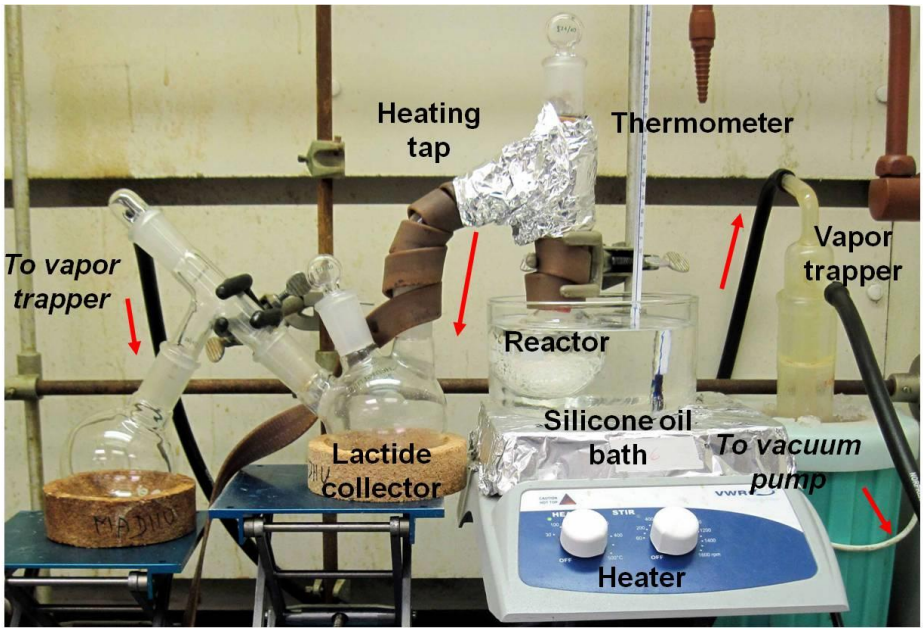

Figure 10.4: Experimental device for depolymerization of PLA materials

The composition of L-, D- and *meso*-lactide in the depolymerized product was dissolved in chloroform (10 g/L) and analyzed using method Agilent GB/T 9722-2006 on an Agilent GC 7820a gas chromatographer equipped with a capillary column DB-17MS (30 meter×0.25 mm) and using hydrogen as carrier gas (1.8 ml/min flow rate). The temperatures of the injector and detector were 200° and 335° C, respectively. The oven temperature was controlled as follows: 50°C for 1 minute, increasing from 50° to 320° C (25°C per min) and holding at 320°C for five minutes. Injection of sample (1 µL) was via auto/splitless mode (splitless valve time: one minute). Optical rotation was analyzed in accordance with method USP 781 using a Shanghai Precision Scientific Instrument Auto Optical Rotation Analyzer. Samples were dissolved in chloroform solvent (0.5 g in 50 mL) prior to analysis.

PLA resin (20.0 gram) was added to a 100 ml reactor flask. Melting occurred at 170° to 175° C. After 30 minutes, the temperature increased to 190° to 195° C and depolymerization ensued as the melted PLA began to boil and gas bubbles appeared in the reactor. The lactide vapor began to collect in the three-neck flask. The reaction proceeded rapidly and boiling stopped after 45 minutes. Most of the PLA mass (94 percent) was transferred to the gas phase, but a small amount of dark-brown residue remained. The dark colored residue presumably contained the catalyst. Yellowish-white lactide-like products were collected in the first lactide collector (>90% recovery by weight).

In one follow-up test, additional PLA resin (19.0 g) was added to the dark brown residue in the depolymerization reactor. After the resin melted with the residue,

depolymerization was observed above 185° C and ended within 40 minutes. The recovery efficiency was 94 percent. This indicated that the catalyst remained active in the residue.

In a second test, bits of PLA cups were added to give a total mass of 19.9 g. After temperature increased to 180°C, depolymerization initiated. The reaction proceeded to completion within one hour. A total of 18.89 g of lactide-like materials were collected in the collection flask and transferred in a storage vial for analysis of composition. The recovery efficiency was greater than 92 percent.

In a third test, a PLA/PBAT blend (50:50 by weight) of 20.14 g was mixed with the tin(II) catalyst in the depolymerization reactor. The material melted at 155° to 165° C. Depolymerization and formation of lactide bubbles occurred at more than 185°C, and lactide was generated at 195° to 200° C, as noted in previous tests. At the end of test (i.e., when bubbling stopped), the amount of lactide collected was 5.69 g. The recovery of lactide was 57 percent, assuming a PLA content of 50 percent in the original blend. This result indicates that recovery of lactide from a 50:50 PLA/PBAT blend was feasible but the efficiency of lactide recovery was relatively low (56.5 percent) compared to the values obtained for PLA resin and PLA cups.

To determine whether tin(II) catalyst was deactivated in PBAT blend residues, PLA resin (5 g) was added to the reactor containing residues from the blend test (PLA/PBAT, initially 50:50) to determine whether the residue still contained active catalyst. The added PLA melted at 195° to 200° C, but after for two hours no bubbles were observed and no lactide was recovered. This indicated that the tin (II) catalyst in the residues was likely inactivated.

To confirm that the catalyst in the residue was inactive, additional tin(II) catalyst (0.14 g) was added to the reactor flask. After increasing the temperature to more than 180°C, the reaction occurred, but at a slow rate. After two hours, the total mass loss was only 0.92 g. Based on the mass of PLA added, the recovery was only 18 percent. This indicates that the activity of the catalyst is adversely affected after mixing with residues, preventing efficient depolymerization of PLA.

To assess lactide recovery at a PLA:PBAT mass ratio of 90:10, 8.0 g of PLA resin was mixed with 2.0 g of PLA/PBAT blend (50:50, by weight), resulting in a ratio of PLA:PBAT mass ratio of 90:10 where the total mass of PLA in the mixture was 9.0 g. After the temperature reached 175°C, the test was completed within two hours and the mass loss was 8.83 g due to formation of lactide-like vapor, indicating that 98 percent of the available PLA had depolymerized. This also indicated that a low fraction of PBAT did not affect PLA depolymerization.

To assess the effects of lower fractions of PBAT on lactide recovery, 5.0 g of PLA resin was mixed with 5.0 g of PLA/PBAT (50:50,by weight) to give a PLA/PBAT mass ratio of 75:25 where the total mass of PLA in the mixture was 7.5 g. The reaction proceeded to completion within two hours, with a mass loss of 7.24 g, indicating that 97 percent of the available PLA had depolymerized.

These results suggest that PBAT affects PLA depolymerization when an extremely high fraction of PBAT is present. In general, such an effect would be limited during the depolymerization of recycled PLA wastes since most commercial PLA materials do not contain a high percentage of PBAT.

The depolymerized products recovered in all tests were white colored crystals. The recovered crystals were melted by transferring them inside the lactide collector to a hot water bath (>90^{o}C), then poured into small tubes for analysis. The solidified products were light yellow in color at ambient conditions. As shown in **Table 10.1**, analysis of samples recovered in the above tests confirmed that lactide was the major product at a purity of 96 to 99 percent. The products for each of the five tests are shown in **Figure 10.5**. The major isomer was L-lactide (88-93.5%). They also contained a small fraction of D-lactide (6%) and trace amount of *meso*-lactide (<0.2%). The presence of D-lactide is important because commercial PLA are copolymers of poly(L-lactic acid) and poly (D,L-lactic acid) (Aruas, et al., 2004). The trace amount of *meso*-lactide could be the result of racemization during thermal depolymerization, but it may not affect the properties of the product within the recycled feedstock because its levels are low.

Table 10.1. Composition of recovered thermal depolymerization products.

Sample	*L*-lactide % (w/w)	*meso*-lactide % (w/w)	*D*-lactide % (w/w)	Optical rotation	Test material
No.1	86.79	0.1530	6.70	-225.32	PLA resin
No.2	86.89	0.1550	6.60	-225.61	PLA resin
No. 3	84.63	0.1536	5.80	-211.35	PLA /PBAT (50%: 50%)
No. 4	82.28	0.1540	5.89	-219.21	PLA /PBAT (90%:10%)
No.5	85.59	0.1528	6.20	-219.92	NatureWorks PLA cups

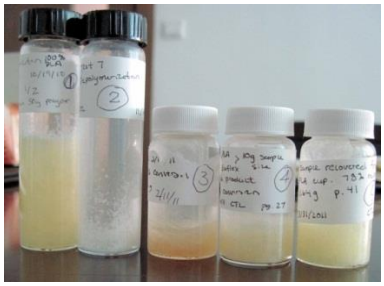

Figure 10.5: Depolymerization products collected for analysis. From left to right: samples No.1 to No.5 in **Table 10.1**.

10.5 Key findings

For enzyme-mediated hydrolysis:

1. Genes encoding PLA-degrading activity were identified, and the encoded enzymes purified and characterized for hydrolytic activity. More than 22 novel PLA depolymerases were identified.
2. PLA depolymerase activity is present in a diverse range of microorganisms from different habitats.

For thermal depolymerization:

1. Recovery of lactide as feedstock from recycled PLA appears feasible. Production of lactide from recycled PLA materials is rapid at 190° to 200° C with tin(II) catalyst (<0.1% w/w) and using vacuum extraction.
2. Thermal depolymerization enabled recovery efficiency of 94 percent or higher.
3. Major products of thermal depolymerization are L-lactide and D-lactide with trace amount of *meso*-lactide.
4. The presence of a high fraction of PBAT blend (50 percent or higher) has a negative impact on the depolymerization of lactide but the impact could be limited by maintaining a low percentage of PBAT in recycled PLA streams.

11. Life Cycle Analysis for the Methane-PHB Cycle and PHA-based Biocomposites

11.1 Executive summary

The environmental impact of bioplastic production from biogas methane must be evaluated to determine whether the use of biogas as a substrate is environmentally preferable when compared to currently prevailing production of bioplastics from agricultural feedstocks. A cradle-to-gate model for life cycle assessment was developed to evaluate the environmental impacts of PHB production from biogas up to the point of extracted polymer resin. PHB production from biogas methane is shown to be energetically preferable to production from corn-based carbohydrates due to the large inputs of land and energy required for growth and processing of agricultural feedstocks. Energy and chemical inputs during recovery of PHB and energy requirements for aeration and agitation during PHB production were the main impacts of methane-based PHB production. These impacts could be largely mitigated through the use of renewable energy sources; use of 18 to 26 percent of incoming biogas methane for energy demands and the remainder for PHB production would eliminate the need for grid-sourced electricity and its associated environmental impacts.

Key publication:

Rostkowski, K., C. Criddle, and M. Lepech. 2012. Cradle-to-gate life cycle assessment for a cradle-to-cradle cycle: biogas-to-bioplastic (and back). Env. Sci. Tech. 46:9822-9829.[31]

11.2 Cradle-to-gate assessment methodology

A cradle-to-gate model was used as the basis for process comparisons, with impacts evaluated for PHB production and PHB recovery. These impacts include substrate requirements, energy for aeration and mixing, nutrients for bacterial growth, energy and chemical requirements for PHB recovery, and disposal of excess cell materials remaining after polymer recovery. Impacts for energy consumption are based upon standard impacts for grid-sourced electricity. The processing steps used in this model are outlined in **Figure 11.1**. Impacts from manufacturing, use, collection, and disposal of plastic products were not evaluated as these impacts are common across all resin production processes. Nine

environmental impact categories were evaluated using the Tool for the Reduction and Assessment of Chemical and Other Environmental Impacts (TRACI). This tool was developed by the U.S. EPA and includes the following impact categories: global warming, acidification, carcinogenics, noncarcinogenics, respiratory effects, eutrophication, ozone depletion, ecotoxicity, and smog. Results are normalized for the production of one kilogram of PHB produced according to annual U.S. emissions by impact category, using the U.S. Environmental Protection Agency (EPA) database values.

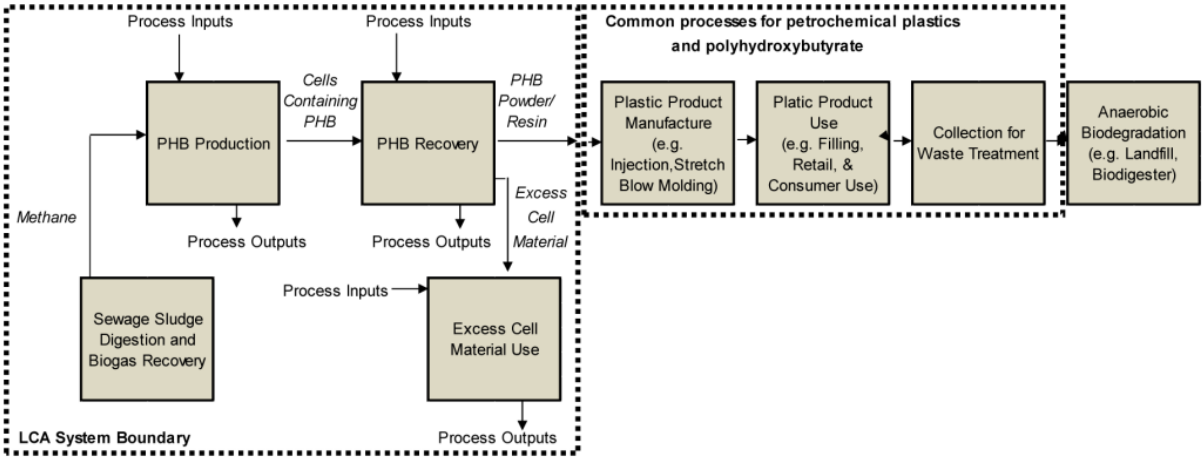

Figure 11.1: Process flow diagram (PFD) of LCA system

11.3 Materials flow for the methane-to-PHB process

Parameters used to determine environmental impacts of PHB production from methane gas are listed in **Table 11.1**. These values are used to determine inputs and outputs required for production and extraction of PHB polymer. Production of biodegradable polymer from biogas produces two forms of organic solids: residual cell material following PHB extraction and PHB products disposed of at end-of-life. Both of these sources of organic material can be digested anaerobically to produce methane for further production of energy or bioplastics as documented in **Figure 11.2**, or could be directly combusted for energy production. Using the parameters in **Table 11.1**, 5.3 grams of methane are required per gram of PHB produced (a conservative value), of which 0.8 grams may be produced by anaerobic digestion of PHB products and residual biomass. The remaining 4.5 grams of methane could then be supplied through digestion of 16.9 grams of organic waste.

Table 11.1: Parameters used for PHB production from methane

parameter	value	reference
% PHB achieved	50% (0.5 g PHB/g total mass)	measured value
yield of PHB on methane	0.55 g PHB/g methane	lumped average of measured and theoretical values
growth yield	0.345 g biomass/g methane	average value
oxygen requirement	4 g oxygen/g methane	thermodynamic estimate
nitrogen requirement	0.12 g nitrogen/g biomass	typical 12% N in microbial biomass.
PHB recovery by extraction	90%	reported value
methane recovery from biomass waste	0.32 g methane/g biomass	calculated from the empirical formula for biomass waste
methane recovery from carbohydrate organic waste	0.27 g methane/g organic waste	calculated from the empirical formula for carbohydrate organic waste
methane recovery from PHB	0.38 g methane/g PHB	calculated from the empirical formula for PHB

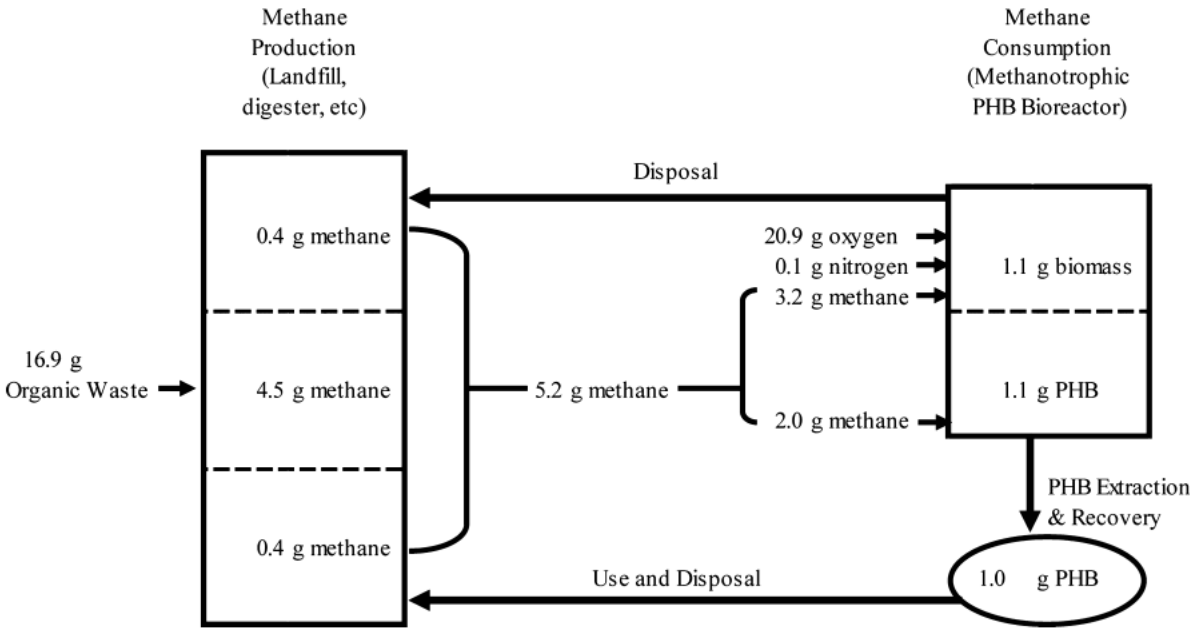

Figure 11.2: Materials flows in the methane-PHB cycle

11.4 Impact assessment for PHB production from waste biogas

Relative environmental impacts for the nine categories evaluated are listed in **Table 11.2**. Values are presented for biological production of intracellular resin and for the entire resin production process including extraction. For each category, the use of solvent (chloroform) to recover PHB from intracellular resin represents more than 90 percent of the total impact. Extraction impacts, while high, are common to all processes involving intracellular PHB production. When considering only the production of intracellular resin the majority of impacts are associated with energy use. These impacts are based on use of grid-sourced electrical energy and include the detrimental effects of coal-burning, among other impacts. Use of on-site renewable resources including combustion of available biogas and combustion of residual cell material could mitigate impacts attributed to grid-sourced electrical energy.

Table 11.2: Relative impacts per 1kg of PHB produced from waste biogas.

impact indicator	unit	cradle-to-resin value	cradle-to-intracellular-resin value	normalization value[60]	cradle-to-intracellular-resin normalized value
global warming	kg CO_2 equiv	9.42×10^{2}	−1.94	6.85×10^{12}	-2.83×10^{-13}
acidification	H^+ moles equiv	9.25×10^{1}	2.62	2.08×10^{12}	1.26×10^{-12}
carcinogenics	kg benzene equiv	1.02	1.02×10^{-2}	7.21×10^{7}	1.42×10^{-10}
noncarcinogenics	kg toluene equiv	8.84×10^{2}	3.15×10^{1}	4.11×10^{11}	7.66×10^{-11}
respiratory effects	kg PM2.5 equiv	3.95×10^{-1}	1.42×10^{-2}	2.13×10^{10}	6.65×10^{-13}
eutrophication	kg N equiv	1.06	1.11×10^{-3}	5.02×10^{9}	2.22×10^{-13}
ozone depletion	kg CFC-11 equiv	5.08×10^{-4}	4.32×10^{-7}	8.69×10^{7}	4.97×10^{-15}
ecotoxicity	kg 2,4-D equiv	4.20×10^{1}	4.08	2.06×10^{10}	1.98×10^{-10}
smog	kg NO_x equiv	3.28	1.83×10^{-2}	3.38×10^{10}	5.41×10^{-13}

11.5 Impact assessment for PHB extraction

Extraction and purification of PHB accounts for more than 90 percent of environmental impacts in each impact category, with production of intracellular resin accounting for less than 10 percent. Minimizing the impacts of PHB extraction is therefore the most critical step toward reducing environmental impact. In **Figure 11.3**, two alternatives to solvent extraction are compared across impact categories. Both surfactant digestion and selective dissolution are significantly lower impact alternatives, although even at these levels PHB extraction still accounts for the majority of total impacts. Further research is therefore needed to develop economically viable, environmentally benign extraction methods. With regard to PHB extraction, cost, efficiency, and preservation of molecular weight must be weighed against environmental impacts.

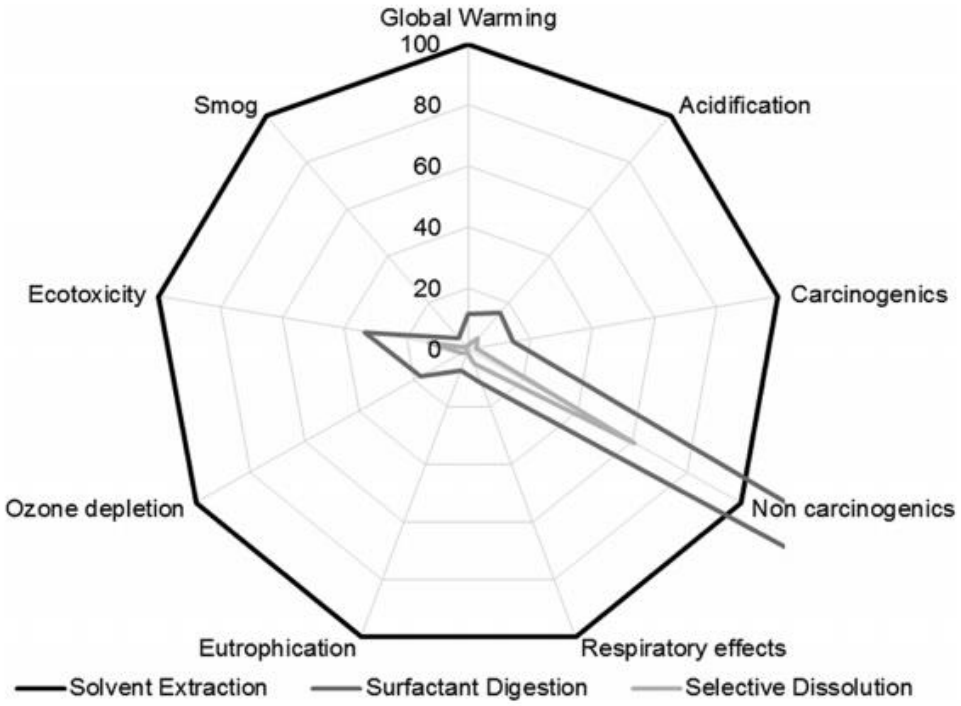

Figure 11.3: Relative impact assessment of PHB extraction methods. Use of surfactants and selective dissolution dramatically shrinks the envelope of detrimental impacts for all categories except non-carcinogenic compounds.

11.6 Comparison with agricultural feedstock

Including the combustion of residual solids for increased energy production, the total energy requirement for production of 1 kg PHB from methane is 37.4 MJ. This can be compared to an energy requirement of 41.9 MJ for PHB produced from corn. While higher yields of PHB may be achieved using corn as a source of carbohydrates for PHB production, energy and land requirements for feedstock cultivation and fermentation result in a higher overall energy impact. The energy requirement for PHB production from methane could be met through oxidation of 18 to 26 percent of incoming methane, resulting in an energy-independent process and leaving the remaining 74 to 82 percent of methane for PHB production. With regard to global warming potential, use of currently uncaptured biogas[49] could result in a net decrease in total emissions due to the prevention of atmospheric methane releases.

11.7 Impact assessment for biocomposites

Biobased composites offer a potentially low environmental impact material option for the construction industry. Designing these materials to meet performance requirements for an application while minimizing environmental impacts requires the ability to refine composite constituents (e.g., matrix, fibers, additives) based on environmental impact and resulting mechanical properties. To investigate environmental impact of PHA-based natural fiber materials, composites with varying natural fiber reinforcement (e.g., hemp Lenin [HL], hemp burlap [HB], jute burlap [JB], wood flour [WF]) in a PHBV matrix were characterized through life cycle assessments. These biobased composites were found to have competitive flexural properties with certain short-chopped glass fiber reinforced plastics (GFRPs). Using experimental mechanical results, multi-criteria material selection techniques were applied to weigh desired material properties with greenhouse gas emissions, fossil fuel demand, and a weighted single score. An example is shown in **Figure 11.4**. The dashed lines represent lines of equivalent performance. Materials that lie along a line with the slope of these plotted equivalency lines are considered equal in terms of the specified environmental impact and mechanical property. Higher flexural modulus and low environmental impact is preferred. Thus, materials that are closer to the upper-left-hand corner are considered most favorable.

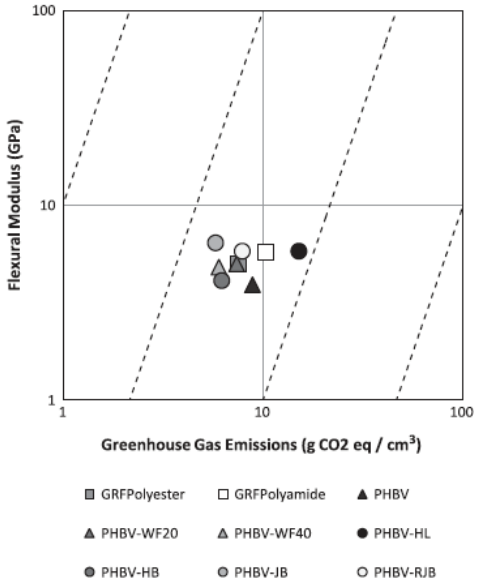

Figure 11.4: Example of a materials selection chart for PHA-based composites and GRFPs for a flexural application

Materials selection charts comparing flexural stiffness to environmental impact provide a fast visualization for comparison between material performances. For example, the low greenhouse gas emissions (GHG) and respectively high

flexural modulus associated with jute burlap reinforced PHBV makes these composites the most desirable for the GHG impact category.

Life cycle assessment methods were also used to examine the environmental impact of and improvements to production processes for biobased composites made of a PHBV and natural fiber fabric. Investigated production improvements include targeting reduced thermal energy use, biomass reuse as a fuel source, and design alterations such as reduced waste and fiber replacement. It was found that the application of thermal energy recycling mechanisms did not exceed 15 percent of the environmental impact categories considered. The greatest reductions in greenhouse gas emissions, energy consumption, and weighted impact score were found to be possible through incineration of excess biomass and the use of alternate fiber types.

11.8 Key findings

1. Organic solids generated during PHB extraction and disposal of PHB products can be anaerobically digested to contribute positively toward energy and biogas requirements.
2. Environmental impacts for PHB production from biogas are largely related to extraction of intracellular resin.
3. Selection of extraction technology is a critical determinant of environmental impact.
4. Energy requirements for PHB production from methane compare favorably to energy requirements for PHB production from corn.
5. Combustion of residual solids and use of 18 to 26 percent of incoming methane for energy generation results in an energy-independent process and eliminates impacts related to grid-sourced electrical energy.
6. In the case of biocomposites, the greatest reductions in greenhouse gas emissions, energy consumption, and weighted impact score were achievable through incineration of excess biomass and the use of alternate fiber types.

12. Economic Analysis of PHB Production from Biogas Methane

12.1 Executive summary

Methane in biogas or natural gas is a cost-effective feedstock for PHB production. Existing landfills in California could potentially support PHB production at more than 5,000 tonnes of PHB per year. Anaerobic digesters sized to digest 200,000 tonnes of MSW per year could sustain PHB production of 10,000 tonnes per year. Collection and digestion of concentrated organic waste streams, such as animal wastes, could enable PHB production at smaller treatment facilities with excess digester capacity. Waste PHB products can be used as raw materials for methane production and further enhance overall PHB production. The cost of PHB production with biogas could compete with PLA and petroleum-based plastic resins at facilities producing more than 5,000 tonnes of PHB per year. At smaller-scale facilities, labor costs become critical, while at large scale, energy efficiency becomes the critical cost factor. At all scales, chemical costs, especially for PHB extraction and purification, are important. The PHB conversion yield has a large impact on production cost, as does the efficiency of PHB recovery from microbial biomass. Pilot- and full-scale studies are needed to assess the stoichiometry and kinetics of PHB production at a realistic scale and to accurately assess capital and operational cost.

12.2 The effects of feedstock cost

Polydroxyalkanoate (PHA) biopolymers, including polyhydroxybutyrate (PHB), are currently produced from plant-derived sugar and oils. Corn and sugar cane are the primary sugar sources. Major producers that use a sugar-based feedstock include Tianjin GreenBio Materials Co., Ltd.,[32] with a production capacity of 10,000 tonnes per year, and TianAn Biopolymer,[33] with a production of 2,000 tonnes per year. Meredian, Inc., a privately held biopolymer producer in Bainbridge, Georgia, reportedly produces 15,000 tonnes of PHA per year and plans to expand production to 300,000 tonnes per year.[34] The company reportedly uses plant-derived oils that do not compete with food.[35]

In this study, we focus on utilization of biogas or methane gas generated from landfills and anaerobic digesters as a raw material for PHB production to achieve full life-cycle use of carbon. In general, the market value of biogas is related to the market price of natural gas (which contains more than 80 percent methane). As shown in **Figure 12.1**, the cost of corn-derived feedstock is variable because it is driven by weather patterns and the availability of food. An alternative carbon source is methane. Methane availability is not tied to the food supply, so its price

is less sensitive to factors affecting the price of food. Natural gas, especially shale gas, is largely methane and is increasingly accessible with new extraction technology. Over the past decade, the price of natural gas in North America has declined (**Figure 12.2**). This trend is likely to continue as additional reservoirs are tapped. Therefore, the market value of methane in biogas should also follow the same trend and becomes attractive for PHB production.

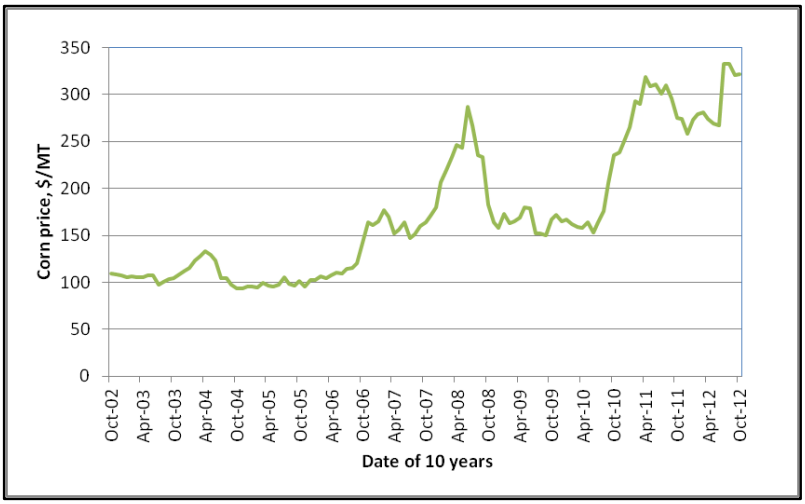

Figure 12.1: Corn price ($/MT) for the last 10 years (Source: World Bank).

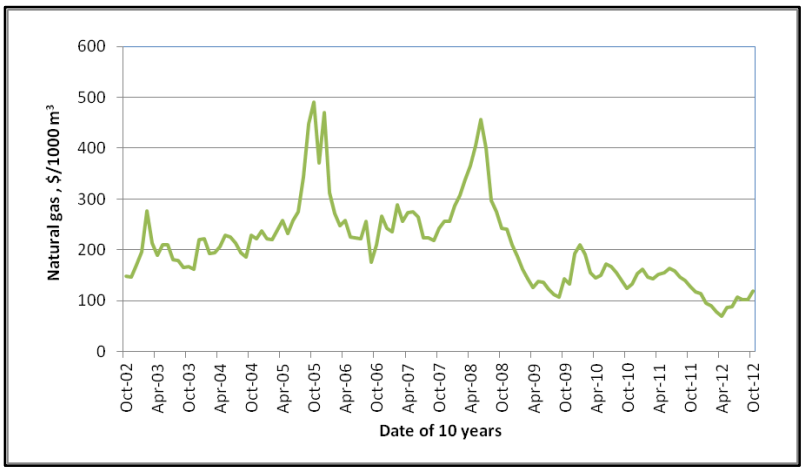

Figure 12.2: Natural gas price ($/1000 cubic meters) for the last 10 years (Source: World Bank)

Table 12.1 compares PHA conversion yields—the mass of PHA produced per unit mass of carbon source—for glucose, palm oil, and methane. For glucose, this value ranges from 0.25 to 0.34 g PHA per g, depending upon culture and growth conditions.[36,37] For these conversion yields and the corn price of October 2012 of $321 per tonne,[38] the raw material cost for PHA production exceeds

$0.94 to 1.46 per kg PHA. For palm oil, the conversion yield is 0.61 g oil/g PHB.[39] At a palm oil price of $0.73/kg oil,[40] (the feedstock cost is $0.45 per kg PHB. For methane, the PHB conversion yield of *Methylocystis parvus* OBBP is 0.49 g PHB per g methane.[41] This is consistent with the reported value of 0.50 g PHB per g methane for *Methylocystis sp.* GB 25 DSM 7674.[42]

For this conversion yield and a natural gas price of $154 per metric tonne (October 2012), the raw material cost is $0.28 per kg PHB. At present, there is no available market price of biogas generated from landfill and WWTP. We assume that the price of methane in biogas should be less than that of natural gas, so that a biogas cost estimate based on natural gas is conservative. **Figure 12.3** compares corn as feedstock and natural gas as feedstock, using cost data for the past decade. Prior to 2008, use of natural gas was not an attractive feedstock, but natural gas became an attractive alternative when the costs fell to less than half those of corn.

Table 12.1: PHA/PHB yield values for production of PHA/PHB from glucose, palm oil, and methane.

Substrate	Value
Glucose	0.25 g PHA/g glucose 0.34 g PHA/g glucose
Palm oil (emulsion)	0.61 g PHB/g palm oil
Methane	0.49 g PHB/g methane 0.50 g PHB/g methane

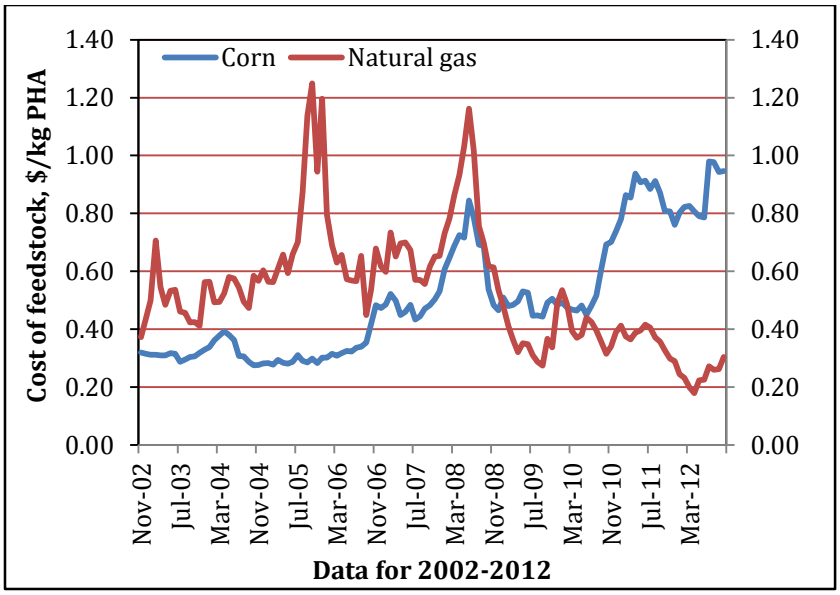

Figure 12.3: Comparison of feedstock type (corn, natural gas) on production costs over the past decade. Assumed product yields are 0.34 g PHB/g glucose and 0.49 g PHB/g methane.

12.3 Environmental and economic considerations

Use of plant feedstock to produce PHB creates a three-step cradle-to-cradle cycle: (1) photosynthesis drives fixation of CO_2 in plant biomass, (2) sugars or oils extracted from plant biomass are used for production of PHB, and (3) PHB is oxidized at end-of-life (via composting or combustion) back to CO_2. While this cycle is often viewed as "carbon neutral," it does not account for the energy required for planting, harvesting, and processing of crops or for land, water, and fertilizer requirements. These factors adversely impact PHB life cycle and production costs. As shown in **Table 12.2**, the result is high prices compared to functionally similar petrochemical-based plastics and bioplastics. Commercial PHB currently sells at $3.5-5.0/kg. These high prices have likely limited application. The current global annual production is less than 50,000 tonnes; decreasing production cost and sale price will expand the market potential. A price closer to polylactic acid (PLA) at approximately $2 to $2.50 per kilogram would likely be attractive for large-scale commercial applications and could potentially replace functionally similar petrochemical based polymers such as polypropylene.

Table 12.2: Market prices of various polymers

Polymer	Market price, $/kg
Petroleum based, nonbiodegradable	

Polystyrene (PS)	1.87-2.14
Polyethylene (PE)	1.27-1.43
Polypropylene (PP)	1.38-1.43
Polyethylene terephthalate (PET)	1.7-1.9
Petroleum based, biodegradable	
Polycaprolactone (PLC)	5.8-7.8
Ecoflex (PBAT)	4.0-6.0
Renewable, biodegradable	
Polylactic acid (PLA)	2.0-2.5
Polyhydroxybutyrate (PHB), PHB valerate (PHBV)	3.5-5.0

Note: Data from U.S. Plastic News and Alibaba.com on June 12, 2012

In contrast to the economics of the three-step process above, use of methane in biogas as a carbon and energy source creates a two-step cycle: (1) methanotrophic aerobic oxidation of methane drives fixation of carbon as PHB, and (2) methanogenic anaerobic oxidation converts PHB back to methane in anaerobic digesters or landfills. This cycle avoids the need for crop cultivation to generate feedstock and breaks the link between PHA production and the price of food.

Biogas is mainly produced at municipal solid waste (MSW) landfills and in the anaerobic digesters of municipal wastewater treatment plants (WWTPs). As shown in **Figure 12.4**, landfills already in place in the United States contain large quantities of organic matter. Such landfills can sustain production of a reliable stream of methane for decades. But landfill space is increasingly limited, particularly in urban environments, and, like natural gas, biogas from landfills can leak to the atmosphere during collection and conveyance, contributing to global warming. Instead, use of anaerobic digesters for biogas production eliminates leaks and enables production of methane under optimal conditions.

Systems designed for recycling through methane should therefore focus on the use of anaerobic digesters. Nevertheless, use of methane from “legacy” sources (natural gas, landfills) is also needed to mitigate global warming through sequestration of carbon as PHB, especially in the near future until adequate digester capacity comes online.

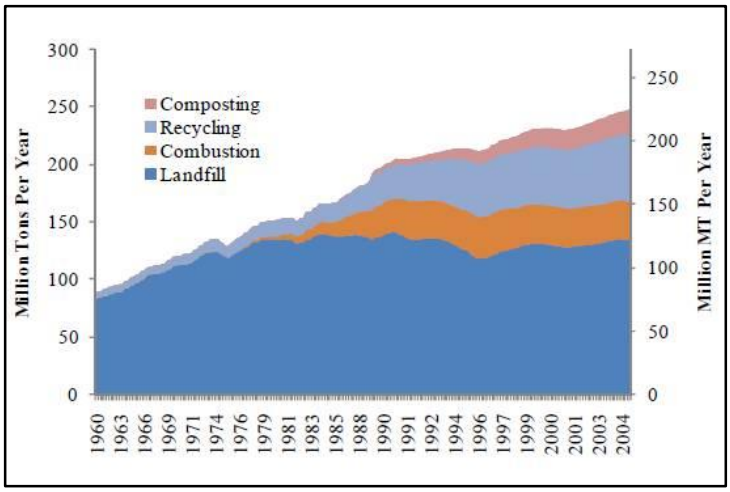

Figure 12.4: Trends in the disposal and recovery of MSW in the United States[54]

12.4 Production of polyhydroxybutyrate (PHB) from biogas

PHB production potential at California landfills

Over the past 50 years, the rate of municipal solid waste generation in the United States has increased from 2.6 pounds to 4.3 pounds per person per day,[43] but the amount of material that has been landfilled has remained stable. In California, this can be attributed to large gains in waste reduction and diversion for recycling driven by the passage of California State Assembly Bill 939, which mandated cities and counties to implement plans for achieving recycling and landfill diversion goals. Despite these gains, huge amounts of materials are still landfilled. In 2006, Californians landfilled 38 million tonnes of solid waste and generated 3 million metric tonnes of green waste for alternative daily cover.[44] Roughly 40 to 60 percent of landfilled solid waste is organic.

Landfill data from CalRecycle indicates that California has more than 371 landfills. Complete operational data including annual waste-in-place (WIP), biogas flow, and methane content are available for 98 of them. These landfills have a WIP of 1.146 billion tonnes, supporting a captured biogas flow of 199,473 scfm. The average biogas methane content of the waste is 39 percent, with a range of 20 to 60 percent depending upon the individual landfill. This corresponds to an annual methane production of approximately 1.1 billion cubic meters per year (~840,000 tonnes/yr)**.** For a PHB conversion yield of 0.49 tonnes of PHB per tonne of methane (**Table 12.1**), the PHB production capacity from California landfills is 410,000 tonnes PHB per year. But because many landfills flare biogas, the recovered biogas is 0.6 billion cubic meters (~430,000) tonnes per year. Accounting for this loss, the PHB production capacity is 210,000 tonnes per year, a value equivalent to current U.S. production of polylactic acid (PLA) of approximately 200,000 tonnes per year (Green Chemical Blog, 2012).

The size of landfills in California varies from a WIP of 0.25 million to 120 million tonnes (**Figure 12.5**). The largest is Puente Hills Landfill, Whittier, in Los Angeles County. This landfill opened in 1957 and closed in 2003. It has a WIP of 120.6 million tonnes, and currently uses turbines to generate 35 MW of electricity, with plans to add 8 MW.[45] If this biogas were instead used to make PHB, the production capacity would be approximately 53,000 tonnes PHB per year. Most landfills are much smaller; the average size is 12 million tonnes of WIP. A landfill of this size could sustain a biogas flow rate of 2,000 scfm (~8,500 tonnes of methane per year). Such a mass flow could support production of 4,100 tonnes PHB per year.

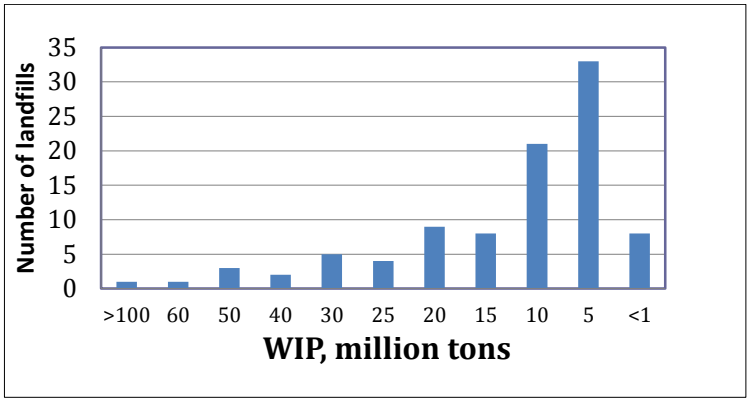

Figure 12.5: WIP for municipal landfills in California [46]

The annual methane production of a landfill, and hence the annual capacity for PHB production, is a function of the WIP. About 28 of 98 landfills (28.6%) produce biogas at a rate exceeding the average. **Figure 12.6A** illustrates the relationship between methane production potential and WIP

$$y = 1.09x \qquad (r^2 = 0.898) \qquad \text{(Equation 1)}$$

in which y = methane in biogas produced (million cubic meters per year); x = WIP in landfill (million tonnes).

Figure 12.6B illustrates the relationship between PHB production potential to landfill WIP (assuming a conversion factor of 0.49 kg PHB/kg CH_4, per **Table 12.1**)

$$y = 382x \qquad (r^2 = 0.898) \qquad \text{(Equation 2)}$$

in which y = PHB production potential (tonnes per year); x = WIP in landfill (million tonnes).

As shown in **Figure 12.6A**, most California landfills are small. Thirteen support biogas flow rates greater than 20 million cubic meters per year, a value that could sustain PHB production of 10,000 tonnes per year (**Figure 12.6B**). This is a capacity equivalent to that of Tianjin GreenBio Materials Co., Ltd. On the other

hand, 54 landfills (or 55 percent of total) could support a PHB production capacity >2,000 tonnes per year. In California, most large landfills are already equipped for electricity generation. The existing investment in gas purification and power production equipment may preclude a near-term switch to PHB production, though a mix of energy and PHB production may offer benefits.

From the above analysis, we conclude that most current California landfills have the potential to sustain PHB production at levels higher than 2,000 tonnes per year, and 13 could support production levels exceeding 10,000 tonnes per year. Large, centralized landfills would be favored by economies of scale for PHB production and proximity to markets. In addition, new and existing landfills should ensure efficient methane recovery and may benefit from PHB production as an alternative or adjunct to energy production.

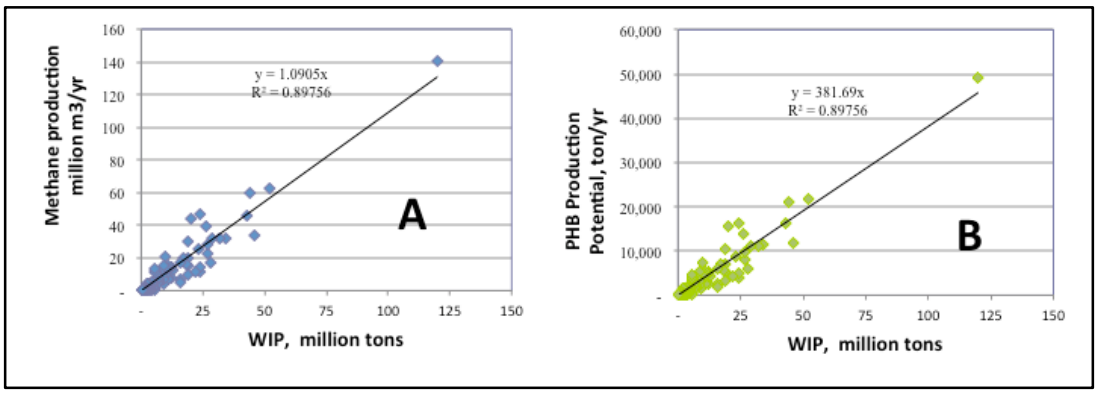

Figure 12.6: (A) Annual methane production and (B) PHB production potentials versus WIP

PHB production capacity of anaerobic digesters in California

Anaerobic digestion is commonly used throughout the world to stabilize biosolids, animal manure, food residues, and concentrated organic wastewaters. In Europe, municipal solid waste is also digested, with more than 240 anaerobic digesters in 17 countries processing approximately 8 million tonnes per year.[56] In California, large anaerobic digesters are used at municipal wastewater treatment plants (WWTPs) near major cities such as San Francisco and Los Angeles. The U.S. EPA database contains data for 84 California WWTPs:[47] 66 have anaerobic digesters (78.6%), 16 have unknown capabilities for anaerobic digestion (19%), and 2 (2.4%) lack digesters. Most WWTPs are net energy consumers, so the biogas generated at WWTPs is often used as a supplementary energy source. Increasingly, however, wastewater treatment utilities are augmenting biogas production by trucking in organic solid and liquid wastes, such as food residues and fats, oils, and grease. With increasing production of biogas, there are more opportunities for its use as feedstock for applications besides energy production, such as production of PHB.

12.5 Revenue for biogas to electricity and biogas to PHB

Use of biogas to produce heat and electricity is common practice. For small digesters, biogas is used for heating (cooking, boilers, etc.). For large landfills and digesters, electrical power production can be attractive. Internal combustion engines with combined heat and power (CHP) operate at an efficiency of 35 percent, and turbines operate at an efficiency of 40 percent. Accordingly, we carried out an analysis of the revenue for biogas-to-electricity conversion compared to projected revenue from conversion of biogas to PHB. Our analysis depends strongly upon the market price of electricity and PHB. Both may vary.

For this analysis, we assumed:

1. The factor for conversion of methane to energy is 213 kcal/mol (ref 57).
2. The factor for conversion of energy to electricity is 0.00116 kWh/kcal (ref 57).
3. The efficiency of electricity generation is 35% for a gas engine and 40% for a gas turbine.
4. The anaerobic digester is operated continuously with 50% solid removal and a methane yield of 0.32 m^3/kg solid removed; and the conversion yield for PHB production is 0.49 kg PHB/kg methane.

The relationship between digester design capacity and power production capacity is

Electrical power production capacity (MW) y= kx (Equation 3)

in which k=0.00007 for 35 percent electrical energy conversion efficiency, and k=0.00008 for a 40 percent efficiency; x= digester design capacity (MT per year). The results are illustrated in **Figure 12.7.**

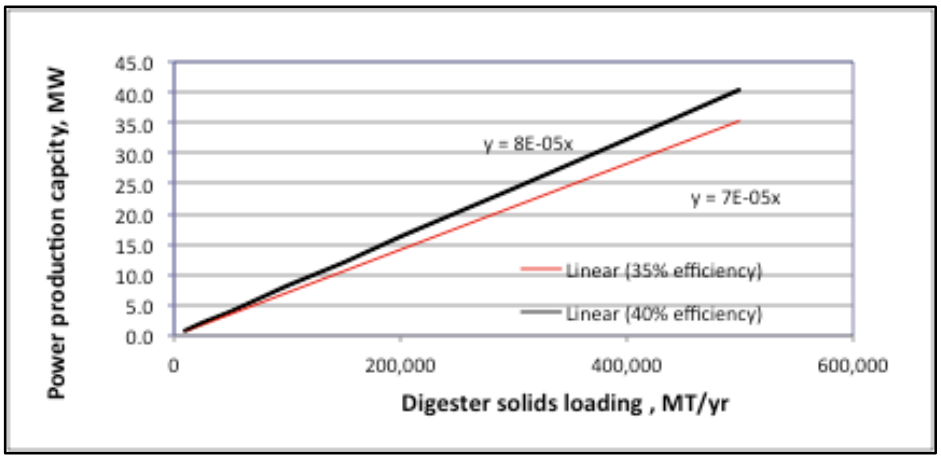

Figure 12.7: Electrical power production verses anaerobic digester solids loading, where the assumed efficiencies of energy conversion to electricity are 35 and 40 percent, respectively

To achieve a capacity of 35 MW, the required solids loading is 440,000 to 500,000 tonnes per year. This is similar in scale to the Joint Water Pollution Control Plant (JWPCP) wastewater treatment plant near Los Angeles (service for 3,500,000). To achieve a capacity of 6 MW, the required solid loading is 75,000 to 85,714 tonnes per year. This is similar to that of the East Bay Municipal Utilities District (EBMUD) wastewater treatment plant in Oakland (service for 650,000).

We can now compare the capacity for power (MW) and PHB production when methane is the feedstock. The results are shown in **Figure 12.8** where

Electrical power generation capacity (MW) y = kx (Equation 4)

in which k=0.0013 for a conversion efficiency of 35% and 0.0014 for a conversion efficiency of 40%; x= PHB production capacity if all the biogas is used for PHB production. For an electrical power production capacity similar to that of the JWPCP treatment plant (35 MW) and EBMUD treatment plant (6 MW), the estimated capacities for PHB production are 27,000 to 32,000 and 4,600 to 5,500 tonnes, respectively.

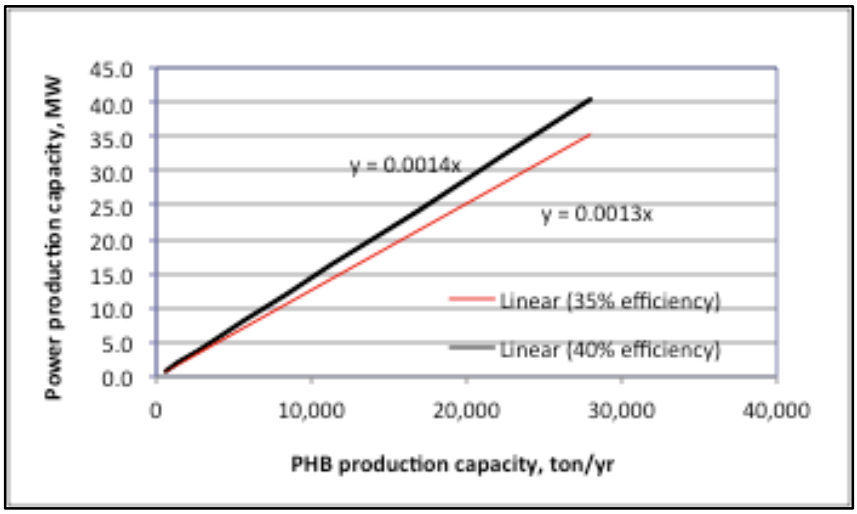

Figure 12.8: Power production capacity, assuming energy conversion of efficiencies of 35% and 40 percent, versus annual capacity for PHB production from the same amount of methane.

The scale of municipal WWTPs required for PHB production can be estimated from service populations and typical per capita wastewater generation data. For this analysis, we assumed:

- Wastewater flow: 340 L per capita per day
- COD concentration 330 mg/L
- COD removal: 90 percent

- Suspended solid (SS) concentration: 300 mg/L
- SS removal: 98 percent
- Sludge yield: 0.3 g SS/g COD removed
- SS removal in anaerobic digester: 50 percent
- CH_4 yield in the anaerobic digester: 0.32 L/g SS removed.

The relationship between wastewater treatment plant service population and solids loading, including primary solids and biosolids generated during secondary treatment, is

$$y = 0.0484x \qquad \text{(Equation 5)}$$

in which y = solids loading (tonnes per year); x = Population served by the WWTP.

Figure 12.9 illustrates this relationship.

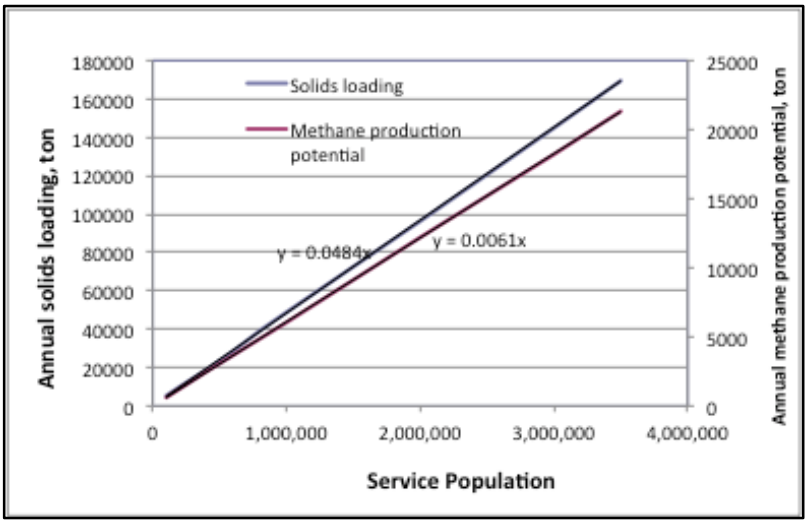

Figure 12.9: Annual solids produced (blue line, left axis) and methane production capacity (red line, right axis) in wastewater treatment plants as a function of service population

The methane produced as a function of treatment plant service population is given by

$$y = 0.0061x \qquad \text{(Equation 6)}$$

in which y = methane generated (tonnes per year); x = WWTP service population.

Figure 12.10 illustrates this relationship. For a given service population, the power production capacity can be estimated from Equation 5. For the Joint Water

Pollution Control Plant, with a service population of 3,500,000, the estimated capacity is 15 MW, slightly less than the current operational capacity (20 MW). For the EBMUD wastewater treatment plant, with a service population of 650,000, the estimated power capacity is 2.8 MW. While this value is roughly half of the current EBMUD power capacity, it appears reasonable given that EBMUD trucks in additional organic wastes for digestion.

Assuming methane production as described by Equation 6 and a PHB conversion yield of 0.49 g PHB/g CH_4

$$y = 0.003x \qquad \text{(Equation 7)}$$

in which y = PHB production potential (tonnes per year); x = Population of WWTP service.

To achieve an annual PHB production potential of 2,000 tonnes per year at a wastewater treatment plant, the service population of the plant would need to be at least 500,000, a population similar to that served by the East Bay MUD plant. A plant capable of producing 10,000 tonnes per year would require a treatment plant with a service population of 3,000,000, similar to that of the Joint Water Pollution Control Plant.

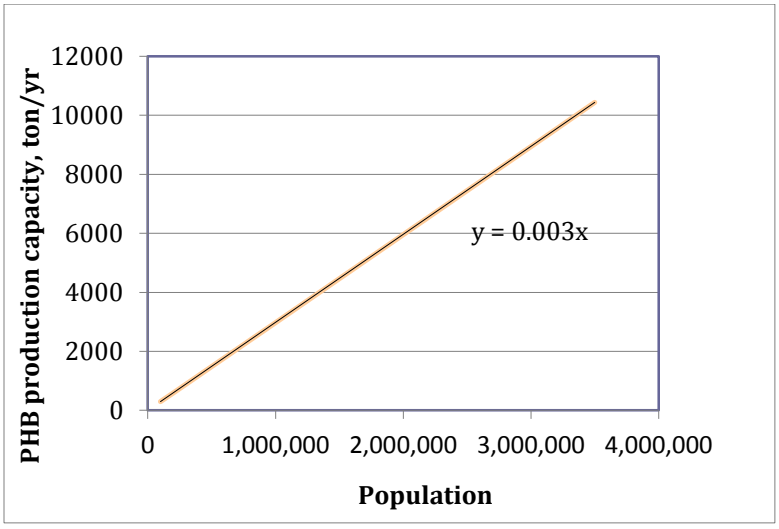

Figure 12.10: PHB production capacity from biogas generated at a wastewater treatment plant as a function of the service population of the WWT plant. Assumption: Anaerobic digestion removes 50 percent of the solids with generation of 0.32 L CH_4 per g SS removed.

Revenue from electricity depends upon market prices. Currently, the retail price of electricity in the United States varies from state to state and ranges from $0.08 to 0.17 per kWh (EIA, Electric Power Monthly: Average Retail Price of Electricity pg. 106). California prices range from $0.11 to $0.13 per kWh (Source: California Energy Commission). To estimate electrical energy production revenues for methane, we assumed energy conversion efficiencies of 35 percent and 40

percent and prices spanning the historical and projected range. Revenue from PHB depends upon its market price. To estimate revenues for PHB, we assumed a conversion yield to PHB of 0.49 g PHB/g methane, the current price of $4 to $5/kg, a target price of $2 to $2.50/kg, and a price typical of petroleum-based plastics ($1.5/kg). The results are summarized in **Table 12.3**.

PHB production is attractive at its current price ($4 to $5/kg) and remains attractive at greater than $2.0/kg, close to the current price of biodegradable PLA and nonbiodegradable PET (**Table 12.2**). PHB production becomes less attractive, or not attractive, if the price approaches that of PE and PP ($1.27 to $1.43/kg). Though the potential for revenue is large, the economic viability of PHB production depends upon the cost of production. The following sections assess this issue.

Table 12.3: Revenue per tonne of methane when methane is used for power or PHB production based on energy efficiencies of 35 percent and 40 percent and for different PHB sale price assumptions

Electricity price ($/kWh)	PHB sale price ($/kg)	Electricity revenue ($/tonne) at 35% efficiency	Electricity revenue ($/tonne) at 40% efficiency	PHB revenue ($/tonne)
0.06	1.50	320	370	820
0.09	2.00	490	560	1,100
0.12	2.50	650	740	1,400
0.15	3.00	810	930	1,700
0.18	4.00	970	1,100	2,200

12.6 Cost of biogas as feedstock for PHB production

The following analysis was conducted using chemical engineering data from different sources and current market prices for industrial fermenters. The analysis involves many assumptions related to process engineering and design, as well as the following:

1. Biogas is available free of charge.
2. The PHB production plant is located near a landfill, a wastewater treatment plant with anaerobic digestion, or a biogas pipeline. Cost for transport of biogas or natural gas is not included.
3. Electricity is available for PHB production. It may be generated locally from biogas or imported from an external network.
4. Water is available near the plant area for PHB production and electricity generation.
5. Waste and wastewater generated during PHB production can be disposed to a landfill or used as a source for biogas to enhance biogas production.
6. A lifetime of 15 years is assumed for capital investment depreciation.
7. The following costs are excluded:
    a. Capital cost and maintenance for electricity generation.
    b. Water supply system and sewer for wastewater discharge.
    c. Road construction to outside area.
    d. Cost for marketing and sale of PHB products.
    e. Wastewater treatment and solid waste disposal.

Note: All of the above assumptions require testing at the pilot scale.

12.7 PHB production costs

Figure 12.11 illustrates the process schematic developed to estimate PHB production costs. The process includes four major units:

1. Bioreactors, including both production fermenters for growth of PHB-rich biomass and culture fermenters for maintenance of seed cultures;
2. PHB extraction units including tanks, biomass filters, and centrifugation equipment;
3. Equipment for product drying, extrusion, packaging, and storage; and
4. Supporting facilities including an analytical laboratory, workshop for mechanics, electrical control room, and office buildings.

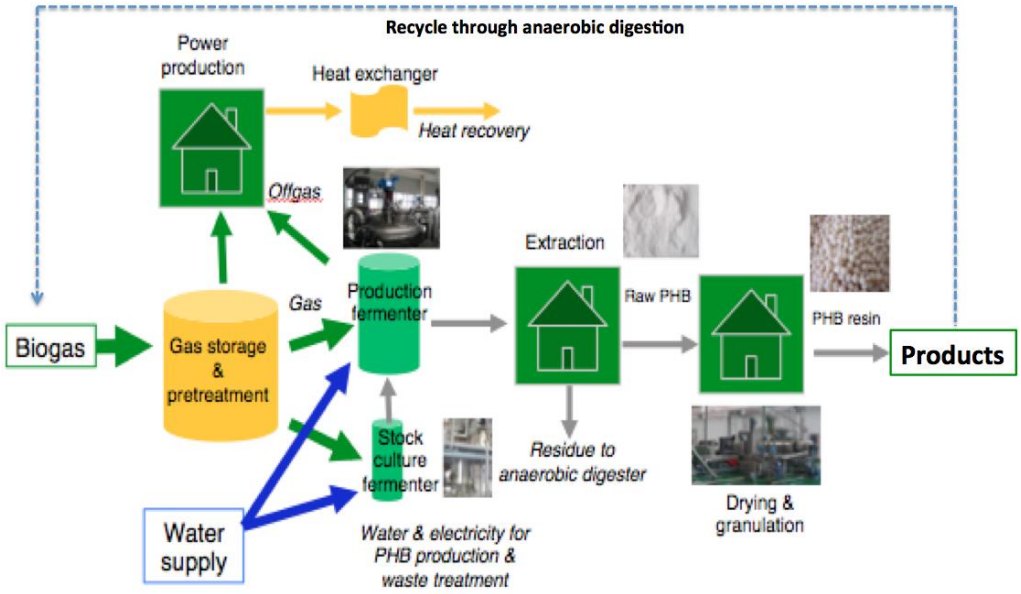

Figure 12.11: Schematic for proposed PHB production process from biogas methane

Table 12.4 summarizes major parameters for the fermentation. Biogas from a landfill and/or anaerobic digester is compressed in a storage tank prior to delivery to bioreactors (i.e., fermenters). The fermenters are operated at 25 kPa (2.5 atm) at a cell density of 100 g dry weight/L (maximum density 120 g/L). This is a high cell density, reported for *E. coli*, but not yet attempted with methanotrophs. Confirmation that this cell density can be achieved will require pilot-scale testing.

One or two small fermenters are operated for culture maintenance. These cells are incubated continuously in an ammonium-rich medium (6 mM as NH_4-N) to maintain a stock of Type II methanotrophs. After harvesting and dewatering of the cake, the SDS-hypochlorite method is used to extract PHB. The residues of extraction are used as fertilizer or anaerobically digested for biogas production. This could potentially generate additional values that offset costs.

In the final step, PHB powder is purified, dried, and granulated via extrusion to produce commercial resins. The power supply is assumed to be an electrical power generation system in which biogas is used as fuel but the capital and operational costs were not estimated. The total cost of production includes: a) annual depreciation of the capital investment; b) operational costs (chemicals, labor, electricity, etc.); and c) management and other maintenance costs.

Stoichiometric and kinetic parameters used for the following analysis (**Table 12.4**) were determined in laboratory experiments and/or obtained from published literature. These parameters were used to envision a plausible large-scale reactor design and to determine the capacity for PHB production, but these projections must be viewed with great caution in the absence of pilot-scale testing.

Table 12.4: Design parameters for methanotrophic PHB production at large-scale (T = 30°C)

Parameter	Value
Biomass PHB content	0.5 g PHB/g dry weight[48]
Conversion yield	0.49 g PHB/g methane[49]
Growth yield	0.345 g biomass/g methane[50]
Growth rate	0.09/hr on nitrate as N source[51]
Cell concentration	100 g/L (Max. 120 g/L)
PHB production duration	168 hrs including growth (120 hrs) and PHB accumulation phase (48 hrs)

The cost of PHB production is a function of reactor capacity and configuration. In this analysis stainless steel, pressurized, well-mixed fermenters are assumed. The proposed reactors are a modification of reactors now used for PHBV production with glucose as feedstock. Other reactor configurations could be more economical, but none have been demonstrated at a sufficiently large scale. The following additional assumptions and parameters were used to define capital and operational costs:

1. The fermenter system of the plant is composed of four production reactors to produce PHB and one culture reactor to maintain an active seed for inoculation of the production reactor;
2. The capital investment recovery time is 15 years at a 4 percent effective rate;
3. The medium is synthesized with the desired nutrients (N, P, and trace elements) to achieve C, N and P balance of 200:5:1 for the growth phase and 50 percent PHB for the PHB accumulation phase;
4. For the PHB production phase, the primary design parameters were:
    - Harvest cell density in the production reactor: 100 g/L
    - Pre-growth phase cell density: 5 to10 g/L
    - Final PHB content: 50 percent of dry weight
    - Temperature: 25^{o} to 30^{o} C
    - pH: 5-6

- Batch fermentation duration of 168 hours (7days) with 48 hours (2 days) for clean-up and refill of culture
- The number of production cycles per year for each fermenter is 37, including time for maintenance

Major capital investment costs were estimated in three steps: Step 1 included costs for equipment (fermentation vessels, extraction equipment, driers, compressors, pipes, mixers, pumps, etc.); Step 2 included costs for the equipment plus a PHB production building; and Step 3 included costs for the equipment plus a PHB production building, installation of equipment, building construction, and construction of supporting facilities (offices, laboratory, storage, road access, etc.). Step 3 gave the total capital cost. Details are provided below.

Step 1: Investment cost for equipment

The size of the fermenter depends upon its capacity for PHB production. We assume annual PHB production capacities of 500, 2,000, 5,000, 10,000, 50,000 and 100,000 metric tonnes. A capacity of 2,000 tonnes per year is similar to that of the third-largest PHBV producer in the world and represents the PHB production capacity of a wastewater treatment plant comparable in size to the East Bay Municipal Utility plant; 5,000 tonnes per year is the mean PHB production capacity of a California landfill; 10,000 tonnes per year is the capacity of a treatment plant similar to the Joint Water Pollution Control Plant near Los Angeles; and 50,000 tonnes per year would represent the PHB production capacity of the largest landfill in California. No current biogas source in California could support 100,000 tonnes of PHB production. This capacity is of interest because it is half the capacity of the NatureWorks PLA production facility and about one third the size of many polyethylene and polypropylene plants that produce approximately 300,000 tonnes per year.

The fermentation unit is the core of a PHB production facility. **Table 12.5** summarizes the fermenter size, power for stirring, power for supply of biogas and oxygen, and footprint for the fermentation unit with four fermenters for growth. The capital investment of extraction unit and product package unit are based on the production capacity, varying from 15 to 40 percent of fermentation unit.

Table 12.5: Pressurized fermenters with stirrer and compressed air and biogas supply for PHB production. Cost is for each fermenter. The fermenter is made from stainless steel and operated at 25 kPa (2.5 atm). Market prices were obtained from a private consultant. The footprint is for a four-fermenter unit.

Fermenter size (m^3)	Fermenter price ($)	Power of stirrer (kW)	Air or CH_4 gas (m^3/min)	Vortex blower power (kW)	Fermentation footprint (m^2)

320	650,000	650	270	950	150
200	430,000	400	180	650	120
150	350,000	300	130	450	100
100	240,000	200	90	320	85
50	170,000	95	45	160	46
20	130,000	50	23	80	30

For a plant that produces 500 tonnes PHB per year, the annual capital investment depreciation is $89 per tonne of PHB production capacity per year; for a plant that produces 100,000 tonnes per year, it is $15 per tonne of PHB production capacity per year (**Table 12.6**).

Table 12.6: Capital investment for equipment to produce PHB.

Plant capacity (tonne/yr)	Fermenter			Extraction ($)	Drying, packaging ($)	Sum ($)	Specific Investment ($/tonne)	Annual ($/tonne-yr)
	Size (m^3)	No.	Cost ($)					
500	20	2	260,000	130,000	100,000	490,000	990	89
2,000	50	4	690,000	280,000	210,000	1,200,000	590	53
5,000	100	4	950,000	330,000	240,000	1,500,000	300	27
10,000	150	4	1,400,000	420,000	280,000	2,100,000	210	19
50,000	320	10	6,500,000	2,000,000	650,000	9,100,000	180	16
100,000	320	18	12,000,000	3,500,000	1,200,000	16,000,000	160	15

Note: Annual cost is the equivalent uniform annual cost per tonne ($/tonne-yr) calculated for a fixed interest rate of 4 percent over a 15-year design life.

Step 2: Investment cost for PHB production equipment and building

Table 12.7 summarizes the capital investment for equipment and for a PHB production building at different PHB production capacities. Currently available fermenters range in size from 20 to 320 cubic meters (**Table 12.5**). A pressurized fermenter larger than 320 m^3 could be expensive and technically difficult to operate. Accordingly, we assume two or four fermenters operating as a unit, and we select different sized fermenters to meet the PHB production capacities indicated in **Table 12.7**. The capital investment for equipment includes fermenters, extraction, and packaging equipment. The equivalent uniform annual cost per tonne of PHB produced ($/tonne-yr) was used to estimate operational costs. The annual capital investment depreciation for a plant that produces 500 tonnes per year is three times that of a plant that produces 5,000 tonnes per year and six times that of a plant that produces 100,000 tonnes per year. Large plants near a site with a rich source of biogas are favored.

Table 12.7: Capital investment for fermentation unit and PHB production capacity

Plant capacity (tonne/yr)	Fermentation unit building			Equipment ($)	Equipment + building ($)	Specific Investment ($/tonne)	Annual ($/tonne-yr)
	Foot print (m^2)	Rate ($/$m^2$)	Building Cost ($)				
500	**30**	4000	120,000	260,000	380,000	760	68
2,000	**46**	4000	180,000	690,000	880,000	440	39
5,000	**85**	3500	300,000	950,000	1,200,000	250	22
10,000	**100**	3500	350,000	1,400,000	1,700,000	170	16
50,000	**375**	3000	1,100,000	6,500,000	7,600,000	150	14
100,000	**675**	3000	2,000,000	12,000,000	14,000,000	140	12

Total PHB production capacity has a significant impact on capital investment for equipment. The total equipment investment increases as capacity increases (**Figure 12.12A**), but the specific capital investment (normalized to one tonne of PHB produced per year) decreases significantly as PHB production capacity increases from 500 tonnes per year to 10,000 tonnes per year, then decreases slowly thereafter (**Figure 12.12B**). The relationship between specific capital investment for equipment and PHB production capacity roughly fits a power function (**Figure 12.12B**)

$y = 7123.2x^{-0.345}$ ($r^2 = 0.899$)

in which y = specific capital investment (dollar per tonne PHB); x = PHB production capacity (tonnes per year). This equation can be used to estimate the capital investment required for different-size plants.

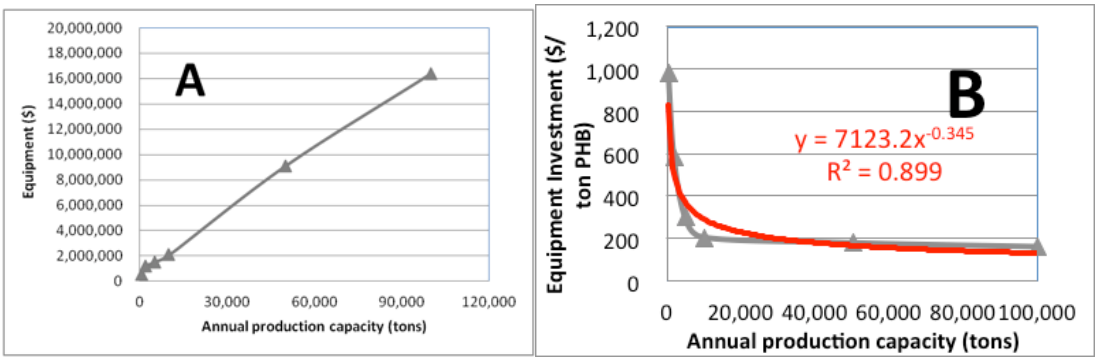

Figure 12.12: Influence of (A) capital equipment investment and (B) capital equipment investment per tonne of PHB produced on PHB production capacity.

Figure 12.13A illustrates the relationship between the capital cost for the fermentation unit and plant capacity; **Figure 12.13B** illustrates the relationship between capital investment ($/tonne PHB) and plant capacity.

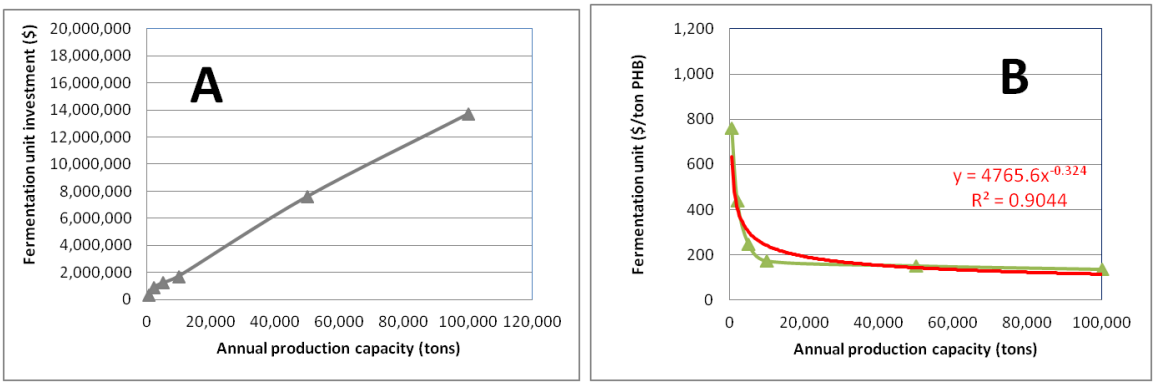

Figure 12.13: The effects of (A) capital investment for equipment and building and **(**B**)** the specific capital investment on PHB production

The relationship between the specific capital investment for equipment and building ($ per tonne of PHB produced) roughly fits power function equation:

$$y = 4765.6x^{-0.324} \ (R^2 = 0.9044)$$

in which y = specific capital investment of the PHB production equipment plus building ($ per tonne PHB); x = annual PHB production capacity (tonne).

Step 3: Total investment cost

It is difficult to estimate the total capital investment for a full-scale plant with all of the supporting facilities, particularly without pilot- and full-scale data. Even with such data, the cost is highly site-specific. Published data for a full-scale PHB or PHBV plant does not include construction costs, nor does it include itemized information about construction costs and supporting facilities. However, consultants experienced in high cell density fermentations have reported that the total investment cost, including construction, installation, and supporting facilities (offices, laboratories, landscape, roads), can be estimated at roughly 5 to 10 times the cost of the PHB production equipment and the PHB production building. For the purposes of this report, a mean of 7.5 is assumed. The results are summarized in **Table 12.8** and in **Figure 12.14**. **Figure 12.14A** illustrates the total capital investment versus PHB production capacity. **Figure 12.14B** shows that the relationship between the specific capital investment ($ per tonne of PHB produced) and the PHB production capacity fits a power law function:

$$y = 36438x^{-0.324} \qquad (r^2 = 0.904)$$

in which y = specific total capital investment ($ per tonne PHB); x = annual PHB production capacity (tonne). This equation can be used to roughly estimate the total capital investment for plants with different PHB production capacities.

Table 12.8: Total capital investment for PHB production facilities that have different production capacities, including equipment costs for extraction, drying, and packaging.

Plant capacity (tonne/yr)	Total capital cost ($)	Specific capital cost ($/tonne)	Annual cost with depreciation ($/tonne-yr)
500	2,900,000	5,700	510
2000	6,600,000	3,300	300
5000	9,400,000	1,900	170
10000	13,000,000	1,300	120
50000	57,000,000	1,100	100
100000	100,000,000	1,000	90

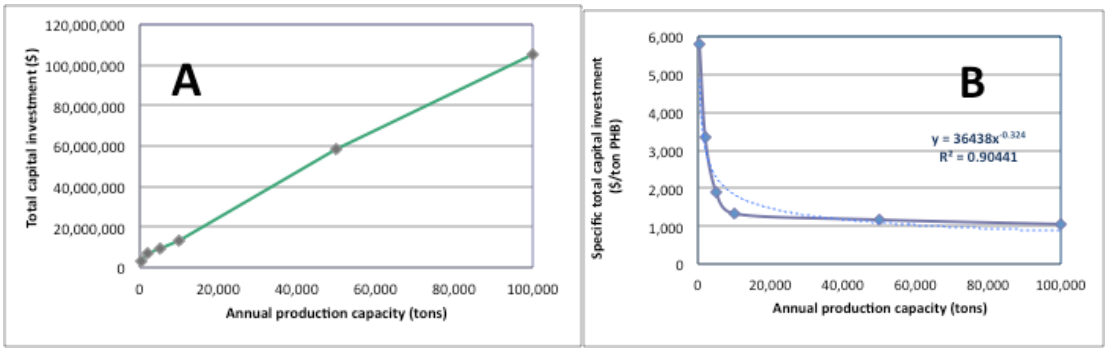

Figure 12.14: Influence of (A) the total capital investment for PHB production and (B) the specific total capital investment on PHB production capacity

Operational costs

Operational costs include the costs of chemicals, utilities, and labor. **Table 12.9** summarizes the mass of chemicals required per tonne of PHB produced, the unit price of chemicals, and the contribution of each chemical to the cost of PHB. This includes nutrients in the growth medium (sodium nitrate, ammonia chloride, and potassium phosphate) and reagents for extraction. Nutrient requirements are based on biomass N and P requirements, and buffer is proved at 20 mM of soda ash as $NaHCO_3$. Chemicals for extraction are sodium hypochlorite and sodium dodecysulfate (SDS). Consumption of these chemicals is estimated from batch extraction experiments. These estimates are conservative because chemical recycling is not considered. More accurate estimates require pilot- and full-scale testing of cell growth and PHB accumulation and extraction.

Table 12.9: Chemical requirements for PHB production

Chemical	Requirement (tonne/tonne PHB)	Market price $/tonne of chemical	Chemical cost ($/tonne PHB)
$NaNO_3$	0.14	320	46
K_2HPO_4	0.011	900	10
KH_2PO_4	0.0081	900	7
NH_4Cl	0.0010	100	0.0048
Soda ash	0.0019	200	0.38
Sodium hypochlorite	0.20	700	140
SDS	0.14	320	45
Sum			249

Electrical power consumption results from stirring, use of vortex blowers to supply biogas and air, medium pumping, filtering, extraction and extrusion, and

lighting and office use. These numbers were obtained from a consultant with experience in high-density cell cultivation and are considered conservative. The source of electricity can be biogas or external sources. A unit price of $0.10/ kWh is assumed. This value is conservative; biogas-producing utilities are currently able to sell electricity at approximately $0.08/kWh.

Table 12.10 summarizes electricity consumption for fermenters of different size, and **Table 12.11** summarizes electricity consumption for plants with different capacities for PHB production. A plant producing only 500 tonnes of PHB per year consumes twice the electricity per unit of PHB produced ($627 per tonne of PHB produced) of a plant producing 10,000 tonnes per year ($363 per tonne of PHB produced). However, when plant capacity exceeds 10,000 tonnes of PHB per year, power requirements per kg of PHB produced are relatively stable at approximately 340 to 380 kWh per year (**Table 12.11**).

Table 12.10: Power and electricity consumption for fermenters of different size

Fermenter size (m^3)	Stirrer (kW)	Air vortex blower (kW)	Biogas blower (kW)	Electricity per cycle (kWh)	Electricity per year (kWh)
320	650	950	950	430,000	16,000,000
200	400	650	650	290,000	11,000,000
150	315	450	450	200,000	7,600,000
100	200	320	320	140,000	5,200,000
50	95	160	160	70,000	2,600,000
20	50	80	80	35,000	1,300,000

Note: Each PHB production cycle lasts 168 hours, and 37 cycles are employed per year.

Table 12.11: Annual electricity costs at an assumed electricity price of $0.10 per kWh

Plant capacity (tonne/yr)	Reactor size (m^3)	No.	Power (kwh)	Extraction (kwh)	Package (kwh)	Sum (kwh)	Cost	
							Sum($)	$/tonne PHB
500	20	2	2,600,000	260,000	260,000	3,100,000	310,000	630
2,000	50	4	10,000,000	1,000,000	1,000,000	12,000,000	1,200,000	620

5,000	100	4	21,000,000	2,100,000	2,100,000	25000,000	2,500,000	500
10,000	150	4	30,000,000	3,000,000	3,000,000	36,000,000	3,600,000	360
50,000	320	10	160,000,000	16,000,000	16,000,000	190,000,000	19,000,000	380
100,000	320	18	290,000,000	29,000,000	29,000,000	340,000,000	34,000,000	340

Labor costs are incurred for straight-time labor associated with the three major operational units (**Table 12.12**) and for indirect labor including management, sales personnel, and supporting technicians (**Table 12.13**). For straight-time labor, the assumed pay rate is $60,000 per year with an average indirect labor cost of $75,000 per year. This assumes a work schedule of 2,080 hours per yr.

Table 12.12: Straight-time labor and annual cost at a rate of $60,000 per year

Plant capacity (tonne/yr)	Fermentation	Extraction	Pack -age	Total personnel	Sum of labor cost ($)	Labor cost ($/tonne PHB)
500	10	2	2	14	840,000	1,680
2000	10	3	2	15	900,000	450
5000	10	4	3	17	1,020,000	204
10000	12	6	5	23	1,380,000	138
50000	24	10	8	42	2,520,000	50
100000	50	15	14	79	4,740,000	47

Table 12.13: Indirect labor and annual cost at a rate of $75,000 per year

Plant capacity (tonne/yr)	Manager	Sale	Supporting	Total personnel	Sum of labor cost ($)	Labor cost ($/tonne PHB)
500	2	1	1	3	225,000	450
2000	2	2	2	4	300,000	150
5000	3	3	4	6	450,000	90
10000	3	4	6	7	525,000	53

50000	4	4	11	8	600,000	12
100000	4	5	16	9	675,000	7

Table 12.14 gives the total labor cost and a breakdown of labor costs. In general, straight labor (direct wages and salaries) constitutes more than 70 percent of the total labor cost. The cost of labor for anaerobic digestion may be offset by tipping fees and is thus not included in the analysis. Indirect costs include employee benefits, office supplies, insurance, legal and license fees, product promotion costs, etc. Miscellaneous costs include costs for maintenance and repair. These costs are estimated at 30 percent of direct costs except for capital depreciation. During field operations, solid waste is generated and will need to be managed. These costs are not included in this analysis.

Table 12.14: Total labor costs

Plant capacity (tonnes/yr)	Total personnel	Total wages ($)	Labor cost ($/tonne PHB)	Straight labor (%)	Indirect labor (%)
500	17	1,100,000	2100	79	21
2000	19	1,200,000	600	75	25
5000	23	1,500,000	290	69	31
10000	30	1,900,000	190	72	28
50000	50	3,100,000	60	81	19
100000	88	5,400,000	54	88	13

12.8 PHB production: Breakdown of costs

Table 12.15 provides a breakdown of costs as a function of PHB production capacity. **Figure 12.14** illustrates these data. For small plants (<2,000 tonnes PHB produced per year), labor costs are the main contributor to the cost of PHB production. For large-scale production (>5,000 tonnes of PHB per year), energy consumption (electricity) can contribute up to 38 percent of the total production cost. The cost of electricity is assumed to be $0.10/kWh, but it is possible that electricity generated from biogas will be less expensive and may offset or stabilize operational costs. The second-largest cost is chemicals.

Figure 12.15 illustrates the estimated cost of PHB production ($/kg) with biogas as feedstock as a function plant production capacity. Also shown are the current

market prices of major polymers, including PHBV, PLA, PE (polyethylene), PPE (polypropylene), and PS (polystyrene). These data suggest that PHB production can be cost-competitive, particularly at a large scale.

Table 12.15: Cost breakdown for PHB production with biogas as feedstock

Capacity (tonne/yr)	Cost ($/tonne)	Chemical (%)	Electricity (%)	Labor (%)	Indirect & misc (%)	Depreciation (%)
500	4400	6	14	48	20	12
2000	2200	11	28	27	20	14
5000	1500	16	33	19	21	11
10000	1200	21	31	16	21	10
50000	1000	25	38	6	21	10
100000	900	27	37	6	21	10

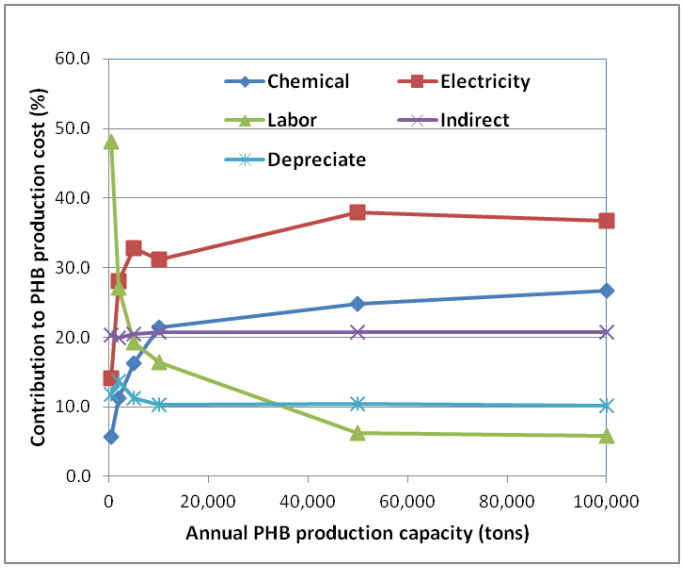

Figure 12.14: Breakdown of costs for PHB production (labor, chemicals, depreciation, electricity, indirect) as production capacity increases. This analysis assumes that capital depreciation over 15 years at a 4 percent interest contributes 10 to 13 percent of the total production cost.

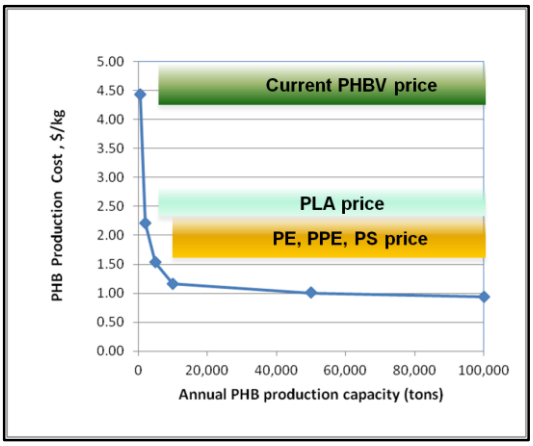

Figure 12.15: Estimated PHB production cost from biogas verses the scale of PHB production (PHB production capacity) for current market prices of PHBV, PLA, and major petroleum-based plastic resins.

12.9 Incremental capital cost of anaerobic digesters

An assumption in the analysis up to this point is that biogas feedstock is available at existing anaerobic digesters or at existing landfills. In such cases, the recycling of PHB-based products occurs when the product has reached its end-of-life and is disposed of in one of these facilities. In such cases, the costs of construction of new anaerobic digestion facilities can be ignored. For many applications, however, an anaerobic digester will be required, and its amortized cost will need to be included in the cost of PHB production. In this section, the contribution of this additional cost is estimated.

The construction cost of an anaerobic digester depends upon its capacity. Clarke (2000)[52] estimated the cost for an anaerobic digester treating MSW as

Capital cost ($million) $y = 1.72x^{0.5581}$

in which x = digester design capacity (1000 dry MT of MSW per yr).

Tsilemou and Panagiotakopoulos[53] estimated the cost as

Capital cost ($million) $y = 1.60\ x^{0.5099}$

in which x = digester design capacity (1000 dry MT of MSW per yr).

Figure 12.16 illustrates solutions to the above equations. The cost estimates of Tsilemou and Panagiotakopoulos[54] exceed those of Clarke,[55] likely because of inflation and details of digester configuration, but the basic patterns are similar. Economies of scale are evident: The larger the digester capacity, the lower the capital cost per tonne.

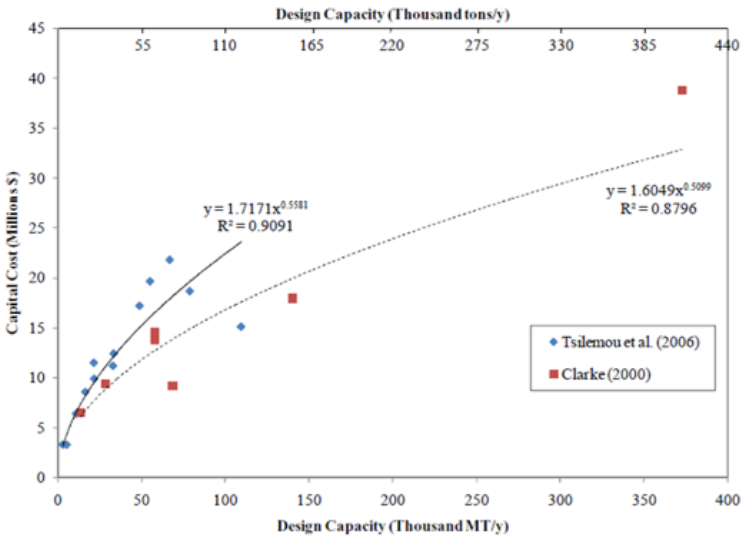

Figure 12.16: Cost of anaerobic digesters as a function of design capacity[56, 57]

The added capital cost of anaerobic digestion can be determined using the model of **Figure 12.16**, with the following assumptions:

1. Solids removal is 50 percent during anaerobic digestion.
2. The methane yield is 0.32 cubic meter (STP) per kg solid removed.
3. The PHB conversion yield is 0.49 kg PHB per kg methane.
4. Costs for transport of waste to the digester are not considered, nor are tipping fees.

Figure 12.17 illustrates the added capital cost of anaerobic digestion and economies of scale. The incremental cost ranges from $0.02 to 0.08/kg PHB produced. Economies of scale are evident: independent of the cost model, the cost per dry tonne of MSW decreases as capacity increases, stabilizing at more than 200,000 MT of solids per year (**Panel A**). This corresponds to a plant with a PHB production capacity of more than 10,000 tonnes of PHB per year (**Panel B**).

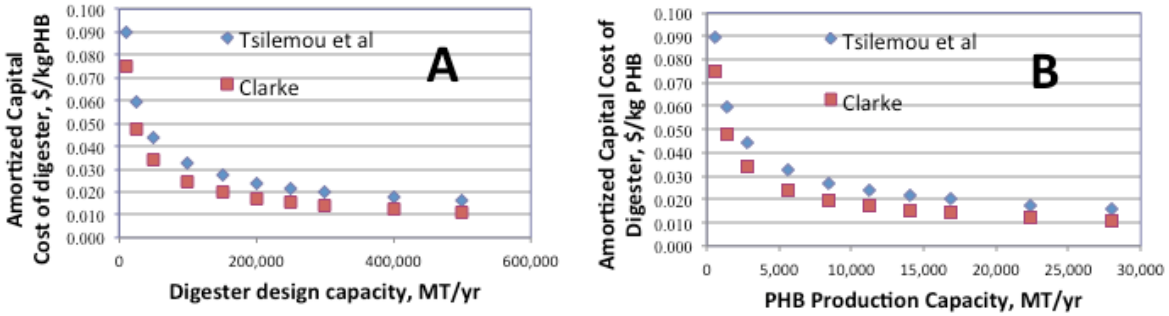

Figure 12.17: Amortized cost of an anaerobic digester in a recycling system that produces PHB. (A) Effect of digester capacity (MT/yr) on the cost of one

kg PHB. (B) Effect of PHB production capacity (MT/yr) on the cost of one kg PHB. The design models are from Clarke (2000)[58] and Tsilemou and Panagiotakopoulos (2006).[59]

12.10 Sensitivity analysis

A sensitivity analysis was conducted to determine which factors have the greatest impact on the cost of PHB. This analysis assumes that the largest practical scale for PHB production is 50,000 tonnes of PHB per year. A plant capable of producing 100,000 tonnes per year would likely require natural gas or shale gas as feedstock.

The main factors influencing the cost of PHB production are:

1. Microbial kinetics and stoichiometry of PHB production, including growth rates, rates of PHB accumulation, and final PHB percentage in the biomass.
2. Effect of process scale-up (efficiencies of fermentation and PHB extraction).
3. Price of feedstock (biogas methane, in this case) and chemicals for nutrients and extraction reagents.
4. Price of energy (electricity and heating source).
5. Capital investment.
6. Labor costs.

The sensitivity of production costs to the above factors is analyzed in the following sections.

Microbial stoichiometry and kinetics have major impacts upon the cost of production. For example, if the growth rates are slower than that those assumed in this analysis (i.e., 0.09/h), the duration of the incubation cycle will be increased and consumption of electricity will increase. Capital investment and energy consumption will also increase. Because the capital investment is only about 10% of the total cost (**Table 12.15**), an increase in the operational cycle of one to two days will increase the cost of the fermentation unit, labor costs, and energy costs, but will have only a small effect on the total cost (10 to 20 percent). These considerations again underscore the need for pilot-scale testing.

Both the percentage of PHB produced in dry cells (as a fraction of the dry weight) and conversion yield (PHB mass produced per unit mass of methane consumed) have significant impacts on production costs. Selection and maintenance of cultures with high conversion yields is critical. For a PHB content of 50 percent, production costs increase significantly at conversion yields less than 0.30 g PHB/g CH_4 (**Figure 12.18**).

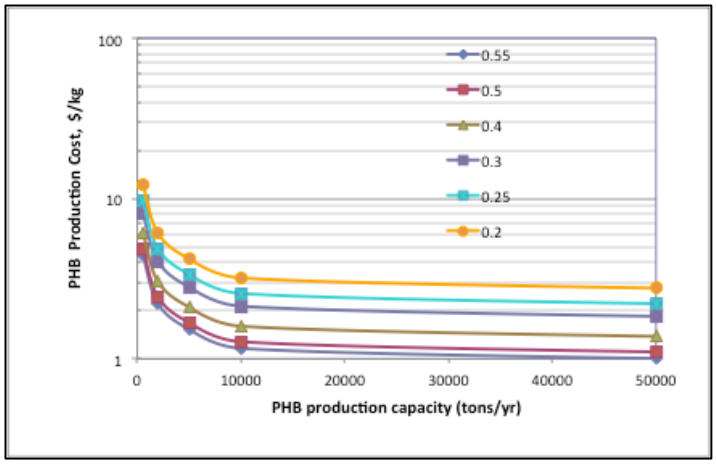

Figure 12.18: Effects of PHB conversion yield (kg PHB/kg CH_4) on the cost of PHB production for plants with different capacities for PHB production.

PHB extraction efficiency also impacts production cost (**Figure 12.19**), but the effects are somewhat less than PHB conversion yield. To achieve a low production cost, the extraction procedure should ensure a recovery efficiency greater than 70 to 80 percent. This is generally achievable but should be tested at large-scale.

Up to this point in the analysis, the cost of methane feedstock has been neglected. The cost is assumed to be zero if a supply of biogas is available on site (landfill, WWTP digester, or digester for agricultural wastes, such as cow and chicken manure). Because of scale effects, large facilities are expected to be most cost-effective, but this requires large landfills and WWTPs. If such a supply is unavailable or unreliable, use of natural gas may be advisable as a supplement. As shown in **Figure 12.20**, if natural gas is used, PHB production costs will increase by 22 to 26 cents per kg PHB, assuming current market prices for natural gas.

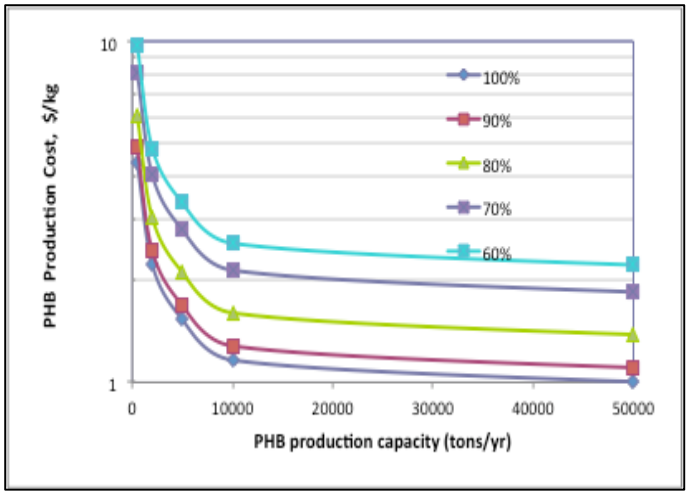

Figure 12.19: Effects of PHB extraction efficiency on the cost of PHB production for plants with different capacities for PHB production.

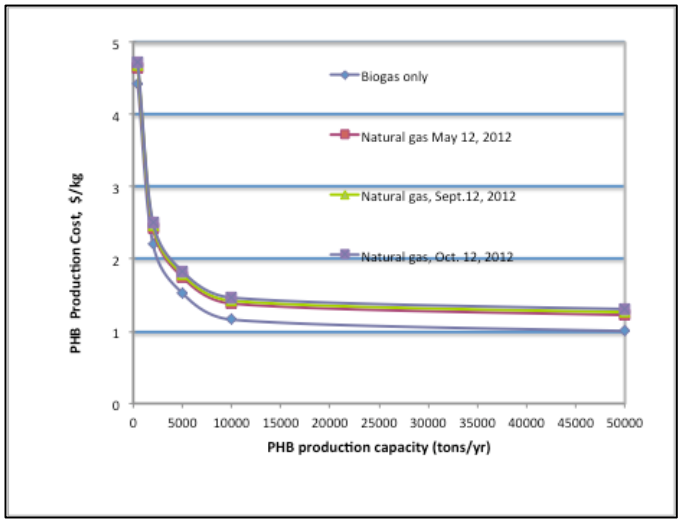

Figure 12.20: Effects of methane source on the cost of PHB production: biogas (no cost) and natural gas at recent market prices.

Energy is a significant part of the total cost and constitutes about 40 percent of the total cost for a large plant (**Table 12.15** and **Figure 12.17**). If electricity is purchased, the variation in its price will significantly impact production costs. If current trends continue, long-term costs for power generation from natural gas may decrease. To stabilize this effect, use of a fraction of the biogas to satisfy energy requirements for PHB may be desirable.

12.11 Key findings

1. Methane in biogas or natural gas can be a cost-effective feedstock for PHB production and could economically displace glucose or other cultivated feedstock.
2. In general, the value of PHB produced from a unit of methane exceeds the value of electricity generated from a unit mass of methane.
3. Existing landfills in California can provide feedstock for mid- to large-scale PHB production with plants producing more than 5,000 tonnes of PHB per year.
4. Anaerobic digesters sized to digest 200,000 tonnes of municipal solid waste per year could sustain PHB production of 10,000 tonnes per year.
5. Some wastewater treatment plants can provide sufficient biogas for mid- to large-scale PHB production from human wastes (i.e., those with a service population of 1 million to 3 million). Collection of and digestion of additional concentrated organic waste streams could enable PHB production at smaller treatment plants.
6. Scale has a large effect on the capital investment for PHB production, but the effect tends to level off when plant sizes reach production volumes of 5,000 to 10,000 tonnes of PHB per year.
7. The cost of PHB production with biogas is attractive at facilities producing more than 5,000 tonnes PHB per year. Costs of PHB production at this scale could compete with PLA and petroleum-based plastic resins.
8. At small scale, labor costs are critical. Such costs might be reduced with effective labor management and training of the existing staff. At large scale, energy efficiency becomes critical. At all scales of operation, chemical costs, especially for extraction and purification of PHB, become important. Some chemicals may be recycled.
9. The PHB conversion yield has a large impact on production costs. Selection of high-performing cultures and maintenance of cultures that can produce high levels of PHB is critical.
10. The efficiency of PHB recovery in the extraction process has a significant impact on production cost. Advances in extraction technology can have a significant impact on costs.
11. Complete or partial replacement of biogas by natural gas or shale gas increases the cost of PHB production by a relatively small amount; the cost of production remains attractive.
12. Pilot- and full-scale studies are critically needed to assess the stoichiometry and kinetics of PHB production at a realistic scale and to accurately assess capital and operational cost.

Appendix: PHA extraction cost estimates

Professor Hunchan Shi, Environmental Science and Technology School, provided cost estimates for PHA extraction. Professor Shi's research group

compared electricity consumption and chemical costs for five extraction methods. The results are summarized in **Table A1.** For these studies, data were obtained for a PHA-producing enrichment fed volatile fatty acids as the carbon source. The PHB content was 40 to 74 percent, close to that achieved in methanotrophic cultures. The most cost-effective extraction method was use of sodium dodecysulfate (SDS)-sodium hypochlorite.

Table A1: Cost of PHA extraction by different methods

Method	Extraction efficiency	% PHA	% Purity	Cost $/kg	Cost $10k/tonne
Sodium hypochlorite -chloroform	77%	74	88	32	3.20
SDS-sodium hypochlorite	96%	74	97	0.34	0.034
SDS-EDTA	90%	74	76	0.88	0.088
Acid method	100%	74	94	0.49	0.049
Alkali method	90%	74	88	0.54	0.054

13. Project Summary and Outcomes

13.1 Summary

Synthesis and Degradation of PHB and PLA

1. PHB production in nature appears limited to Type II methanotrophs. This finding has important implications for industrial biotechnology in open systems because PHB-producing methanotrophs will compete for methane, oxygen, and nutrients with methanotrophs that do not produce PHB. Because Type I strains can outcompete Type II strains, Type II-selective conditions are needed for sustained PHB production. Creating bioreactor conditions that mimic the ecological niche of PHB-producing Type II methanotrophs confers a competitive advantage for methanotrophs that produce PHB. This requires understanding of the physiological and ecological role of PHB in methanotrophs that produce it.

2. The likely role of PHB is to serve as a source of reducing power (fuel) to drive the initial step in methane oxidation and assimilation of nitrogen. An unexpected finding was that the model Type II methanotroph *Methylocystis parvus* OBBP does not use PHB as its sole growth substrate in the absence of methane, even when all other required nutrients are present. The likely physiological function of PHB is to serve as a source of reducing equivalents (fuel). A plausible hypothesis is that strategies favorable for PHB-producing methanotrophs can be based upon the use of PHB as a fuel to drive rapid uptake of methane and facilitate rapid metabolism of nutrients, especially those forms of nitrogen that impose high energy demands (ammonium<N_2). Methane limitation during PHB consumption led to increased PHB production over time in a defined mixed culture. Growth on ammonium selected for Type II methanotrophs, but limited culture densities. Methane limitation can be combined with cycling nitrogen sources for long-term PHB production in enrichment culture, but long-term exposure to high levels of ammonium induced functional instability.

3. A high-throughput system for growth and analysis of methanotrophs enabled screening and optimization of strains and culture conditions. Use of this system enabled an order of magnitude improvement in handling time and effective selection of conditions for increased PHB production. Media composition dramatically impacted PHB production in *M. parvus* OBBP. Calcium and copper, in particular, had significant impacts. The results with calcium were not expected and could not have been predicted from the existing literature. A PHB content of 3.43g/L was achieved in pure culture *M. parvus* OBBP under optimized conditions.

4. Methane required per unit of PHB produced is highly strain-specific and dependent upon growth conditions. Growth rates vary with yield, with doubling times of two to 11 hours, and are highly dependent upon the nitrogen source, with slow growth on N_2 and rapid growth on nitrate. PHB yields of 0.49 g PHB/g methane, and approximately 50 percent PHB by weight, were achieved with *Methylocystis parvus OBBP*, a model Type II methanotroph. Up to 46 percent by cell weight was achieved in enrichments inoculated with activated sludge and grown under selective conditions.

5. Molecular weight in Type II enrichment cultures was consistent over time at around 1.0×10^6 Da. The production of a uniform product is of value for many commercial applications.

6. Biocomposites containing PHB biodegrade eight to 25 times faster than biocomposites containing cellulose acetate and soybean oil. Fully biobased composites exhibit a high level of anaerobic degradability; almost all composites tested produced 80 percent or greater of the theoretical methane expected based on stoichiometry.

7. Biocomposites with fiber and matrix treatments (silination and maleation) reached 80 percent of theoretical degradation by four to six weeks, indicating little or no adverse effect on biodegradation due to chemical treatments.

8. The microbial biodegradation rate of P3HB-*co*-3HHx depends upon the copolymer composition and processing history. Increasing the 3HHx fraction in P3HB-*co*-3HHx resulted in increased rates of biodegradation that are likely due to the decreased crystallinity.

9. PLA degrades relatively slowly under anaerobic conditions. The release of biogas from PLA is noteworthy, however, given that PLA is typically viewed as resistant to anaerobic degradation. The amount of biogas generated at 55°C for PLA is approximately double that observed at 37°C, indicating that further testing of anaerobic biodegradability at 55°C is warranted.

10. Base-catalyzed depolymerization of PHB can be used to rapidly recover hydroxybutyrate and crotonate from PHB products at end of life. Crotonate is a potential feedstock for polycrotonates, a class of polymers with promising material properties, but conversion yields must be improved and end-of-life options investigated. Hydrolysis of PHBV yields both hydroxyvalerate and pentenoate.

11. Biological reassembly of hydroxybutryate monomer back to PHB is feasible. An enrichment of aerobic heterotrophic microorganisms can recycle HB back to PHB. PHB percentages of up to 50% by weight are observed in mixed cultures fed hydroxybutyrate and grown under feast-famine conditions.

12. Enzyme-mediated hydrolysis of PLA can enable its rapid depolymerization. Several microbial genes for novel PLA depolymerases have been identified and expressed. These genes derive from a diverse range of microorganisms and different habitats. They may thus be of value for accelerating PLA degradation in environments where degradation kinetics are known to be slow (seawater, compost, anaerobic conditions).

13. PLA is efficiently depolymerized to lactide under a vacuum at relatively low temperatures (190° to 200° C) with a tin(II) catalyst. Recovery efficiency was 94 percent or higher. Major products of thermal depolymerization are L-lactide and D-lactide with a trace amount of *meso*-lactide. The process is insensitive to low levels of blended PBAT, but sensitive to high levels (>50%), suggesting that lactide recovery from recycled PLA is technically feasible by maintaining a low percentage of PBAT in recycled PLA streams.

Biocomposites

1. Addition of oak wood flour (OWF) increases overall composite density, increases composite stiffness and decreases strength and elongation-to-break. Density increases due to a collapse of matrix infill in the OWF during the injection molding process.

2. Both silane- and maleic anhydride (MA)-treated composites exhibited improved mechanical properties. Both treatments increase fiber wettability and distribution and enhance mechanical interlock between fibers and the matrix phase, improving mechanical properties. The crystallinity of neat PHBV decreases after MA-grafting via reactive extrusion, and the overall crystallinity of neat PHBV and MA-grafted PHBV decreases with the incorporation of OWF. The initial modulus softening of MA-PHBV was overcome with as little as 17 percent by volume of OWF.

3. Use of natural textile woven reinforcement can double the initial stiffness of PHBV. Different weave types lead to a change in ultimate tensile strength of the composites, but most fibers examined result in composites with similar tensile stiffness.

4. Exposure to moisture, heat, and UV results in mass loss in PHB polymer films, decreases molecular weight, decreases cross-sectional area, increases elastic modulus, and decreases ultimate strength and strain. PHB and PHBV films increase in modulus and decreases in ultimate strain at break, while ultimate tensile strength remained relatively unchanged.

5. Moisture exacerbated polymer and composite mechanical degradation, cracking, and fading. PHB-hemp composites experienced extensive cracking generated by fiber expansion and contraction arising from cyclic hygrothermal conditions. Cracking is the primary physical and mechanical property degradation mechanism in the composites. The PHB-hemp composites

weathered in a manner similar to several synthetic polymer biobased composites, but they typically experienced faster degradation rates or greater aggregate deterioration. Changes in physical, mechanical, and visual properties of the polymer and composite specimens did not stabilize, indicating that these properties would likely further degrade with continued weathering.

6. During ambient storage, both PHB and PHBV polymer films exhibit significant increase in modulus and decrease in ultimate strain at break, while ultimate tensile strength remains relatively unchanged for both materials. The dominant mechanism is likely glassy aging of amorphous regions over a span of months. Excess free volume is eliminated, which stiffens the amorphous material. This explains the increase in tensile modulus and decrease in strain at break.

7. PHB-hemp fiber composites exhibit mass loss, increase in cross-sectional area, and decrease in ultimate strength and modulus, while ultimate strain increases in the presence of moisture and decreases otherwise.

8. The water absorption processes for all families of wood flour/PHBV composites exhibited Fickian diffusion behavior. Fickian diffusion coefficients for all samples exhibit a temperature dependency as expressed by an Arrhenius rate law. These coefficients are comparable in magnitude to conventional polyolefin-based wood-plastic composites.

9. Silane- and MA-treatments of wood flour/PHBV composites improved resistance to moisture uptake. Fickian activation energies increase for the silane- and MA-treated composites indicating that improved hydrophobicity is due to better wettability and dispersion of fibers in the PHBV matrix.

10. Highly processed hemp fibers provided biobased composites with higher flexural stiffness and strength than the less processed fibers. Recycled jute burlap composites are similar to PHBV-HL composites in flexural stiffness, but use of virgin jute burlap results in stiffer composites. The strength of all burlap composites is significantly lower than that of the highly processed hemp linen composites.

Foams

1. Blending PHBV with cellulose acetate butyrate increases its viscosity and results in foams that have lower bulk density and better cell uniformity, but cell density is reduced. Higher melt viscosity and elasticity and decreased gas solubility retard cell coalescence and collapse during foam expansion, resulting in more uniform cell size distribution and better homogeneity of cellular morphology.

2. Using a gas with higher solubility, such as carbon dioxide, can lead to significant reductions in foam bulk density. Addition of sodium bicarbonate decreases the bulk density compared to azodicarbonamide blowing agents, but with loss of a closed-cell structure.

3. To prevent loss of closed-cell structure, PHBV foams were quenched with water, leading to faster crystalline formation in the polymer matrix. Faster solidification leads to a more uniform, closed-cell bubble morphology and foam with a higher expansion ratio.

4. PHBV, a material with poor melt strength, has enhanced melt properties for foaming applications and can be used to make foams with high cell density when crystallization is induced on the same time scale as cell coalescence. Rapid quenching with water is an effective method for cooling PHBV foamed with sodium bicarbonate to maintain high cell density.

5. Low concentrations of silica nanoparticles can provide cell stabilization to promote lower bulk density and more uniform bubbles. Inclusion of nanoparticles within a foamed polymer matrix provides several advantages, including increased bubble nucleation rates and enhanced cell stability. Hydrophilic silica particles can interact with PHBV through hydrogen bonding, inducing crystallization at high temperatures such that crystalline regions reinforce the low melt strength of PHBV to give low-density foams. These reinforcing effects are more pronounced when the foams are rapidly quenched upon extrusion so that crystalline structures are generated at even shorter time scales.

6. Viscoelastic parameters for PHB-HHx copolymers are readily tunable by varying the HHx content, making them attractive as ‘‘green’’ substitutes for nondegradable thermoplastics. Shear viscosities for a series of microbially synthesized poly(3-hydroxybutyrate-co-3-hydroxyhexanoate)s (PHB-HHxs), with varying comonomer (HHx) content, show dependence on the rate of deformation, temperature, molecular weight, and copolymer compositions.

7. Solvent-cast films of poly(3-hydroxybutyrate-*co*-3-hydroxyvalerate) (PHBV) and silk fibroin (SF) blends were immiscible at all compositions studied. SF morphology changed from amorphous to 38.2 to 47.6 percent crystallinity in the presence of PHBV. SF acts as a crystal-nucleating agent for PHBV, but concentrates in noncrystalline regions during PHBV crystal growth. After melting and fast cooling, SF generally reduces the melting temperature and crystallinity of PHBV films. Mobile SF likely nucleates new PHBV crystals in regions of higher SF content, but immobile SF creates more disorder near the nuclei resulting in overall lower crystallinity.

8. The solubility of nitrogen gas solubility in PHBV affects foam microstructure and properties when N_2 is used for foaming. There is a step change from low to high cell density below and above a specific N_2 pressure threshold associated with N2 solubility in PHBV.

Life cycle assessment

1. The major adverse impacts of PHB production from biogas methane are due to energy requirements for aeration and chemical inputs for PHB extraction and purification. Adverse energy impacts could be offset by combusting approximately 25 percent of the biogas methane to generate the energy needed to produce PHB from the remaining 75 percent. Such a strategy would eliminate the need for grid-sourced electricity and its associated environmental impacts. Adverse impacts due to extraction and recovery steps are decreased by using surfactant and hypochlorite for extraction, but improved separation and purification methods are needed.

2. The major adverse impacts due to biocomposite production are process energy for fiber refinement and polymer production. The greatest reductions in greenhouse gas emissions, energy consumption, and weighted impact score were achievable through incineration of excess biomass and the use of alternate fiber types.

3. Material selection charts are useful tools for concurrent visualization of the mechanical and thermal properties and environmental impacts for biocomposites with different fibers. For example, material selection charts comparing flexural stiffness to environmental impact quickly illustrate that wood flour PHBV composites have low environmental impact relative to textile-reinforced PHBV composites in terms of fossil fuel demand and single score impact, but the low greenhouse gas emissions associated with the jute burlap-reinforced PHBV makes these composites most desirable for that impact category. In fact, for thermal application and single score impact, the burlap-reinforced biobased composites are consistently the most desirable. These charts also quickly show that virgin jute burlap and recycled jute burlap provide a favorable combination of material properties and environmental impacts.

4. Analysis of the material and energy flows for the production of the composite constituents facilitated studying the influence of each flow. The greatest environmental impacts were due to electricity and thermal energy consumption during processing of each constituent. For manufacturing improvements, the greatest benefit was identified as reduction of steam energy use in polymer production through air-to-air exchangers. Incineration of field waste from fiber cultivation provided the greatest benefit for waste reuse. Replacement of highly refined fiber with a less processed reinforcing fiber led to the largest improvements.

5. When analyzing the environmental impacts of biocomposite fabrication, reductions in adverse impacts associated with improvements in the polymer were less substantial than those associated with improving or altering the fiber.

Cost analysis

1. Biogas or natural gas can be a cost-effective feedstock for PHB production, and could potentially displace cultivated feedstock. Cultivated feedstock currently adds $0.50 to $1.50 to the cost of producing one kilogram of PHA. Natural gas would add about $0.30 per kg PHB. Waste biogas from existing landfills and digesters is a reliable and continuous supply that could be free in situations where biogas is currently captured and flared. If new digesters are constructed, the additional cost is estimated to be less than $0.10 per kg PHB.

2. In general, model predictions indicate that the revenue from sale of PHB produced from a unit of methane will exceed the revenue from sale of the electricity generated from a unit mass of methane.

3. The cost of PHB production with biogas appears attractive at facilities producing more than 5,000 tonnes of PHB per year, with production costs approaching $1 per kg. These costs could be competitive with PLA and petroleum-based plastic resins.

4. Scale is likely to have a significant impact on production costs. At large scale, energy efficiency becomes critical. Energy is about 40 percent of the production cost for a large plant. If electricity is purchased, changes in its price will impact costs. Use of a fraction of the biogas to satisfy energy requirements may be desirable to stabilize costs. At small scale, labor costs are critical. Such costs might be mitigated through effective labor management or by retraining of the staff at existing waste treatment facilities. At all scales of operation, chemical costs, especially for extraction and purification of PHB, are important.

5. The PHB conversion yield has a large impact on production costs. Selection of high-performance cultures and maintenance of such cultures is critical. Fast growth rates and a high percentage of PHB are desirable.

6. The efficiency of PHB recovery in the extraction process has a significant impact on production cost. Advances in extraction technology are needed.

7. Pilot and full-scale studies are needed to assess the stoichiometry and kinetics of PHB production at a realistic scale and to accurately assess capital and operational costs.

13.2 Outcomes

To date (December 2013), the knowledge and experience gained through this project has resulted in 21 published peer-reviewed manuscripts, three

manuscripts under review, nine student theses, eight pending patent applications, one issued patent, and a start-up company. Details are provided below.

Peer-reviewed publications

1. Liao, Q., I. Noda, and C.W. Frank. 2009. "Melt viscoelasticity of biodegradable poly(3-hydroxybutyrate-co-3-hydroxyhexanoate) copolymers." Polymer 50 (25):6139-6148.

2. Morse, M.C., Q. Liao, C.S. Criddle, and C.W. Frank, 2010. "Anaerobic biodegradation of the microbial copolymer poly(3-hydroxybutyrate-co-3-hydroxyhexanoate): effects of comonomer content, processing history, and semi-crystalline morphology." Polymer. 52:547-556. * co-first author.*

3. Pieja, A.J., K.H. Rostkowski, and C.S. Criddle, 2011. "Distribution and selection of poly-3-hydroxybutryate production capacity in methanotrophic proteobacteria." Microbial Ecology 62:564-573.

4. Pieja, A.J., E.R. Sundstrom, and C.S. Criddle, 2011. "Poly-3-hydroxybutyrate metabolism in the Type II methanotroph Methylocystis parvus OBBP." Applied Environ. Microbiol. 77(17): 6012-6019.

5. Pfluger, A., W.M. Wu, A.J. Pieja, J. Wan, K.H. Rostkowski, and C.S. Criddle, 2011. "Selection of Type I and Type II methanotrophic proteobacteria in a fluidized bed reactor." BioResource Technology 102:9919-9926.

6. Pieja, A.J., E.R. Sundstrom, and C.S. Criddle. 2012. "Cyclic, alternating methane and nitrogen limitation increases PHB production in a methanotrophic community." BioResource Technology 107:385–392.

7. Rostkowski, K., C.S. Criddle, M.D. Lepech. 2012. "Cradle-to-gate life cycle assessment for a cradle-to-cradle cycle: biogas-to-bioplastic (and back)." Environ. Sci. Technol. 46(18):9822-9829.

8. Michel, A.T., S.L. Billington. 2012. "Characterization of poly-hydroxybutyrate films and hemp fiber reinforced composites exposed to accelerated weathering." Polymer Degradation and Stability. 97(6): 870-878.

9. Srubar III, W.V., Z.C. Wright*, A. Tsui, A.T. Michel, S.L. Billington, C.W. Frank. 2012. "Characterizing the Effects of Ambient Aging on the Mechanical and Physical Properties of Two Commercially Available Bacterial Thermoplastics." Polymer Degradation and Stability; 97(10): 1922-29. *equal contribution.*

10. Srubar III, W.V., C.W. Frank, S.L. Billington. 2012. "Modeling the Kinetics of Water Transport and Hydroexpansion in a Lignocellulose-Reinforced Bacterial Copolyester." Polymer; 53(11): 2152-61.

11. Srubar III, W.V., S. Pilla, Z.C. Wright, C.A. Ryan, J.P. Greene, C.W. Frank, S.L. Billington. 2012. "Mechanisms and Impact of Fiber-Matrix Compatibilization Techniques on the Material Characterization of PHBV/Oak Wood Flour Engineered Biobased Composites." Composites Science and Technology; 72(6): 708-15.

12. Michel, A.T., and Billington, S.L. 2012. "Characterization of Poly-Hydroxybutyrate Films and Hemp Fiber Reinforced Composites Exposed to Accelerated Weathering." Polymer Degradation and Stability, published online, http://dx.doi.org/10.1016/j.polymdegradstab.2012.03.040, April.

13. Srubar III W.V., Wright Z.C.*, Tsui A., Michel A.T., Billington S.L., and Frank C.W. 2012. "Characterizing the effects of ambient aging on the mechanical and physical properties of two commercially available bacterial thermoplastics." Polymer Degradation & Stability, 97:1922-1929. *equal contribution.*

14. Liao, Q., A. Tsui, S. Billington, and C.W. Frank. 2012. "Extruded foams from microbial poly(3-hydroxybutyrate-co-3-hydroxyvalerate) and its blends with cellulose acetate butyrate." Polym. Eng. Sci. 52 (7):1495-1508.

15. Miller, S.A., Billington, S.L., and Lepech, M.D. 2013. "Improvement in Environmental Performance of Poly(b -hydroxybutyrate)-co-(b-hydroxyvalerate) Composites through Process Modifications". Journal of Cleaner Production, 40:190-198.

16. Rostkowski, K.H., A.R. Pfluger, and C.S. Criddle, 2013. "Stoichiometry and kinetics of the PHB-producing Type II methanotrophs Methylosinus trichosporium OB3b and Methylocystis parvus OBBP." BioResource Technology 132C:71-77.

17. Srubar III, WV, S.L. Billington. 2013. "A Micromechanical Model for Moisture-Induced Deterioration in Fully Biorenewable Wood-Plastic Composites." Composites Part A: Applied Science and Manufacturing; 50: 81-92.

18. Miller, S.A., M.D. Lepech, S.L. Billington. 2013. "Application of multi-criteria material selection techniques to constituent refinement in biobased composites." Materials and Design. 52: 1043-1051.

19. Miller, S.A., S.L. Billington, M.D. Lepech. 2013. "Improvement in environmental performance of poly(β-hydroxybutyrate)-co-(β-hydroxyvalerate) composites through process modifications." Journal of Cleaner Production. 40:190-198.

20. Srubar, W.V. III, A. T. Michel, C.S. Criddle, C.W. Frank, and S.L. Billington, 2011. "Engineered biomaterials for construction: A cradle-to-cradle design

methodology for green material development." The International J. of Environmental, Cultural, Economic and Social Sustainability 7(5):157-166.

21. Tsui, A., X. Hu, D.L. Kaplan, and C.W. Frank. 2013. "Biodegradable films and foam of poly(3-hydroxybutyrate-co-3-hydroxyvalerate) blended with silk fibroin." Green Polymer Chemistry II, American Chemical Society. November 22, 2013 | doi: 10.1021/bk-2013-1144.ch018

22. Tsui, A., Z.C. Wright, and C.W. Frank. 2013. "Prediction of gas solubility in poly(3-hydroxybutyrate-co-3-hydroxyvalerate) melt to inform process design and resulting foam microstructure." Submitted for publication.

23. Wright, Z.C. and C.W. Frank. 2013. "Increasing cell homogeneity of semicrystalline, biodegradable polymer foams with a narrow processing window via rapid quenching." Submitted for publication.

24. W.M. Wu, C. LaFeldt, J. Ren, Q. Wang , R, Narayan, and C. S. Criddle, 2013. "Recovery of lactide by thermal depolymerization of poly(lactic acid) materials." Submitted for publication.

25. Myung, J., N. I. Strong, W. M. Galega, E. R. Sundstrom, J. A, Flanagan, S.-G. Woo, and R. M. Waymouth. 2014. "Disassembly and reassembly of polyhydroxyalkanoates: Recycling through abiotic depolymerization and biotic repolymerization." Submitted for publication.

Theses

Eleven graduate students completed theses with funding provided in part through this project.

Engineer's Degree Thesis

1. Andrew Pfluger, 2010. Thesis: "Growth of Type 1 and Type 2 Methanotrophs in a Fluidized Bed Reactor."

Doctoral Degree Theses

1. Margaret-Catherine Morse. 2009. Thesis: "Anaerobic Biodegradation of Biocomposites for the Building Industry."

2. Qi Liao, 2010. Thesis: "Biodegradable poly(hydroxyalkanoates): Melt, Solid, and Foam."

3. Allison Pieja 2011. Thesis: "Methanotrophic Production of Polyhydroxybutyrate."

4. Katherine Rostkowski, 2012. Thesis: "Understanding Methanotrophic Polyhydroxybutyrate (PHB) Production Across Scale: Life Cycle Assessment, Pure Culture Experimentation, and Pathway/genome Database Development."

5. Eric Sundstrom, 2013. Thesis: "Selection and Optimization Strategies for Production of Polyhydroxybutyrate in Methanotrophic Bacteria."

6. Zachary Wright, Z.C. 2013. Thesis: "Poly(3-hydroxybutyrate-co-3-hydroxyvalerate) Biodegradable Foams: the Effects of Processing, Nanoscale Additives, and Aging."

7. Aaron Michel, 2013. Thesis: "Characterization and Modeling of Biobased Composites and Structural Insulated Panels."

8. Wil Srubar, 2013. Thesis: "Hygrothermal Durability of Biorenewable Composites for Construction."

9. Sabbie Miller, 2014. Thesis: "Application of Time-Dependent Material Properties and Environmental Impact Analysis in Bio-based Composite Design."

10. Amy Tsui, 2014. Thesis: "Complex Interplay of Thermal Constraints, Rheological Performance, and Process Design on Extrusion Foaming of Biodegradable Polyhydroxyalkanoates."

Patents

The table below summarizes the status of patent filings as of Nov 2013: In total, 11 patents were filed, two were subsequently abandoned, one has issued, and eight are pending office actions.

Title	**Date Filed**	**Status**	**Serial Number**
Intermittent nutrient addition for synthesis of polyhydroxyalkanoic acids biopolymers by methane-oxidizing bacteria	12/08/09	Pending. Published Dec 8, 2010	61/283,784
High solids fermentation for synthesis of polyhydroxyalkanoates from gas substrate	10/08/10	Pending. Published Feb 2, 2011	12/901,343
Use of hydroxyalkanoic acids as	12/8/10	Pending.	12/928,323

substrates for production of polyhydroxyalkanoates by methane-oxidizing bacteria		Published Jun 30, 2011	
High throughput system for isolation, growth, and detection of lipid inclusions in bacteria	12/07/10	Pending. Published Jun 30, 2011	12/928,312
Method for anaerobic biodegradation of bioplastics	09/29/11	Pending. Published Mar 29, 2012	13/200,731
Process for the selection of PHB-producing methanotrophic cultures	08/21/12	Pending. Published Feb 28, 2013	13/590,603 US20130052681 A1
PHBV/ground bone meal and pumice powder engineering biobased composite materials for construction	2/7/12	Issued Aug 13, 2013	United States Patent 8,507,588
Production of PHA using biogas as feedstock and power source	03/15/12	Abandoned 10/07/13	13/421,771
Lactide production from thermal depolymerization of PLA with applications to production of PLA or other bioproducts	03/15/12	Abandoned 10/07/13	13/421,780
Intermittent application of reduced nitrogen sources for selection of PHB producing methanotrophs	05/29/13	Pending	US2013/043069
Coated biodegradable building article	07/11/13	Pending	App no. 13/939868

Two inventions were awarded prior to CalRecycle support and are relevant to this work. These patents are now in force:

U.S. Patent No. 7887893. (Filed Dec 12, 2007; issued Feb 15, 2011). App no. US 12/002,001 Bacterial poly(hydroxyalkanoate) polymer and natural fiber

composites." S.L. Billington, C.S. Criddle, W.C. Frank, M.C. Morse, S.J. Christian, and A.J. Pieja.

U.S. Patent No. 8,030,021 B2 (priority: June 24, 2008; filed June 24, 2009; issued Oct 4, 2011; expires June 3, 2030). App. no. US 12/456,988. "Use of selection pressures to enable microbial biosynthesis of polyhydroxyalkanoates from anaerobic degradation products." C.S. Criddle and A.J. Pieja.

Startup company

Mango Materials[60] is an internationally recognized startup company that produces biodegradable plastics from waste methane gas. The company spun out of Stanford University and was incorporated in Palo Alto in August 2010. Dr. Molly Morse (Ph.D., Stanford University, 2009) is CEO, and Dr. Allison Pieja (Ph.D., Stanford University, 2011) is CTO. The company has focused on scaling up production of PHA from methane and PHA commercialization. Mango Materials was a Cleantech Open semi-finalist (2010), is the recipient of Phase I (2012) and Phase II (2013) Small Business Innovation and Research Awards from the National Science Foundation, and won the grand prize in the Postcode Lottery Green Challenge International Business Plan Competition in 2012.

Literature Cited

[1] http://www.calrecycle.ca.gov/plastics/ *(January 2014)*

[2] http://www.nrel.gov/docs/fy14osti/60178.pdf *(January 2014)*

[3] *A.J. Pieja, K.H. Rostkowski, and C.S. Criddle, "Distribution and selection of poly-3-hydroxybutyrate production capacity in methanotrophic proteobacteria," Microbial Ecology, 62, October 2011, pp.564-573.*

[4] *K. Rostkowski, A. Pfluger, and C.S. Criddle. 2013. "Stoichiometry and kinetics of the PHB-producing Type II methanotrophs Methylosinus trichosporium OB3b and Methylocystis parvus OBBP" Bioresource Technology, Vol. 132, March 2013, pp. 71-77.*

[5] *A.J. Pieja, E.R. Sundstrom, and C.S. Criddle, "Poly-3-hydroxybutyrate metabolism in the Type II methanotroph Methylocystis parvus OBBP," Applied Environmental Microbiology, Vol. 77, January 2011, pp. 6012-6019.*

[6] *E.R. Sundstrom, "Selection and optimization strategies for production of polyhydroxybutyrate in methanotrophic bacteria," Ph.D. thesis, Department of Civil and Environmental Engineering, Stanford University, 2013.*

[7] *Ibid.*

[8] *A.J. Pieja, E.R. Sundstrom, and C.S. Criddle. "Cyclic, alternating methane and nitrogen limitation increases PHB production in a methanotrophic community," BioResource Technology, Vol. 107, March 2012, pp.385–392.*

[9] *A. Pfluger, W. Wu, A. Pieja, J. Wan, K. Rostkowski, and C.S. Criddle. "Selection of Type I and Type II methanotrophic proteobacteria in a fluidized bed reactor under non-sterile conditions," Bioresource Technology, Vol. 102, November 2011, pp. 9919-9926.*

[10] *E.R. Sundstrom, "Selection and optimization strategies for production of polyhydroxybutyrate in methanotrophic bacteria," Ph.D. thesis, Department of Civil and Environmental Engineering, Stanford University, 2013.*

[11] *Z.C. Wright, "Poly(3-hydroxybutyrate-co-3-hydroxyvalerate) biodegradable foams: the effects of processing, nanoscale additives, and aging," Ph.D. thesis, Stanford University. 2013*

[12] *W.V. Srubar III, S.L. Billington. 2013. "A Micromechanical Model for Moisture-Induced Deterioration in Fully Biorenewable Wood-Plastic Composites," Composites Part A: Applied Science and Manufacturing, Vol. 50, July 2013, pp. 81-92.*

[13] *S.A. Miller, M.D. Lepech, S.L. Billington. "Application of multi-criteria material selection techniques to constituent refinement in biobased composites." Materials and Design, Vol. 52, Dec. 2013, pp. 1043-1051.*

[14] *S.A. Miller, S.L. Billington, M.D. Lepech. "Improvement in environmental performance of poly(β-hydroxybutyrate)-co-(β-hydroxyvalerate) composites through process modifications." Journal of Cleaner Production, Vol. 40, February 2013, pp. 190-198.*

[15] *A.T. Michel, S.L. Billington. "Characterization of poly-hydroxybutyrate films and hemp fiber reinforced composites exposed to accelerated weathering." Polymer Degradation and Stability, Vol. 97, January 2012, pp. 870-878.*

[16] *W. V. Srubar III,* Z. C. Wright,* A. Tsui, A.T. Michel, S.L. Billington, C.W. Frank, "Characterizing the Effects of Ambient Aging on the Mechanical and Physical Properties of Two Commercially Available Bacterial Thermoplastics." Polymer Degradation and Stability, Vol. 97, January 2012, pp. 1922-29. *equal contribution*

[17] *W.V. Srubar III, C.W. Frank, S.L. Billington, "Modeling the Kinetics of Water Transport and Hydroexpansion in a Lignocellulose-Reinforced Bacterial Copolyester." Polymer, Vol. 53, December 2012, pp. 2152-61.*

[18] *W.V. Srubar III, S. Pilla, Z.C. Wright, C.A. Ryan, J.P. Greene, C.W. Frank, S.L. Billington, "Mechanisms and Impact of Fiber-Matrix Compatibilization Techniques on the Material Characterization of PHBV/Oak Wood Flour*

Engineered Biobased Composites." Composites Science and Technology, Vol. 72, November 2012, pp. 708-15.

[19] Q. Liao, A. Tsui, S. Billington, and C.W. Frank, "Extruded foams from microbial poly(3-hydroxybutyrate-co-3-hydroxyvalerate) and its blends with cellulose acetate butyrate." Polymer Engineering Science, Vol. 52, November 2012, pp. 1495-1508.

[20] A. Tsui, X. Hu, D.L. Kaplan, and C.W. Frank, "Biodegradable films and foam of poly(3-hydroxybutyrate-co-3-hydroxyvalerate) blended with silk fibroin." Green Polymer Chemistry: Biocatalysts and Materials II, Vol. 1144, November 2013, pp. 251-279.

[21] Z.C. Wright, "Poly(3-hydroxybutyrate-co-3-hydroxyvalerate) biodegradable foams: the effects of processing, nanoscale additives, and aging." Ph.D. thesis, Stanford University. 2013.

[22] A. Tsui, Z.C. Wright, and C.W. Frank, "Prediction of gas solubility in poly(3-hydroxybutyrate-co-3-hydroxyvalerate) melt to inform process design and resulting foam microstructure" Polymer Engineering and Science, Submitted December 2013.

[23] Z.C. Wright, and C.W. Frank, "Increasing cell homogeneity of semicrystalline, biodegradable polymer foams with a narrow processing window via rapid quenching." Polymer engineering and Science, Submitted December 2013.

[24] M.C. Morse, "Anaerobic biodegradation of biocomposites for the building industry." Department of Civil and Environmental Engineering, Ph.D. Thesis. Stanford University, 2009

[25] C.A. Ryan, "Closed-loop life cycle engineering of biopolymer composites: end-of-life degradation and reuse." Ph.D. Thesis. Stanford University, 2014 Expected.

[26] M.C. Morse, Q. Liao, C.S. Criddle, and C.W. Frank, "Anaerobic biodegradation of the microbial copolymer poly(3-hydroxybutyrate-co-3-hydroxyhexanoate): Effects of comonomer content, processing history, and semi-crystalline morphology." Polymer, Vol. 52, January 2011, pp. 547–556.

[27] A.M. Buswell, and H.F. Mueller, "Mechanism of methane fermentation." Industrial
and Engineering Chemistry, Vol. 44, March 1952, pp. 550-552.

[28] http://www.marketsandmarkets.com/PressReleases/polymethyl-methacrylate.asp (January 2014)

[29] M. Hajighasemi, A. Tchigvintsev, W. Wu, C.S. Criddle, E.A. Edwards, and A.F. Yakunin, "Enzymatic degradation of polylactic Acid." In preparation, 2013.

[30] *W.M. Wu, C. LaFeldt, J. Ren, Q. Wang , R, Narayan, and C.S. Criddle, 2013. "Recovery of lactide by thermal depolymerization of poly(lactic acid) materials." Submitted for publication, 2013.*

[31] *K. Rostkowski, C. Criddle, and M. Lepech, "Cradle-to-gate life cycle assessment for a cradle-to-cradle cycle: biogas-to-bioplastic (and back)." Environmental Science and Technology, Vol. 46, July 2012, pp. 9822-9829.*

[32] *http://www.tjgreenbio.com/en/index.aspx (January 2014)*

[33] *http://www.tianan-enmat.com (January 2014)*

[34] *http://www.meredianpha.com (January 2014)*

[35] *http://www.meredianpha.com/technology (January 2014)*

[36] *J. Wang, and H.Q. Yu, "Biosynthesis of polyhydroxybutyrate (PHB) and extracellular polymeric substances (EPS) by Ralstonia eutropha ATCC 17699 in batch cultures," Applied Microbiology and Biotechnology, Vol. 75, June 2007, pp.871-878.*

[37] *M. Mahmoudi, et al, "Kinetic model for polyhydroxybutyrate (PHB) production by Hydrogenophaga pseudoflava and verification of growth conditions," African Journal of Biotechnology, Vol. 9, No. 21, 2010, pp. 3151-3157.*

[38] *http://www.indexmundi.com/commodities/?commodity=palm-oil (January 2014)*

[39] *H.F. Listewnik, et al, "Process design for the microbial synthesis of poly-beta-hydroxybutyrate (PHB) from natural gas," Engineering in Life Sciences, Vol.7, June 2007, pp.278–282.*

[40] *http://www.indexmundi.com/commodities/?commodity=sunflower-oil (January 2014)*

[41] *K. Rostkowski, et al, "Stoichiometry and kinetics of the PHB-producing Type II methanotrophs Methylosinus trichosporium OB3b and Methylocystis parvus OBBP," Bioresource Technology, Vol. 132, March 2013, pp.71-77.*

[42] *Listewnik, H.F. et al, "Process design for the microbial synthesis of poly-beta-hydroxybutyrate (PHB) from natural gas," Eng Life Sci, Vol.7, 2007, pp.278–282.*

[43] *U.S. EPA, "Municipal solid waste in the United States: 2005 facts and figures," U.S. EPA, Office of Solid Waste, Washington, D.C., 2009. http://www.epa.gov/osw/nonhaz/municipal/msw99.htm*

[44] *R.H. Zhang, et al, "Current anaerobic digestion technologies used for treatment of municipal organic solid waste," Publication #IWMB-2008-011,*

California Integrated Waste Management Board, Sacramento, Calif., March, 2008. Available at http://www.ciwmb.ca.gov/Publications/

[45] http://www.energyjustice.net/map/displayfacility-69956.htm (January 2014)

[46] U.S. EPA, "Municipal solid waste in the United States: 2005 facts and figures," U.S. EPA, Office of Solid Waste, Washington, D.C., 2009. http://www.epa.gov/osw/nonhaz/municipal/msw99.htm

[47] http://water.epa.gov/scitech/datait/databases/cwns/ (January 2014)

[48] K. Rostkowski, A. Pfluger, and C.S. Criddle. 2013. "Stoichiometry and kinetics of the PHB-producing Type II methanotrophs Methylosinus trichosporium OB3b and Methylocystis parvus OBBP" Bioresource Technology, Vol. 132, March 2013, pp. 71-77.

[49] Ibid.

[50] Ibid.

[51] A.J. Pieja, E.R. Sundstrom, and C.S. Criddle. "Cyclic, alternating methane and nitrogen limitation increases PHB production in a methanotrophic community," BioResource Technology, Vol. 107, March 2012, pp.385-392.

[52] W.P. Clarke, "Cost-benefit analysis of introducing technology to rapidly degrade municipal solid waste," Waste Management and Research, Vol. 18, January 2000, pp. 510-524.

[53] K. Tsilemou and D. Panagiotakopoulos, "Approximate cost functions for solid waste treatment facilities," Waste Management and Research, Vol. 24, August 2006, pp.310-22.

[54] Ibid.

[55] W. P. Clarke, "Cost-benefit analysis of introducing technology to rapidly degrade municipal solid waste," Waste Management and Research, Vol. 18, January 2000, pp. 510-524.

[56] K. Tsilemou and D. Panagiotakopoulos, "Approximate cost functions for solid waste treatment facilities," Waste Management and Research, Vol. 24, August 2006, pp. 310-22.

[57] W.P. Clarke, "Cost-benefit analysis of introducing technology to rapidly degrade municipal solid waste," Waste Management and Research, Vol. 18, January 2000, pp. 510-524.

[58] Ibid.

[59] K. Tsilemou and D. Panagiotakopoulos, "Approximate cost functions for solid waste treatment facilities," Waste Management and Research, Vol. 24, August 2006, pp. 310-22.

[60] http://www.mangomaterials.com